

QATAR UNIVERSITY

COLLEGE OF ENGINEERING

DEVELOPING A FRAMEWORK FOR OPTIMAL PERFORMANCE OF
ACTIVATED CARBON/ GRAPHENE OXIDE/ACTIVATED CARBON-GRAPHENE
OXIDE NANO ADSORBENT FOR THE REMOVAL OF ANTIBIOTICS FROM
WASTEWATER

BY

SUNITA ROSHANKUMAR VARDE

A Thesis Submitted to
the College of Engineering
in Partial Fulfilment of the Requirements for the Degree of
Masters of Science in Environmental Engineering

June 2021

© 2021 Sunita Roshankumar Varde. All rights reserved.

COMMITTEE PAGE

The members of the Committee approve the Thesis of
Sunita Roshankumar Varde defended on 18/04/2021.

Dr. Abdelbaki Benamor
Thesis/Dissertation Supervisor

Dr. Abdul Wahab Mohammad
Committee member

Dr. Alaa Hawari
Committee Member

Dr. Raffaello Furlan
Committee Member

Approved:

Khalid Kamal Naji, Dean, College of Engineering

ABSTRACT

VARDE, SUNITA, R., Masters : June : 2021,

Masters of Science in Environmental Engineering

Title: Developing a Framework for Optimal Performance of Activated Carbon/ Graphene Oxide/Activated Carbon-Graphene Oxide Nano Adsorbent for the Removal of Antibiotics from Wastewater

Supervisor of Thesis: Dr. Abdelbaki Benamor.

Antibiotics are important drugs for treating infectious diseases and they have undoubtedly saved the lives of millions of people. A growing global problem is the emergence of antibiotic resistance, which means that the antibiotic does not work on the bacteria that cause the disease. Likely, many of the resistance genes we find in pathogenic bacteria today have their origin in the environment where, for example, they may have been part of the bacteria's defence mechanism. Adsorption is a physiochemical method widely used in wastewater treatment, is a fast, competent, and economical technology. Nowadays, a carbon-based material, graphene-based material has been extensively utilized because of its properties like high surface area, porosity, and reaction rate. This study emphasizes the removal of major antibiotics, namely Tetracycline and Doxycycline from wastewater. To achieve the objective of this study, nano adsorbent like activated carbon (AC), graphene oxide (GO) and composite nano adsorbent AC-GO (Activated carbon -graphene oxide) had been synthesized, characterized, and utilized for studies of adsorption equilibrium and kinetics for the elimination of antibiotics. Langmuir isotherm model was the best fit for equilibrium data obtained for Tetracycline and Doxycycline. For kinetic adsorption,

pseudo-second-order was fitting best with experimental data. Physical and chemical adsorption plays a vital role in adsorption onto nano adsorbent AC, GO, and AC-GO. The adsorption of Tetracycline and Doxycycline on nano adsorbent was owing not only to the larger surface area but also due to π -EDA (electron donor-acceptor interactions), hydrogen bonding, and electrostatic attraction-repulsion theory. After 3 regeneration cycles, the AC-GO still demonstrated a high adsorption capacity and reusability.

Keywords: Adsorption, Nano adsorbent, Antibiotic, Tetracycline, Doxycycline, Activated Carbon

DEDICATION

*I dedicate this thesis to
my loving kids Rudra , Darsh
and
my loving husband Roshankumar*

ACKNOWLEDGMENTS

I hereby wish to thank Dr Abdelbaki Benamor my supervisor for his continuous guidance, motivation, and advice throughout this project. Also, I would like to acknowledge the contribution of Mr Nafis Mahmud for his technical support during various stages of the experiments and Qatar University as a whole for providing this opportunity, including all administrative and support staff.

TABLE OF CONTENTS

DEDICATION.....	v
ACKNOWLEDGMENTS	vi
LIST OF TABLES	xiii
LIST OF FIGURES	xv
CHAPTER 1: INTRODUCTION.....	xv
1.1 Water Consumption Worldwide	1
1.2 Water Pollution and Water Scarcity	1
1.3 Research Motivation	2
1.4 Thesis Objective.....	3
1.5 Systematic Diagram of Overall Research Work.....	4
CHAPTER 2: LITERATURE REVIEW	5
2.1 Sources of Wastewater.....	5
2.2 Occurrence of Antibiotic in Aquatic Environment.....	6
2.3 Major Classes of Antibiotics.....	8
2.3.1 Tetracycline.....	8
2.3.2 Fluoroquinolones (FQs)	10
2.3.3 Sulfonamides.....	12
2.4 Treatment Technologies for Removal of Antibiotics	13
2.4.1 Biodegradation	14

2.4.2	Chlorination	14
2.4.3	Ultraviolet Treatment.....	14
2.4.4	Ozonation Process.....	15
2.4.5	Advanced Oxidation Process (AOPs).....	15
2.4.6	Fenton and Fenton-like Process	16
2.4.7	Ozonation or Catalytic Ozonation	17
2.4.8	Electrochemical Oxidation.....	17
2.4.9	Biological Processes	18
2.4.10	Membrane Bioreactor	18
2.4.11	Membrane Processes.....	19
2.4.12	Adsorption Processes	20
2.5	Nanotechnology – New Trend in Wastewater Treatment.....	21
2.5.1	Nanoadsorbent	22
2.5.1.1	Graphene, Graphene Oxide and rGO	23
2.5.1.2	Carbon Nanotubes.....	25
2.5.1.3	Activated Carbon	26
2.6	Research Gap	28
CHAPTER 3: METHODOLOGY AND EXPERIMENTAL SETUP.....		29
3.1	Material.....	29
3.1.1	Weighing Scale	29

3.1.2	Mixing Tool	30
3.2	Experimental Setup.....	30
3.2.1	Conical Flask (100 ml).....	30
3.2.2	Incubator Shaker	31
3.2.3	Vacuum Gas Pump	32
3.2.4	Vacuum Gas Pump With Beaker and Funnel	33
3.2.5	Ultraviolet-Visible (UV-Vis) Apparatus.....	33
3.3	Nano Adsorbent Synthesis	35
3.3.1	Nano adsorbent Activated Carbon (AC).....	35
3.3.2	Nano Adsorbent Graphene Oxide (GO) Synthesis	35
3.3.3	Nano Adsorbent Composite Activated carbon-Graphene oxide (AC-GO) Synthesis.....	36
3.4	Nano Adsorbent Characterization.....	37
3.4.1	X-Ray Diffraction	37
3.4.2	Scanning Electron Microscope	38
3.4.3	Transmission Electron Microscopy	39
3.4.4	Fourier Transform Infrared Spectroscopy	39
3.4.5	Energy Dispersive X-ray Spectroscopy	40
3.4.6	Brunauer- Emmet -Teller	40
3.5	Experimental Procedure.....	41

3.6	Adsorption Equilibrium:	42
3.7	Adsorption Kinetics	44
CHAPTER 4: RESULTS AND DISCUSSION.....		47
4.1	Characterisation of Nano Adsorbent.....	48
4.1.1	X-Ray Diffraction	48
4.1.1.1.	Activated Carbon (AC)	48
4.1.1.2.	Graphene Oxide (GO).....	48
4.1.1.3.	Activated carbon – Graphene oxide (AC-GO).....	49
4.1.2	Scanning Electron microscopy	50
4.1.2.1	Graphene oxide (GO).....	50
4.1.2.2	Activated carbon-Graphene oxide (AC-GO).....	51
4.1.3	Transmission Electron Microscopy	52
4.1.3.1.	Activated Carbon (AC)	52
4.1.3.2.	Graphene oxide (GO)	53
4.1.3.3.	Activated carbon-Graphene oxide (AC-GO)	53
4.1.4	Fourier Transform -Infrared Spectroscopy	54
4.1.4.1	Activated Carbon (AC).....	54
4.1.4.2	Graphene Oxide (GO).....	55
4.1.4.3	Activated carbon-Graphene oxide (AC-GO).....	56
4.1.5	Energy Dispersive X-Ray Spectroscopy.....	57

4.1.5.1.	Graphene Oxide (GO)	57
4.1.5.2.	Activated carbon -Graphen oxide (AC-GO)	58
4.1.6	Brunauer–Emmett–Teller	59
4.2	Adsorption Equilibrium	60
4.2.1	Analyses	60
4.2.2	Adsorption of Tetracycline on Activated carbon, Graphene oxide, and Activated carbon-Graphene oxide	62
4.2.2.1	Effect of Temperature	62
4.2.2.2	Effect of Solution pH	67
4.2.2.3	Effect of Initial Concentration	70
4.2.3	Adsorption Doxycycline on Activated carbon, Graphene oxide, and Activated carbon-Graphene oxide	71
4.2.3.1	Effect of temperature	71
4.2.3.2	Effect of Solution pH	76
4.2.3.3	Effect of Initial Concentration	79
4.3	Adsorption Kinetics	80
4.3.1	Adsorption of Tetracycline on Activated carbon ,Graphene oxide, Activated carbon -Grpahene oxide.....	80
4.3.1.1	Effect of Time	80
4.3.2	Adsorption of Doxycycline Activated carbon, Graphene oxide, and Activated carbon-Graphene oxide	85

4.3.2.1	Effect of Time	85
4.4	Intraparticle Diffusion Studies of Tetracycline and Doxycycline adsorption on Activated Carbon, Graphene Oxide, and Activated carbon-Graphene oxide	89
4.5	Thermodynamic Study	92
4.5.1	Thermodynamics Study of Adsorption of Tetracycline and Doxycycline on Activated Carbon, Graphene Oxide, and Activated carbon-Graphene oxide.....	93
4.6	Comparative Study of Tetracycline and Doxycycline on Activated Carbon, Graphene Oxide and Activated carbon-Graphene oxide	97
4.6.1	Adsorption Isotherm	97
4.6.2	Adsorption Kinetics	99
4.7	Adsorption Mechanism	100
4.8	Reusability of Nano Adsorbent Composite Activated carbon-Graphene oxide ..	103
4.9	Reproducibility of Results	104
CHAPTER 5: CONCLUSION AND RECOMMODATION.....		106
5.1	Conclusion	106
5.2	Future Work and Recommendation	107
REFERENCES		109
EQUILIBRIUM DATA FOR TETRACYCLINE :APPENDIX A		124
EQUILIBRIUM DATA FOR DOXYCLINE :APPENDIX B		125

LIST OF TABLES

Table 1: Physiochemical Properties of Tetracycline	9
Table 2: Adsorption Capacity of Graphene Based Material for Different Class of Antibiotics.....	24
Table 3: Adsorption Capacity of Carbon Nanotubes for Different Class of Antibiotics..	26
Table 4: Adsorption Capacity of Activated Carbon for Different Class of Antibiotics ...	27
Table 5 : BET Analysis of AC,GO, AC-GO	59
Table 6: Common Equilibrium Isotherm Models Used for Analysis	43
Table 7 : Absorption/Concentration Data for Calibration Curve of Tetracycline (TC) ...	60
Table 8: Absorption/Concentration Data for Calibration Curve of Doxycycline (DC)....	61
Table 9: Parameters of Adsorption Isotherm Model of TC Adsorption of AC	63
Table 10: Parameters of Adsorption Isotherm Model of TC Adsorption of GO	64
Table 11: Parameters of Adsorption Isotherm of DC Adsorption of AC	72
Table 12: Parameters of Adsorption Isotherm Model of DC Adsorption of GO.....	73
Table 13: Parameters of Adsorption Isotherm Model of DC Adsorption of AC- GO.....	89
Table 14: Common Kinetic Model Used in Analysis	94
Table 15: Parameters of Adsorption Kinetic Model of TC Adsorption of AC.....	81
Table 16: Parameters of Adsorption Kinetic Model of TC Adsorption of GO	82
Table 17: Parameters of Adsorption Kinetic Model of TC Adsorption of AC-GO.....	99
Table 18: Parameters of Adsorption Kinetic Model of DC Adsorption of AC	86
Table 19: Parameters of Adsorption Kinetic Model of DC Adsorption of GO	87
Table 20: Parameters of Adsorption Kinetic Model of DC Adsorption of AC-GO	88

Table 21: Intraparticle Diffusion Data of Adsorption of TC and DC on AC, GO, AC-GO	90
Table 22: Thermodynamics Data of Adsorption of TC and DC on AC, GO, AC-GO.....	94
Table 23: Regeneration Data of TC and DC onto AC-GO.....	104

LIST OF FIGURES

Figure 1 : Diagram of Overall Research Work.....	4
Figure 2: Antibiotic Circulation in The Environment.....	7
Figure 3: Molecular Structure of Tetracycline.....	9
Figure 4: Usage of Antibiotics in Individual Countries.....	10
Figure 5: Molecular Structure of FQs.....	11
Figure 6: Molecular Structure of Antibiotic Sulfonamide.....	12
Figure 7: Important Technologies Used in Traditional Wastewater Treatment Plants.....	13
Figure 8: Schematic Description of the Adsorption Process	20
Figure 9: Weighing Scale.....	29
Figure 10: Mechanical Mixing Tool.....	30
Figure 11: Conical Flask (100ml).....	31
Figure 12: Incubator Shaker.....	32
Figure 13: Vacuum Gas Pump.....	32
Figure 14: Vacuum Gas Pump with Beaker and Funnel.....	33
Figure 15: Schematic Diagram of UV-Vis	34
Figure 16: UV-Vis Equipment.....	35
Figure 17: Images of Synthesized GO Solution and GO Powder.....	36
Figure 18: X-Ray Diffraction Equipment	38
Figure 19: Fourier Transform Infrared Spectroscopy Equipment	40
Figure 20: XRD Image of Commercial Powdered AC.....	48
Figure 21: XRD Image of Synthesized Nano adsorbent GO.....	49
Figure 22: XRD Image of Synthesized Nano adsorbent AC-GO.....	50

Figure 23: SEM Images of GO at 30 μ m, 50 μ m, 10 μ m, 50 μ m.....	51
Figure 24: SEM Images of AC-GO at 10 μ m, 3 μ m, 100 μ m, 30 μ m.....	52
Figure 25: TEM Images of AC at 200nm, 100 nm,50 nm, 50 nm.....	52
Figure 26: TEM Images of GO at 1 μ m, 50 nm,10 nm,500 nm.	53
Figure 27: TEM Images of AC-GO at 1 μ m, 100 nm,10 nm, 1 μ m.....	54
Figure 28: FTIR Image of Nano adsorbent AC	55
Figure 29: FTIR Image of Nano adsorbent GO	56
Figure 30: FTIR Image of Nano adsorbent GO	57
Figure 31: EDX Image of GO.....	58
Figure 32: EDX Image of AC-GO.....	59
Figure 33: Calibration Curve for Tetracycline (Abs vs Conc)	60
Figure 34: Calibration Curve for Doxycycline (Abs vs Conc).....	61
Figure 35: Adsorption Isotherm Langmuir (1) and Temkin (2) of TC on AC	64
Figure 36: Adsorption Isotherm Langmuir (1) and Temkin (2) of TC on GO	65
Figure 37: Adsorption Isotherm Langmuir (1) and Temkin (2) of TC on AC- GO	67
Figure 38: Effect of pH on Adsorption of TC onto AC.....	68
Figure 39: Effect of pH on Adsorption of TC onto GO.....	69
Figure 40: Effect Of pH on Adsorption of TC onto AC-GO.....	70
Figure 41: Adsorption Isotherm Langmuir (1) and Temkin (2) of DC on AC.....	73
Figure 42: Adsorption Isotherm Langmuir (1) and Temkin (2) of DC on GO.....	74
Figure 43: Adsorption Isotherm Langmuir (1) and Temkin (2) of DC on AC -GO.....	76
Figure 44: Effect of pH on Adsorption of DC onto AC	77
Figure 45: Effect of pH on Adsorption of DC onto GO	78

Figure 46: Effect of pH on Adsorption of DC onto AC-GO	79
Figure 47: Analysis Models for Adsorption of TC on AC	82
Figure 48: Analysis Models for TC on GO	83
Figure 49: Analysis Models for Adsorption of TC on AC-GO	84
Figure 50: Analysis Models for Adsorption of DC on AC	86
Figure 51: Analysis Models for Adsorption of DC on GO.....	88
Figure 52: Analysis Models for Adsorption of DC on AC- GO.....	89
Figure 53: Intraparticle Diffusion Model Analysis of TC on AC (1), GO (2), AC-GO (3)	91
Figure 54: Intraparticle Diffusion Model Analysis of DC on AC (1), GO (2), AC-GO (3)	92
Figure 55: Thermodynamic Analysis of TCon AC (1), GO(2), and AC-GO (3)	95
Figure 56: Thermodynamic Analysis of DC on AC (1), GO(2), and AC-GO (3).....	96
Figure 57: Adsorption Isotherms of TC (1) and DC (2) on AC, GO, AC-GO at 303 K .	98
Figure 58: Comparative Maximum Adsorption capacity of TC (1) and DC (2) on AC, GO, AC-GO	98
Figure 59: Analysis Models of TC on AC, GO, AC-GO.....	100
Figure 60: Pseudo Second-Order Model of DC on AC, GO, AC-GO.....	100
Figure 61: FTIR Spectra of AC After Adsorption of TC.....	102
Figure 62: Adsorption Mechanism of Tetracycline on AC, GO, and AC-GO	103
Figure 63: Regeneration Capacity of TC (1) and DC (2) onto AC-GO.....	104

CHAPTER 1: INTRODUCTION

1.1 Water Consumption Worldwide

Water is the most important element for humankind as it represents 70% of the body liquids which transmits nutrients and macromolecules through the body. Also, water improves the body to cleanse out toxins and enhances the immune system to keep the body healthy and its energy at the pinnacle. Also, water is a compulsory factor for farming, and it was proven by enhancing the irrigation techniques. According to United Nations, the most commonly used water reserves on earth are oceans, seas, rivers, groundwater, which situated on the sub surface of the soil. The obtained water from all these reserves undergo decontamination processes, so it will be suitable for human use [1]. Clean water has an important role in human's life sustainability, and it is moderately essential for the individual's health. Though, having a clean water source all over the world cannot promise rapid access to fresh water for almost 783 million persons in different continents as well as it cannot give assurance to good health since it increases the percentage of water-related diseases, whether these diseases are triggered by deficient water supply, sanitation or hygiene [2].

1.2 Water Pollution and Water Scarcity

Water pollution and water scarcity are vital issues that people face in the current time. Wastewater is a type of water polluted by the use of human activities. Wastewater is used water that can be generated from numerous sources like household, industrial, commercial, or academic institutions, agriculture actions, surface overflow, stormwater, and sewer inflow or sewer infiltration. Thus, wastewater generation is directly linked to human-based activities like domestic, agriculture, commercial as well as industrial. There are various

techniques available to treat generated wastewater to set standards by federal agencies. Wastewater treatment services process approximately a billion gallons of wastewater on daily basis. Wastewater comprises nutrients like nitrogen and phosphorus from human waste, food, and some soaps and cleansers. When the water is cleaned to set the standard and approved by an authorized committee, it is typically released into a local ocean, where it can become a cause of pollution for nutrients (N and P).

1.3 Research Motivation

Pharmaceuticals drugs in water bodies have been reported worldwide. In a broad range of medicinal drugs, antibiotics have increased concerns about the future threats to human being health and environments. Antibiotics are a source of concern for the subsequent reasons: 1) their widespread consumption, e.g., nearly 17061 loads of antibiotics used in both human being and animal medication in the U.S. in 2011 2) their various sources, e.g., waste flow initiating from domestic areas, STP (sewage treatment plants), hospitals, and swine farms; 3) antibiotic resistance, e.g., introduction to a comparatively little pharmaceutical concentration (4 mg/L) in enabling the development of antibiotic-resistant 4) ineffectual technologies for water treatment, e.g. activated sludge, biological degradation, and photolytic and photocatalytic decomposition.

Among antibiotics, Tetracycline (TC) and Doxycycline (DC), are a class of wide-range antibiotics frequently employed in both human beings and animal medication. Regardless Of their efficacy, these drugs can't be digested in humans being and swine, nor can they be efficiently eliminated using existing wastewater treatment technologies such as activated sludge. As a result, they are released into the environment and become emergent environmental contaminants. TC and DC have been discovered in distinct water systems.

In this work, it was postulated that the above-mentioned antibiotics could be eliminated through the use of nano adsorbent like Activated Carbon (AC), Graphene Oxide (GO), and composite activated carbon -graphene oxide (AC-GO) as an adsorbent.

1.4 Thesis Objective

This thesis discusses a detailed work on the application of nano adsorbent for treating wastewater consisting of emerging contaminants, especially pharmaceutical antibiotics. The thesis focuses majorly on two important pharmaceutical antibiotics namely, Tetracycline (TC) and Doxycycline (TC) and three nano adsorbents namely, activated carbon (AC), Graphene oxide (GO) and Activated carbon – Graphene oxide (AC-GO). Hence, the objective of this thesis, in particular, includes:

- Synthesizing nano adsorbents Graphene oxide (GO) and composite nano adsorbent Activated Carbon-Graphene oxide (AC-GO) that are used to study the adsorption of pollutants on these nano adsorbents.
- Characterisation of nano adsorbents (AC, GO and AC-GO) using various characterization techniques such as XRD, SEM, etc.
- Evaluation of adsorption mechanism of pollutants (tetracycline and doxycycline) with nano adsorbents (AC, GO and AC-GO).
- Comparison of adsorption performance of nano adsorbents for removal of antibiotics to determine the best nano adsorbent for removal of both tetracycline and doxycycline.
- Evaluation of regeneration capability of AC-GO for removal of adsorbate TC and DC, to understand reusability of nano adsorbent.

1.5 Systematic Diagram of Overall Research Work

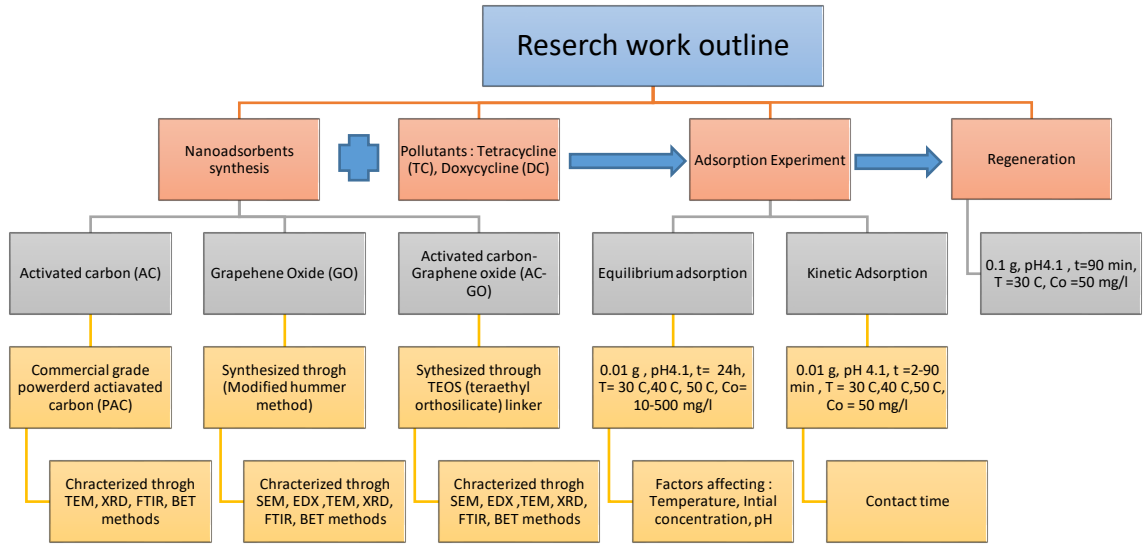


Figure 1 : Diagram of Overall Research Work

CHAPTER 2: LITERATURE REVIEW

Overexploitation of freshwater resources threatens the security of humanity in several parts of the world. Freshwater consumption at the global level is proceeding towards the highest level, irrespective of the estimate used. Due to populace increase, changing water utilization pattern, and environmental change, the contest of keeping water consumption at sustainable levels become even more challenging soon [3]. As a branch of sustainability, water security is critical. Water pollution and water scarcity are thorny issues that people face.

2.1 Sources of Wastewater

There are various types of wastewater produced from several human activities. Two broad groups of wastewaters are 1) Sewage and 2) Non- sewage.

Sewage Water comes from household activities known as sewage water. That contains houses, commercial, public, academic building as well as hospitals. These buildings all generate a lot of wastewater on daily basis, which generally includes urine and faeces. Wastewater treatment plants are employed to handle this sewage and after treatment effluent is finally discharged to nearby water bodies. Sewage is mostly biodegradable and nearly all of it is broken down in the environment [4].

Non- sewage water is further divided into

- 1) Black water
- 2) Grey water
- 3) Agricultural water
- 4) Industrial water and

5) Produced water.

Wastewater produced from the kitchen sink, dishwasher, and toilet is known as blackwater. It consists of all the pollutants expected from these sources including but not limited to human waste, excreta, used paper, washing soap and compounds resulting in highly polluted black water potentially causing diseases[4]. Greywater can be defined as blackwater excluding human waste and food leftovers. Primary sources of greywater are baths, bathroom sinks and washing machines (for clothes). However, it does consist of cleaning compounds and chemicals, but due to this being nonpathogenic is suitable for recycling[4].

Farming is also identified as one of the primary reasons for the degradation of surface and underground water reserves through chemical runoff and erosion[5]. Runoff from agriculture called agricultural water is a major problem that leads to surface and groundwater pollution. Pollutants emitting from industrial sector are severely hazardous to people and the planet. Pollutants from industries include nutrients like nitrates, nitrite, phosphorous, and Sulphur, heavy metals namely lead mercury, and asbestos, oils, and petrochemicals[4].

Oil and gas extraction are two of the activities that possibly very harmful to the environment. The major waste produced through oil and gas extraction activities is a produced water. Produced water is a kind of brackish water that is saline in nature. This water is composed of organic as well as inorganic pollutants which are very harmful. [4].

2.2 Occurrence of Antibiotic in Aquatic Environment

Antibiotic is most common medicine in the medical field and a frequently used drug for human beings and animals to cure disease and to stop bacterial progress[6]. There are

various ways through which antibiotics come into the environment such as wastewater discharge from hospital, agriculture wastewater, medicine manufacturing factory release etc. as illustrated in Figure 1. Consumed antibiotics are partially absorbed by living beings. The antibiotics taken by human or animals as part of disease cure, only a few percentages are digested completely and the rest of it reaches the environmental water bodies through urine excretion or faeces by animals and humans [7]. Since conventional WWTP is not designed to eliminate antibiotics effectively, the wastewater containing antibiotics pass through all the process of a conventional system and finally it discharged from the WWTP to the water bodies or spread over the soil [8]. Then, antibiotics are diffused to the environment through agriculture, and aquaculture [9], This condition provides a good atmosphere for bacteria and antibiotics to interact with each other and develop resistance for antibiotics [10]. The antibiotics remain to exist in the aqueous medium as well as in soil and then enter the person's body and animals through intake water and food chain. In this way, antibiotics keep circulating in the environment and finally accumulated in nature.

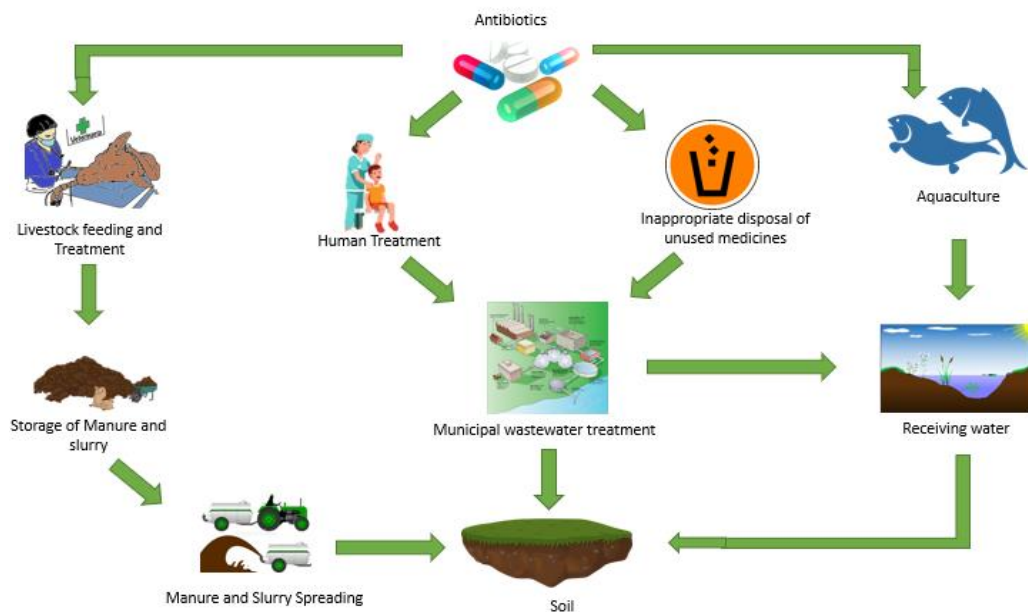


Figure 2: Antibiotic Circulation in The Environment

2.3 Major Classes of Antibiotics

The following are three important classes of antibiotics

Tetracycline

Fluoroquinolones

Sulfonamides

2.3.1 Tetracycline

Tetracyclines are generally used as antibiotics in both human being and animal treatment. This medicine act against gram-positive and negative by combining with 30 ribosomes [11]. Same as other antibiotics, tetracycline antibiotics cannot be entirely absorbed by living being, nor can they completely have eliminated from wastewater using conventional technologies and are ultimately discharged in active form into the environment. The occurrence of tetracycline (0.15-0.97 $\mu\text{g/L}$) in the final effluent from a WWTP in Canada [12]. A higher residual concentration was also reported by Deblonde et al. in the effluent from a WWTP [13]. The antibiotics (e.g., FQs, sulfonamides, tetracyclines) are accountable for the pollution of water resources and have motivated the researchers to develop effective and efficient water treatment technologies. The antibiotics that are usually used in living being medicine, like, Tetracycline and Doxycycline were chosen as the target contaminants in this work.

As the name suggested, the tetracycline is containing four nucleus rings through which a variety of functional groups are attached. Figure 2 below shows the functional groups attached with tetracycline includes hydroxyl, amines, and ketone. This antibiotic is a subclass of polyketides.

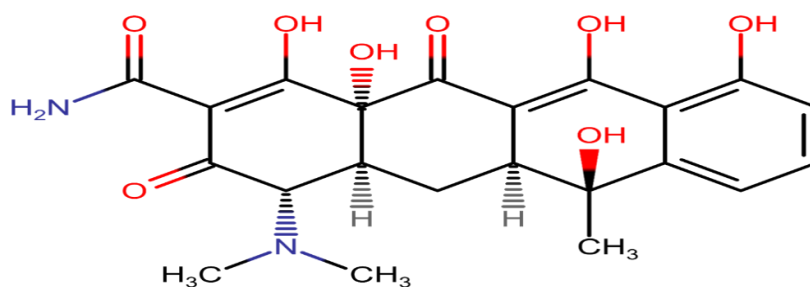


Figure 3: Molecular Structure of Tetracycline

Table 1 : Physiochemical Properties of Tetracycline

Compound	Tetracycline	Reference
Abbreviation	TC	[11]
CAS	60-54-8	[11]
Molecular formula	C ₂₂ H ₂₄ N ₂ O ₈	[11]
Molecular weight (g/mol)	444.44	[11]
Melting point (C)	172.50	[11]
Water solubility (mg/l) (25C)	231	[11]
pKa	3.3,7.68,9.69	[14] [11]
Log Kow	-1.25	[11]

Because of its high production and economic range, tetracycline is also utilized for nutrition stabilization to enhance the progress rate of animals. The animal faeces are used for the production of fertilizer for plants which enables tetracycline residues to enter the soil and aquatic environment because of the high solubility of tetracycline molecules. The growth promoters have also been utilized for the aquaculture and excreta formed by fish contaminate the surface and ground water. Figure 3, shows, the consumption of tetracycline by different countries. It shows that the USA alone consumes around 3200 tonnes.

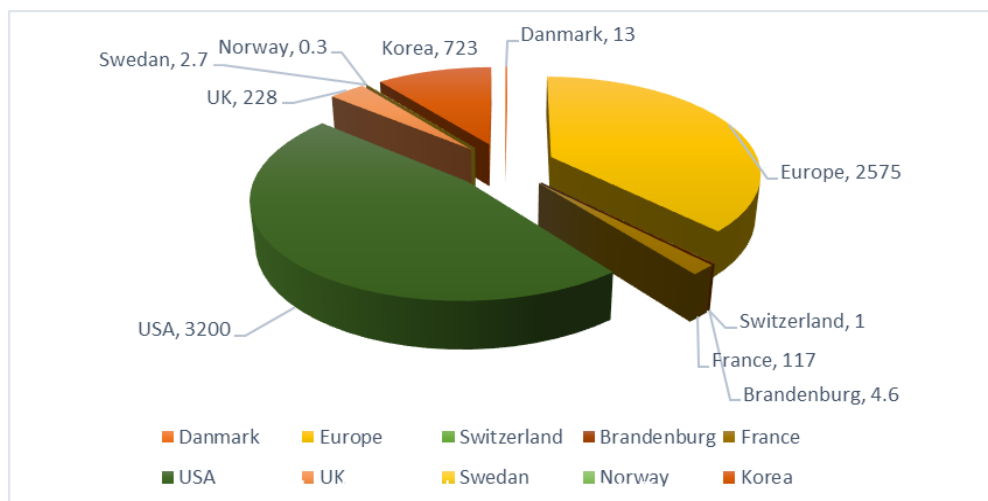
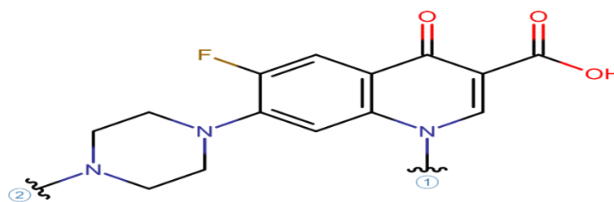


Figure 4: Usage of Antibiotics in Individual Countries

2.3.2 Fluoroquinolones (FQs)

Fluoroquinolone antibiotics (FQs) are an avital class of antibiotic compounds usually used in human being and animal medication. They obstruct key enzymes of bacteria (e.g., DNA gyrase and topoisomerase IV) elaborate in unwinding the DNA [15]. However, FQs may be problematic as cannot be absorbed by the body of a living being, thus are released into the environment. A series of recent studies focused on their occurrence, fate, and environmental risks [16,17,18]. For example, FQs up to 0.40 mg/kg were reported in agricultural soil worldwide, and FQs degraded slowly in soil (half-lives > 60 d) [17]. In tap water four FQs namely Norfloxacin, ciprofloxacin, lomefloxacin, and enrofloxacin was found and the concentration was between 1.0 to 679.7 ng/L [19, 20]. The molecular structure of FQs is shown in Figure 4 below.



Ciprofloxacin: ① = cyclopropyl, ② = H

Norfloxacin: ① = ethyl, ② = H

Enrofloxacin: ① = cyclopropyl, ② = ethyl

Figure 5: Molecular Structure of FQs

The occurrence of FQs in the surface water is becoming an emerging problem. There is a need for methods and regulations which will help to regulate the discharge of antibiotics in the water and improve the water quality[21]. Some published works evaluated different methods which can be utilized in assessing the possible health hazard linked with an indirect introduction to antibiotics, metabolites, and their degradation products in drinking water. For example, the concentration of levofloxacin (LEV, third-generation FQ) was reported in one of the downstream facilities in Pakistan and the concentration found was 8000 ng/L [22]. The Second-generation of FQ, NOR was spotted in Bohai Bay, and the concentration was described to be 6.8 $\mu\text{g} / \text{L}$ [23]. The use of manures to land, sewage sludge, and wastewater farming will lead to the accumulation of FQs in the soils to a very high level [24]. The FQs can interact with heavy metals because of the presence of functional groups such as keto and carboxyl [25].

2.3.3 Sulfonamides

The compounds containing sulfonamide have been widely consumed as antibiotics in human being and animal remedy because of their low cost. These antibiotics contain a sulfonyl group coupled to an amine group and their molecular structure. Sulfonamides obstruct the development of bacterial by contesting para-aminobenzoic acid which works for folic acid synthesis [26].

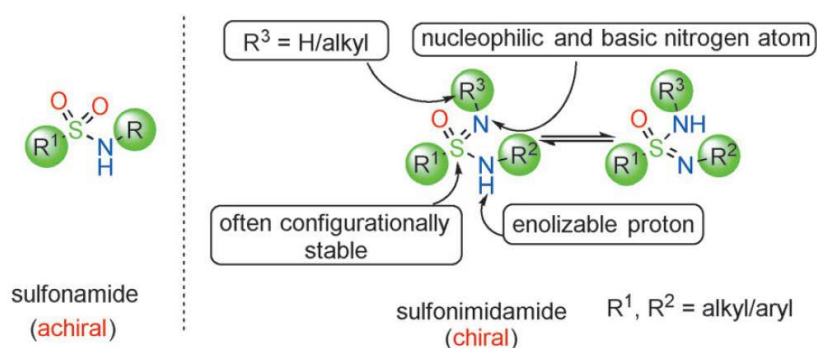


Figure 6: Molecular Structure of Antibiotic Sulfonamide

In the sewage influent of a WWTP in Guangzhou, China, sulfamethoxazole has been noticed with a concentration of 7.91 $\mu\text{g/L}$ [27]. Additionally, in urban water also sulfamethoxazole was stated with a concentration of 5.60 $\mu\text{g/L}$ [28]. The long-time exposure to sulfonamide antibiotics even in a low concentration could lead to a sulfonamide antibiotics resistance that has occurred in bacterial strains [29], which eventually risks human health. There is a necessity to eliminate sulfonamide antibiotics from water bodies to ensure the reuse of the treated effluent quality for numerous purposes and to shield social health as well [30].

2.4 Treatment Technologies for Removal of Antibiotics

The importance of fresh water and the identification of feasible water resources for daily life cannot be abandoned. It is obvious that the recycling of treated antibiotic wastewater not only benefits the environment and human health, but also greatly improves social and economic justice, and decreases the cost of water due to the increase in the water supply, which is good practice.

Conventional wastewater treatment plants (WWTPs) -as illustrated in Figure 6, usually comprise three steps of treatment; primary treatment is the physical treatment which focuses on the removal of suspended solid and steps include for this process are bar screening and sedimentation tank. The secondary treatment is known as biological treatment and it includes processes like activated sludge, rotating biological contactor and membrane bioreactor intended to degrade the complex organic chemicals into non-toxic elements. Tertiary treatment, applied in some WWTPs includes among others, chlorination, activated carbon adsorption, ultraviolet treatment, constructed wetland, and sand filtration treatment for a high degree of water purification[31].

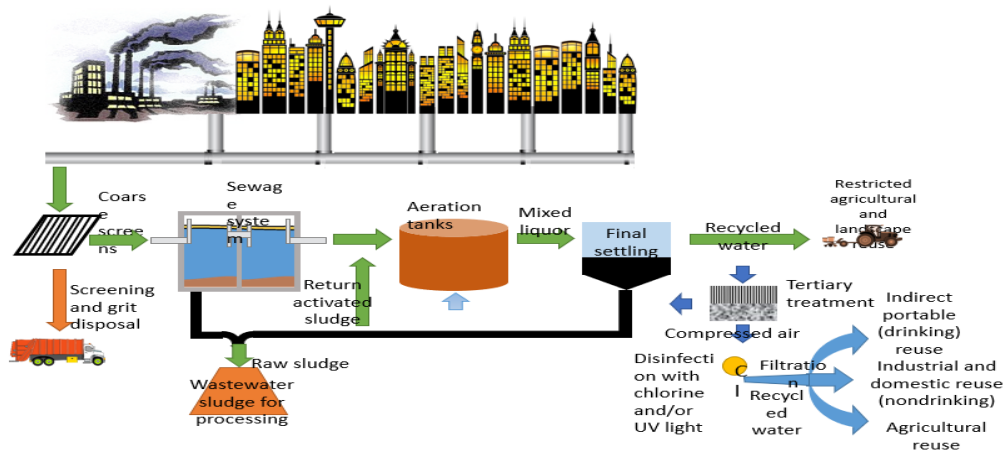


Figure 7: Important Technologies Used in Traditional Wastewater Treatment Plants.

2.4.1 Biodegradation

The Microorganisms mainly aerobic bacteria converts the organic substance into simple substances, like CO_2 , H_2O , and NH_3 through the process of biodegradation (United Nations Statistical Division). Most of the study results demonstrated that the biodegradability of antibiotics at aerobic conditions by bacteria was low. For example, the biodegradation of 18 antibiotics based on the rules of the Organization of the Economic Cooperation and Development (OECD), in 28 days, benzylpenicillin sodium salt (27%), amoxicillin (5%), nystatin (4%), and trimethoprim naphthoate (4%) were somewhat degraded and the degradation of the rest antibiotics were less than 4% [32].

2.4.2 Chlorination

To disinfect the drinking water from a harmful pathogen, chlorine is added to the water and the process is known as chlorination. There are different processes available to accomplish safe chlorine levels in drinking water. A solid sodium or calcium hypochlorite or compressed form of chlorine is utilized for the process. The addition of a chemical to water will result in dilution of the solution because of mixing and spreading that will help in killing pathogens because a high concentration of chemical could be harmful[31].

2.4.3 Ultraviolet Treatment

The most effective method to disinfect an aqueous solution from bacteria is the ultraviolet treatment system. UV (Ultraviolet) rays penetrate harmful pathogens in the wastewater and kill microorganism which will cause the illness by attacking their DNA. This technique is extremely efficient in the elimination of pathogens from the drinking water. Ultraviolet treatment is an exceptionally safe, simple, and environmentally friendly process for the disinfection of water. This technique kills 99.9% of harmful pathogens present in the water

or wastewater without adding any chemical and changing the colour or odour of water. Ultraviolet radiation can treat pathogens like bacteria, virus and microbes present in water, but does not function well with the compounds like chlorides, heavy metals, and organic compounds volatile in nature[33]. This treatment is being used very commonly with another form of filtration such as carbon block filter and reverse osmosis to disinfect water. Ultraviolet treatment is chemical-free, taste and odour-free, extremely effective in killing harmful pathogens, require very little energy and low maintenance cost.

2.4.4 Ozonation Process

Ozonation is a process used for the treatment of wastewater related to domestic as well as industries since 1950 (Salzgeber, 1951). Ozonation is the main treatment process in many sectors of science and engineering. The hydroxy radical combined with ozone through biochemical oxidation reaction and achieve high purification [34]. The process of oxidation has been utilized to treat refractory antibiotics [35]. Furthermore, the hydroxyl radical (OH^\cdot) of ozone has been highly utilized to oxidize the organic matter present in the wastewater which is not achievable by conventional oxidation process and it includes the recalcitrant antibiotics as well [36]. Huber et al [37] showed ozone a dose of 2 mg/l was utilized for the elimination of 10 to 11 antibiotics from an aqueous solution. The physio-chemical processes show high efficiency for the elimination of the pharmaceutical products, but the high cost of operation and production of in-between elements could be hindrances for the real usage of these methods.[38].

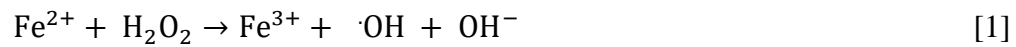
2.4.5 Advanced Oxidation Process (AOPs)

The AOPs (Advanced oxidation process) uses extremely reactive oxygen such as hydroxyl radical for the oxidation of aqueous solution and degrade the antibiotics present in the

solution to a higher degree [39]. Hydrogen peroxide is an oxidation agent, that is not sufficient to oxidize organic substance such as antibiotics, therefore, a combination of other components, catalysts, and Ultraviolet irradiation used for the production of hydroxyl radicals. AOPs include UV/H₂O₂, Fenton (Fe²⁺,³⁺/H₂O₂), and photo-Fenton (Fe²⁺,³⁺/H₂O₂/UV and Fe²⁺,³⁺/H₂O₂ simulated sunlight), and heterogeneous catalysis are most used[40]. For degradation of six antibiotics (i.e., clindamycin, trimethoprim ciprofloxacin, erythromycin, penicillin G, and doxycycline), the effectiveness of UV/H₂O₂ and photolysis by UV sources are utilized and the results demonstrated that all the antibiotics lost commotion when the dose of UV was at or over 500 mJ/cm²[41].

2.4.6 Fenton and Fenton-like Process

Fenton reagent is a mixture of hydrogen peroxide and ferrous salt[42]. In this process, the Fenton reagent reacts to produce hydroxyl radicals ($\cdot\text{OH}$) when added to wastewater and the reactions involved with the process are given in Eqs [1] [3].

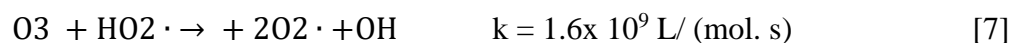
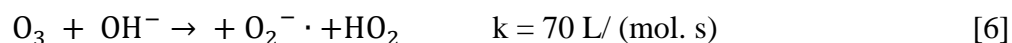
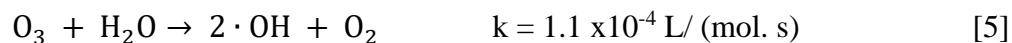


The antibiotics are degraded or oxidized by the radical shown in the equations. This method has advantages like easy operation and a high degradation rate of antibiotics. The variables which affect the process include the concentration of Fe²⁺, Ph, temperature, and concentration of H₂O₂. The process also has numerous disadvantages, like this process is restricted to the acidic condition, sludge produced in the process is most of the ion-containing, which is difficult to dispose of. To deal with the disadvantage associated with

the process, Fe⁺² has been replaced by another catalyst known as the Fenton-like oxidation process [43][44].

2.4.7 Ozonation or Catalytic Ozonation

One of the ecologically responsive technologies used for the treatment of wastewater is known as ozonation or catalytic ozonation[45]. The direct degradation of the organic component can be achieved by the ozone molecule. Ozone will form hydroxyl radical when it gets reacted with water in presence of a catalyst, which has robust oxidation skill, according to given Eqs. [5-10].



The degradation proficiency of homogenous as well as heterogenous organic substances can be enhanced by using the process of catalytic ozonation.

2.4.8 Electrochemical Oxidation

The electric current is used to degrade or oxidize the organic contaminant to non-toxic and inoffensive substance and the process involved is known as Electrochemical oxidation [46] [47]. The process includes both direct and indirect oxidation, and they generally happen concurrently[46, 48,49]. An organic contaminant in an aqueous solution reacts with an anode and lose electrons to make small molecular elements in the direct oxidation process[46, 50]. In the indirect oxidation process, anions in the aqueous solution react with

the anode to make intermediate products with high oxidizing ability, and these in-between products again oxidize and degrade organic pollutant [51][52].

2.4.9 Biological Processes

CAS (Conventional activated sludge), FBR (fixed-bed reactor) and MBR (membrane bioreactor) are biological processes with high abilities to remove antibiotics since they use biological features to meet the desired targets. The most used process for domestic and municipal wastewater treatment is the suspended growth process and known as activated sludge. The activated sludge process provides higher removal efficiency within an economical range with the application of art and science of wastewater treatment. However, Numerous studies debated that the CAS process could not eradicate pharmaceutical products, hence, their direct discharge of effluent or sludge into the environment lead to contaminate water body[53].

2.4.10 Membrane Bioreactor

The alternative technology replaced with CAS (conventional activated sludge treatment) for the recovery of highly simplified wastewater effluent is the MBR (membrane Bioreactor) [54]. The method is widely used in place of the conventional method of activated sludge because of less sludge production and high biodegradation ability. Furthermore, the process has a low cost and simple construction type of advantage also. The MBR with high organic concentration, high sludge holding, and bacterial variety could be a probable technology for the elimination of antibiotic. Radjenovic et al. found that several major antibiotics like ofloxacin (94%), sulfamethoxazole (61%), and erythromycin (67%) were removed by MBR while 24%; 56%; 24% in the CAS process, using a hollow fibre type of MBR. An elimination efficiency of $95.4 \pm 4.5\%$ of sulfamethoxazole at low

concentration with 93% COD and 96.2% NH₄ p-N removal efficiencies, respectively. To improve the biofilm process(attached growth processes) in the carrier, highly porous channels were used to advance the MBR removal efficiency and decrease membrane fouling; Nguyen et al [55] used a flat sheet Sponge-MBR for the removal of antibiotics. He found out that tetracycline was nearly removed, while the removal efficiencies of norfloxacin, ofloxacin (93-99%), ciprofloxacin (73-93%), trimethoprim (76-93%) and erythromycin (67-78%) were obtained.

2.4.11 Membrane Processes

Compared with conventional sewage treatments such as activated sludge, membrane systems (membrane filtration methods and membrane bioreactor) have been described to be more efficient to remove pharmaceutical contaminants and have many advantages, e.g., operation at a high concentration, less sludge production, and a significant reduction of suspended solid. Tetracycline antibiotics removed from water using a hybrid carbon membrane and removal efficiency was 98.9% reported[56]. Removal of FQ antibiotic (i.e., enrofloxacin) was also investigated by Reverse Osmosis (RO) and nano filtration (NF)membranes, the removal efficiencies of enrofloxacin by reverse osmosis (RO)and nano filtration(NF) membranes were higher than 97.2% and 99.1%, respectively. However, the antibiotics were still retained in the wastewater and concentrated in the sludge rather than degraded in the membrane processes. A membrane bioreactor (MBR) is a combination of CAS treatment and membrane filtration technology and is considered a good option for upgrading the existing WWTP. Although MBR systems had higher removal efficiencies than CAS systems, the high cost of membrane materials and high energy consumption limit

the wide application of such technology. There is a need to grow a technology that is low cost and highly efficient in the elimination of antibiotics from aquatic systems.

2.4.12 Adsorption Processes

The technologies are either a combination of economic with low efficiency or expensive with high efficiency. There is a necessity to develop technology that is low cost but high efficiency for pollutant removal. Adsorption is known as an efficient and operative technique, for the elimination of pollutant from wastewater [57][58]. Adsorption is the separation of a pollutant between the fluid (gas or liquid) and solid phase and has been in use for more than a century. Right now, adsorption has been broadly applied for desired bulk separation or purification. The fundamental elements in adsorption theory are illustrated in Figure 7. The solid phase is named an adsorbent; the substance adsorbed on the adsorbent is referred to as adsorbate. The release of an adsorbed substance into the fluid phase is called desorption, which could be accomplished by changing the properties of the fluid phase, e.g., pressure, solution pH, and concentration of adsorbate, and temperature.

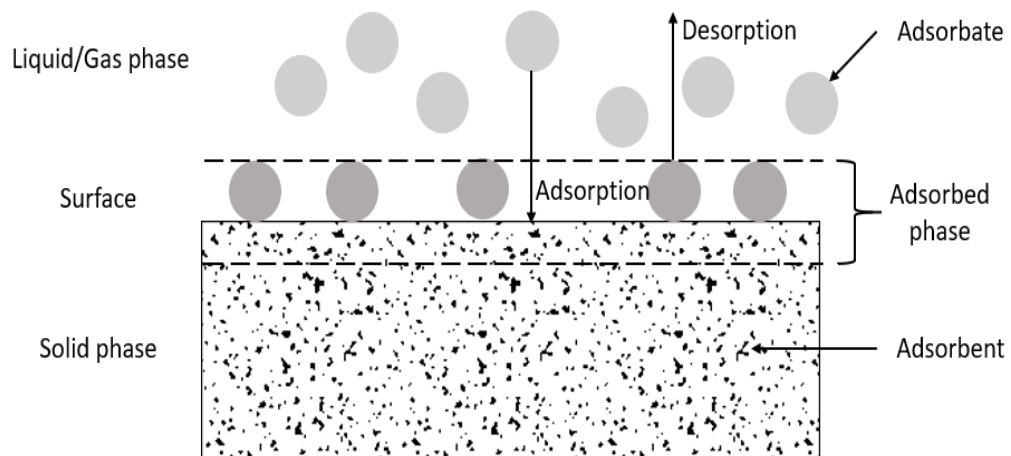


Figure 8: Schematic Description of the Adsorption Process

The adsorption mechanisms are mainly classified into three categories:

- a) steric mechanism- The pores of porous materials such as molecular sieve allow small molecules to enter while excluding large molecules from entry.
- b) Equilibrium mechanism, the solid which is (adsorbent) can accommodate different adsorbates, and the adsorbate that has stronger adsorption attraction with the adsorbent is preferentially adsorbed by the adsorbent.
- c) Kinetic mechanism, it works on the diffusion rate. Different adsorbates have different diffusion rates into the pore of adsorbent, thus adsorption of an adsorbate that has a faster diffusion rate could be achieved by controlling the time of exposure. The high surface area and bigger porous network with the high pore volume will help in the movement of the adsorbent and the adsorbate which possess all these properties will be considered as a good adsorbent.

Based on the adsorption of nitrogen on a wide range of adsorbents at 77.35 K, the pore of solid material was categorized as micropore (<2 nm), mesopore (2-50 nm), and macropore (>50 nm). The adsorbent which satisfies the above-mentioned criteria includes activated carbon, alumina, silica gel and zeolite, which are commonly used in chemical, biological, and biochemical industries. This technique has been applied for the treatment of water and wastewater for decades. Activated carbon most extensively used adsorbent for the treatment of wastewater.

2.5 Nanotechnology – New Trend in Wastewater Treatment

Nanotechnology is about controlling matter on a molecular and atomic scale. The term “nano” is originated from the Greek word ‘Nanos’ and the meaning of the word is ‘Very Short Man’ According to nanotechnological explanation if any dimension among the three

dimensions (Length, depth and width) has to be less than 100 nanometres, are considered as nanocomponents for its original properties. After the intensified research with the invention of Carbon Nanotubes (CNT), this technology got in attention as a new trend for research. Nanotechnology plays a principal role in every sectors and branch of science [59]. Chemistry plays a dominant appearance by improving molecular behaviour sometimes with individually or making assemble atoms and group of atoms well-balanced with their bonds. Now, this technology has immense uses for wastewater treatment. Researchers are trying to enhance the quality of current technology by inventing unique devices and products. Nanotechnology has a chance to permeate as either an adsorption process or by applying photocatalytic degradation aspect to treat active pharmaceutical drugs concentrated into WWTP in ng to mg level. The important criteria of using nanotechnology and nanomaterials are due to economic values (fewer materials), ease to handle and environmentally friendly (biocompatible).

2.5.1 Nanoadsorbent

The characteristics of nanoparticles have diversity in their size changes. The size of nanoparticles is ranging between 1 to 100 nm in the bulk samples of the equivalent materials. Nanoparticles have properties of larger surface area, detention effects with large scale interaction which aids to modify the new dimension of atomic and macromolecular format. Nanoparticles show the properties of the individual magnetic domain, size petite than wavelength, small mean free path for electron and the optical absorption is immense and selective for metals. Nanoparticles are found in different stratum because of their extensive functions. It improves magnetic recording, catalysis behaviour, advanced conductors, R&D of new materials, sensor devices and so on. By modification of the

surface with nanomaterials or by inclusion with solid materials for creating multiphase where any of the dimensions below 100 nm is known as Nanocomposites. The studies have revealed common nanomaterials are, (1) carbon materials that include graphene materials, carbon nanotubes 1) SWCNTs (single-walled carbon nanotubes) and 2) MWCNTs (multi-walled carbon nanotubes) (2) Nanomaterial based on metal oxide includes nano metal oxides [60]. (3) Nano adsorbents, such as chitosan (4) silsesquioxane based materials

2.5.1.1 Graphene, Graphene Oxide and rGO

Graphene, which possesses properties like, wide specific surface area (SSA) ($2630 \text{ m}^2\text{g}^{-1}$), outstanding mechanical, chemical, and thermal properties, as well as high electrical conductivity and stability, made this nanomaterial popular in various field. Graphene is a 2D structure with sp^2 bond organized in a hexagonal form. Graphene contains enormous surface area, good geometry and chemical stability which will make this material, capable of adsorbent for the remedy purposes in the environment, including the treatment of organic and inorganic type pollutant present in wastewater[61][62].

The Graphene oxide with the thickness of one layer, which was anticipated a century ago is known as Graphene oxide. In the current years, GO (Graphene oxide) has involved excessive apprehension because of the high potential of mass production of graphene. Graphene oxide (GO) is a chemical derivative of graphene having a functional group such as alcohol, epoxy and carboxylic acid which are all oxygen-based functional group. The hydrophilicity and negative charge density will increase with the presence of an oxygen functional group. The typical thickness of the GO (graphene oxide) is ranging from 0.7-1.2 nm, which is much larger in comparison with graphene (0.333nm) due to the existence of an oxygen group on both sides of the layer. The structure of GO is not clear because of

its complex nature. There exist different configuration of oxygen and carbon bonding in the layer of graphene.

rGO possesses low conductive in comparison with original graphene but sufficiently conductive for several uses. rGO is formed by GO reduction using thermal consolidation, and chemical reaction methods. The system of graphite can be remodelled by using a basal plane of rGO which allows adjustment in its regular arrangement by non-covalent π - π stacking or by applying van der Waals interactions. As literature stated that because of its distinctive properties, graphene-based material has been utilised for the adsorption of different classes of antibiotics for decades. The maximum adsorption capacity of different class antibiotics has shown in Table 2 below:

Table 2: Adsorption Capacity of Graphene-Based Material for Different Class of Antibiotics

Nano Adsorbent	Antibiotic	Adsorption conditions	Co (mg/l)	qe (mg/g)	Ref .
GO	Tetracycline(TC)	1g/l,700min, pH 6, 25C	100	456.6	[72]
GO	Tetracycline(TC)	66.66 g/l, 600 min, ph 5,35 C	50	106.60	[73]
Graphene	Tetracycline(TC)	1g/l, ph 8,20C,24 h	300	290.70	[71]
GO	Tetracycline(TC)	pH 3.6,25 C, overnight	8.33-333.33	313.48	[68]
GO	Oxytetracycline(OTC)	pH 3.6,25 C, overnight	8.33-333.33	212.31	[68]
GO	Doxycycline (DC)	pH 3.6,25 C, overnight	8.33-333.33	398.41	[68]
GO	Sulfamethoxazole (SMX)	10 mg ,pH4.0 , 30 min, 25C	50	21.33	[77]
GO	Ciprofloxacin (CIP)	50mg, pH 7.0,50min ,25C	5	18.65	[78]
GO	Norfloxacin (NOR)	50mg, pH 7.0,50min ,25C	5	24.93	[78]
rGO	Tetracycline(TC)	70 g/l, ph 4, 25C, 24h	10-100	1233.26	[70]
rGO/magnetite	Ciprofloxacin (CIP)	pH6.2,25C	1-10	18.22	[69]
rGO/magnetite	Norfloxacin (NOR)	pH6.2,25C	1-10	22.20	[69]

2.5.1.2 Carbon Nanotubes

The new arrangement of carbon formed by using the arc-discharge method is known as MWCNTs (multi-walled carbon nanotubes) [63]. He discovered SWCNTs (single-walled carbon nanotubes) only after two years [64]. SCNTs are cylindrical in shape with diameter approximately 0.4-2 nm [73,74]. MCNTs are having a concentric cylindrical shape with inner layer spacing of 0.34 nm and diameter is ranging from 2 to 25 nm [65]. The specific surface of these carbon tubes is ranging from 123.5 m²/g (MCNTs) to 410.7 m²/g (SCNTs). The pore volume and pore diameter of MWCNTs is 0.59 cm³/g and 0.713 nm. The length of SCNTs and MCNTs are ranging from several micrometres to several centimetres. CNTs have been considered as the most anisotropic material ever produced because their aspect ratio commonly exceeds 10,000.

Studies on removal of ciprofloxacin (CIP), Tetracycline (TC), sulfamethoxazole (SMX), Norfloxacin (NOR), and Oxytetracycline (OTC) in an aquatic system, by carbon nanotubes, is shown below in Table 3.

Table 3: Adsorption Capacity of Carbon Nanotubes for Different Class of Antibiotics

Nano Absorbent	Antibiotic	Adsorption conditions	Co (mg/l)	qe (mg/g)	Ref.
MWCNTS	Tetracycline (TC)	12 mg,35 C,24h, pH 4	20	494.91	[83]
MWCNTS	Tetracycline (TC)	8 mg, pH 7.0, 20C	25-50	307	[75]
MWCNTS	Tetracycline (TC)	pH 3-9, 25C	1-200	54.15	[91]
MWCNTS	Oxytetracycline (OTC)	pH 6.7-7, 25C	-	554	[81]
MWCNTS	Tetracycline hydrochloride (TCH)	pH 3-9,25 C	1-200	291.57	[91]
SWCNTS	Ciprofloxacin (CIP)	pH67.7, 25C	-	933.8	[80]
MWCNTS	Ciprofloxacin (CIP)	pH5.0, 25C	10	135	[74]
MWCNTS	Sulfamethoxazole (SMX)	pH 5.6	-	68.5	[80]
MWCNTS	Norfloxacin (NOR)	0.05g ,pH7.0, 15C	20-100	87	[82]
MWCNTS	Oxytetracycline (OTC)	pH 3-9, 25 C	1-200	39.34	[91]

2.5.1.3 Activated Carbon

The activated carbon is a carbon material with a huge volume of micropores, high specific area of surface, constructive distribution of pore size, and high capacity of adsorption [66].

In the present time, AC (activated carbon) is a generally used adsorptive material for the treatment of wastewater as well as water at an industrial scale. There is two-stage method is used to produce AC (activated carbon) namely carbonization and activation. The carbonization step helps to minimize the volatile matter of the material by the pyrolysis process taking place at 400-850 °C, release non-carbon matter mostly hydrogen, nitrogen, oxygen gases, and tar. This step helps to release all the non-carbon content, but still, the material is low on surface area and porosity. So, the second step called activation help to

improve further porosity and high specific surface area of solid material known as activated carbon[67]. The activated carbon is established to be the most effective adsorbent for the removal of an organic compound from wastewater including pharmaceutical drugs like antibiotics. Findings on the removal of antibiotics like ciprofloxacin (CIP), Tetracycline (TC), sulfamethoxazole (SMX), Norfloxacin (NOR), and Oxytetracycline (OTC) in the aquatic system, by Activated Carbon, is shown below in Table 4.

Table 4: Adsorption Capacity of Activated Carbon for Different Class of Antibiotics

Nano Adsorbent	Antibiotic	Adsorption conditions	Co (mg/l)	qe (mg/g)	Ref.
AC	Tetracycline (TC)	0.07g, 5days (120H), pH 4-11	15-300	288.3	[84]
AC	Tetracycline (TC)	24 g/l, 1-day (24h), 25 C pH -7	50-300	455	[85]
AC	Tetracycline (TC)	1 g/l ,3 h, pH 3-10	250-800	455.8	[86]
AC	Tetracycline (TC)	5 h,45C, pH3-11	50-300	344.8	[80]
AC	Tetracycline (TC)	10 mg, 25 C. neutral pH	200-400	500	[87]
AC	Tetracycline (TC)	25-45C,12 h, neutral pH	40-280	418.18	[90]
AC	Tetracycline (TC)	0.1 g, pH4-5, 25C	100-1000	471.1	[92]
AC	Tetracycline (TC)	0.2 g, 25 C, 24h	400	1030.05	[93]
AC	Doxycycline(DC)	0.2 g, 25 C, 24h	400	922.93	[93]
AC	Chlortetracycline (CTC)	0.1 g, pH4-5, 25C	100-1000	309.9	[92]
AC	Oxytetracycline (OTC)	0.1 g, pH4-5, 25C	100-1000	413.2	[92]
AC	Ciprofloxacin (CIP)	pH5.0, 25C	10	231	[74]
AC	Sulfamethoxazole(SMX)	10 mg , pH6.0, 20C,48h	40	93.5	[76]
AC	Norfloxacin (NOR)	8 mg, pH 7.0 25C 0-48 h	1	237	[79]
AC	Ciprofloxacin (CIP)	8 mg, pH 7.0 25C 0-48 h	1	289	[79]
AC	Norfloxacin (NOR)	4 g/l,pH2-10,10 min-24h,25-35 C	1-10	7.25	[88]
AC	Sulfamethoxazole(SMX)	0.025-0.1 g/lpH2-10,4-24h,	2-16	217	[89]

2.6 Research Gap

Adsorption technique is well established in wastewater treatment plants due to advantages such as, but not limited to, easy handling, better proficiency, simple structure and most importantly, highly economic. Several adsorbents were earlier examined for the elimination of pollutants from wastewater such as carbon nanotubes, graphene, graphene oxide, graphene oxide/magnesium oxide, coal fly ash synthesized zeolite, Palm shell activated carbon, agriculture waste activated carbon.

Among the above of mentioned nano- adsorbent, the activated carbon is considered as most successful adsorbent for the removal of organic pollutants. This is due to its high surface area, high thermal stability, and adsorption capacity Graphene oxide (GO) is a single layer sheet with a thickness equal to one carbon atom. Owing to its distinctive composition, GO is considered as the best endorsing materials in the majority of carbon composite like; graphene nano-sheets, graphene/multi-walled carbon nanotube, single-wall carbon nanotubes etc. Consequently, benefits of AC like high surface area, high thermal stability and adsorption capacity can be coupled with GO, for minimizing the cost of composite nano adsorbent (AC-GO) and could possess high adsorption performance. Nevertheless, before this thesis work, no investigation results have been reported on the conjugation of activated carbon-graphene oxide (AC-GO) for the removal of antibiotics. Adsorption of antibiotics namely, tetracycline and doxycycline using nano adsorbent composite (AC-GO) is promising and may deliver an alternative technique for the removal of pharmaceutical contaminant from wastewater.

CHAPTER 3: METHODOLOGY AND EXPERIMENTAL SETUP

3.1 Material

Chemicals used for the synthesis of nonabsorbent GO (graphene oxide) were: Graphite powder, Sodium nitrate (NaNO_3), Sulfuric acid (H_2SO_4), Potassium permanganate (KMnO_4), Hydrogen chloride (HCl), Deionized water (DI). Chemicals used for the synthesis of nonabsorbent AC-GO (activated carbon -Graphene Oxide) were: Graphene oxide (GO), m-AC (milled activated carbon), Ethanol ($\text{C}_2\text{H}_5\text{OH}$), TEOS (tetraethyl orthosilicate- $\text{SiC}_8\text{H}_2\text{O}_4$), Deionized water (DI). These salts were all obtained from Sigma-Aldrich and were used as collected. All chemicals were of analytical grade.

3.1.1 Weighing Scale

An analytical type of weighing scale was used in this work. The analytical balance (Model No. PW 214) Figure 8 was used to precisely weighing the required amount of chemicals as per the experimental aim. The balance was provided by Adam Equipment.



Figure 9: Weighing Scale

3.1.2 Mixing Tool

A high-speed stirrer was used throughout the experiments. It was incorporated in this work for different purposes. It was used to rapidly mix the nano adsorbent (GO, AC-GO) solution while it was mixed to make sure the solution was homogenous.



Figure 10: Mechanical Mixing Tool

3.2 Experimental Setup

3.2.1 Conical Flask (100 ml)

A conical flask of capacity 100 ml was utilized to prepare the solution of desired concentration by mixing adsorbate and denoised water (DI).

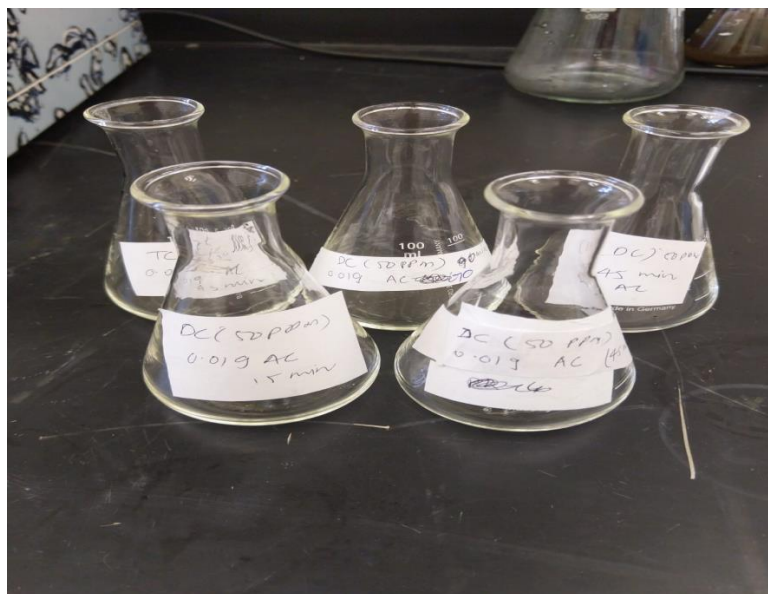


Figure 11: Conical Flask (100ml)

3.2.2 Incubator Shaker

Incubators shaker 10L, the incubator was used to shake solution prepared with the addition of adsorbent and adsorbate. This equipment is manufactured by a benchmark scientific company with a timer range of 1 min to 48 hours or continuous. The shaker is provided with speed increments of 1 rpm. The shaking speed is ranging from 30-300 rpm. The range of temperature is laying between ambient to 60°C. The diameter of orbit is 19 millimetre and the platform size 452 mm x 452mm. This unit is ideal for a variety of incubation applications including culture flask, Petri dishes and staining trays. The equipment is well versed with heat distribution technology which ensures accurate and consistent uniformity.



Figure 12: Incubator Shaker

3.2.3 Vacuum Gas Pump

A vacuum gas pump was utilized to filter the sample of Tetracycline (TC) and Doxycycline (DC) after shaking the solution for desired time.



Figure 13: Vacuum Gas Pump

3.2.4 Vacuum Gas Pump With Beaker and Funnel

The vacuum gas pump is connected with a beaker and funnel as shown in Figure13, below used to filter solution using filter paper. After filtration, the sample is analyzed through equipment called UV-Vis (Ultraviolet-visible)

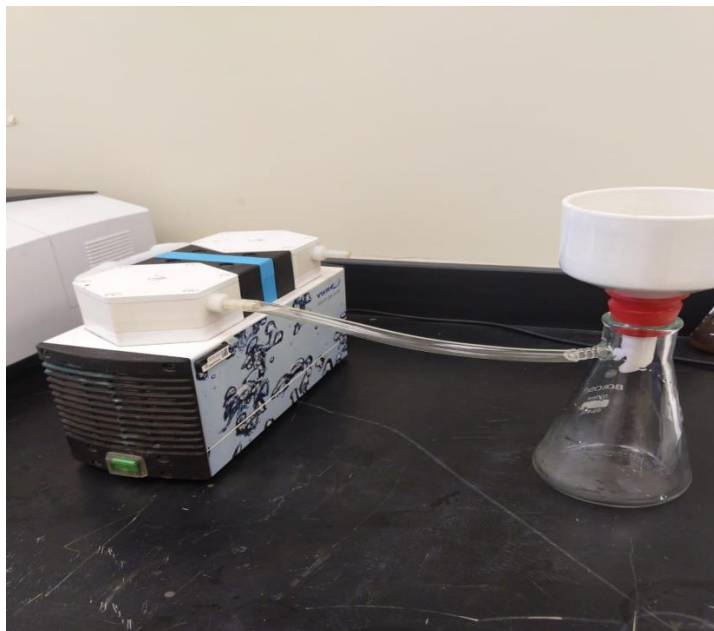


Figure 14: Vacuum Gas Pump with Beaker and Funnel

3.2.5 Ultraviolet-Visible (UV-Vis) Apparatus

The apparatus UV-Vis is known as absorption spectroscopy used to analyze the solution after adsorption of Tetracycline and Doxycycline based onto nano adsorbent. These analyzers use ion-selective electrodes, UV-Vis absorption, turbidometry as an analytical technique in one integrated machine [96]. The study of this spectroscopy is entirely based on the response of light. When a portion of the light passes through a sample, the elements of the sample container absorb some light, and the remainder will pass through the sample as transmission laws. So, let's consider the portion of light enter into the spectroscopy as (I_0) and the intensity of light using for excitation is (I_1). So, the percentage of transmittance

can be expressed as, % of transmittance (By using this equation absorbance (A) can be write down in terms of transmittance can be expressed as,

$$\% \text{ of transmittance } (\% T) = \left(\frac{I_0}{I_1} \right) * 100 \quad [17]$$

By using this equation absorbance (A) can be write down in terms of transmittance,

$$A = -\log T \quad [18]$$

Generally, UV-Vis covers the range of wavelength between (190 – 700) nm or it can vary with modern modification of machine. In this experiment, modern UV-Vis was used with a range of (190-800) nm. This machine can analyze one of the most important principles for adsorption is the “Beer-Lambert Law”. This law states that, if a solution is ideal, absorbance and concentration will possess a linear relationship by keeping the path length constant.

$$A = \epsilon * l * c \quad [19]$$

Where ϵ is the absorptivity of Substance, l is the Path Length and C is the Concentration.

Here, Figure14 illustrates the schematic diagram of UV-vis spectroscopy.

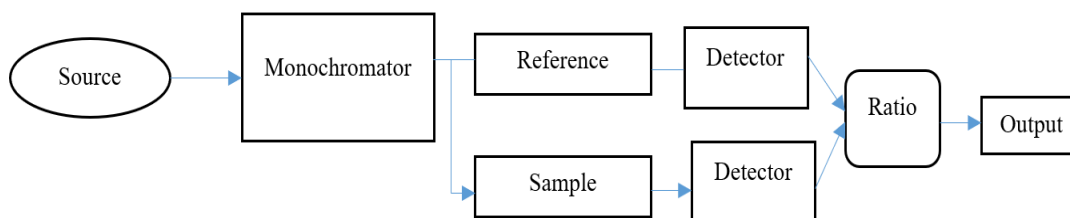


Figure 15: Schematic Diagram of UV-Vis

There are different types of visible sample container are available known as Cuvettes. Cuvettes are available commercially either Quartz or optical glass. According to the condition of this experiment purposes, using optical cuvettes for the absorbance of

transmitting light needed (both are above 300 nm) to measure the absorbance of organic Chemicals (Tetracycline and Doxycycline). Here SHIMADZU UV-1900i UV-Vis spectrometer was used for determining the concentration variation analysis of antibiotics.



Figure 16: UV-Vis Equipment

3.3 Nano Adsorbent Synthesis

3.3.1 Nano adsorbent Activated Carbon (AC)

Commercial grade powdered activated carbon (PAC) was purchased from Sigma-Aldrich and was used as received for an experiment.

3.3.2 Nano Adsorbent Graphene Oxide (GO) Synthesis

Preparation of GO was performed by using modified Hummer's method [94][95]. In a beaker, mix graphite powder (5 g), Sodium nitrate (2.5 g), and Sulfuric acid (115 ml). Keep solution on a mechanical stirrer for around 2 hours for mixing at room temperature. After 2 hours keep the solution in an ice bath to maintain the temperature below 20°C (\approx 15°C). With the help of a thermometer keep checking the temperature. Start adding potassium

permanganate (20 g) very slowly while keeping the temperature lower than 20°C. It took nearly one hour for the slow addition of potassium permanganate and then the solution was kept for one more hour on a mechanical stirrer for mixing. The next step was followed by replacing cold water with warm water to increase solution temperature and slow addition of deionized water (230 ml). Keep stirring manually while adding DI water to the solution. This step took one hour and then the solution was kept an additional one hour on a mechanical stirrer for mixing. After 2 hours, add DI (250 ml) slowly and solution colour changes to orange from dark brown and synthesis of GO was complete. The resulting solution was kept overnight and decanted the next day. After that, the mixture was washed repeatedly with 10% HCl and DI water several times until it reaches neutral pH. Finally, the resulting gel-like structure was kept in the freezer overnight and then vacuum freeze at -40°C to GO Powder.

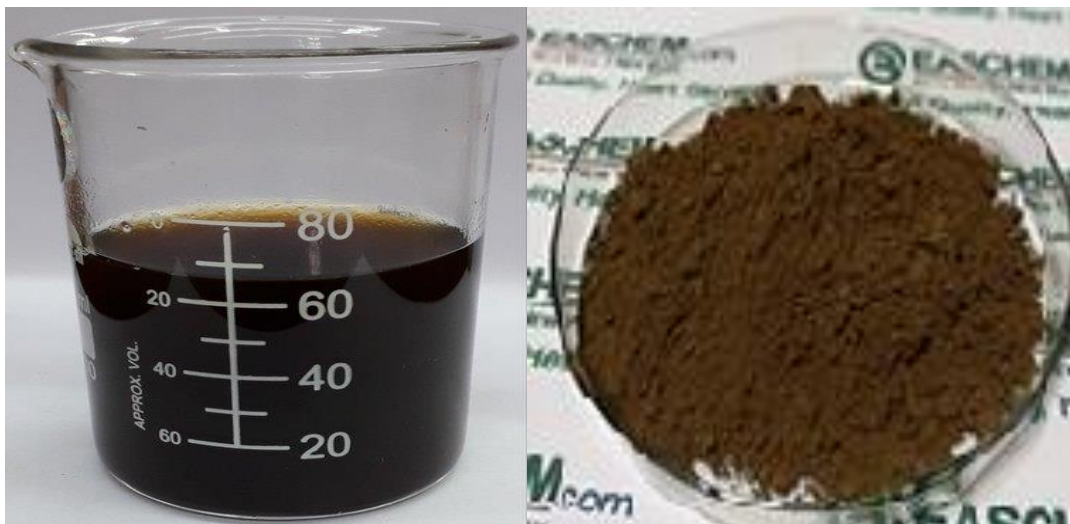


Figure 17: Images of synthesized GO Solution and GO Powder.

3.3.3 Nano Adsorbent Composite Activated carbon-Graphene oxide (AC-GO)

Synthesis

Firstly, graphene oxide (1 g) was added to deionized water (5L) followed by the addition of ethanol (50ml), and tetraethyl orthosilicate (TEOS) of (5ml) at room temperature. In the next step, m-AC (activated carbon) (1.25g) was added to the solution and kept on a mechanical stirrer while slowly increasing the solution temperature to 50°C for 24 h, where the ratio of material in solution kept to (GO: m-AC: TEOS) is approximately (1:1.25:5g). The coupling reaction of solution progress over two-phase 1) hydrolysis reaction of Si (OET)₄ to Si (OH)₄. 2) Condensation reaction was taken place by evaporation of water from the effective group of GO and m-AC and the hydroxyl group of Si(OH)₄ to form the (GO-O-Si-O-AC) composite. The resulted solution of the composite of AC-GO was taken off from the mechanical stirrer and kept for settling. The overabundance of water was eliminated by the decantation method. In the next step, to remove excess TEOS, the solution was cleaned with DI water and then kept for drying in a vacuum oven at 60°C for 72h [95].

3.4 Nano Adsorbent Characterization

The synthesized nano adsorbent and nano adsorbent composite were characterized by various methods such as X-ray diffraction, Scanning electron microscopy, Transmission electron microscopy, Energy Dispersive X-ray spectroscopy, Fourier transform electron microscopy and Branner Emmett Teller. These characterization techniques are discussed in detail in the following section.

3.4.1 X-Ray Diffraction

In this experiment, Rigaku mini flex X-ray diffractometer was used to characterize nano adsorbent AC, GO and AC-GO. This equipment has high precision vertical θ - θ goniometer

and able to handle huge sample than conventional equipment. The eq...equipment is having a goniometer radius of 150mm. The equipment features include scanning range - 3° - 145° , positioning speed $500^{\circ}/\text{min}(2\theta)$, scanning speed 0.01 - $100^{\circ}/\text{min}$, datum angel $2\theta=10^{\circ}$, and X-ray takeoff angle 6° fixed. In addition to qualitative and quantitative, the instrument able to perform a degree of crystallinity calculations, crystalline size, and crystalline strain calculator. The parallel beam optical system with a built poly carpellary unit is available to further expand the range of application. In an X-ray Diffraction experiment, a sample is placed at the centre of an instrument and illuminated with a beam of X-rays. The X-ray tube and detector move in a synchronized motion. The signal coming from the sample is recorded and graphed, where peaks are observed related to the atomic structure of the sample.



Figure 18: X-Ray Diffraction Equipment

3.4.2 Scanning Electron Microscope

SEM, Philips model XL30E, USA is a high-resolution machine that was used to analyze the surface topography of nano adsorbent AC, GO, and AC-GO. The scanning electron

microscope is an instrument that produces sample images by scanning the surface of the sample with a focused beam of an electron. Atoms of sample get interacted with an electron beam and creating numerous signal that comprises information about the topography of surface and composition of the sample.

3.4.3 Transmission Electron Microscopy

Transmission electron microscopy series HT7800 manufactured by Hitachi was used to characterize the nano adsorbent of an experiment. TEM is an instrument based on electron microscopy where a beam of an electron is passed through an ultra-thin specimen and creating and magnifies images through the interaction of the sample with electron. The image is focused on an imaging device that is made by photographic film and images are detected through a sensor functioning as a CCD camera. TEM provides the 2D-Projection image of the 3D structure.

3.4.4 Fourier Transform Infrared Spectroscopy

FTIR series manufactured by Thermo scientific was used for characterization of the nano adsorbent prepared for an experiment. Fourier transformed infrared technique helps to differentiate unknown material in a non-destructive way. This instrument is using infrared spectrum to categorize solid, liquid, or gas surface by adsorption. FTIR coupled with Michelson interferometer to determine the fingerprint of a sample. When an infrared source passes through between the bonds of atoms in a sample, the frequencies of vibrations of specific atoms will express into wavenumbers with a transmittance of absorbance signal.



Figure 19: Fourier Transform Infrared Spectroscopy Equipment

3.4.5 Energy Dispersive X-ray Spectroscopy

EDX is a systematic tool employed for the elemental analysis or chemical characterization of a sample. This technique based on the principle that some source of X-ray excitation interacts with the sample. This instrument based on assumption that each component has a distinctive atomic structure permitting a unique set of peaks on its electromagnetic emission spectrum. EDX analysis was carried to understand the elemental and chemical characteristic of nano adsorbent, GO, and AC-GO.

3.4.6 Brunauer- Emmet -Teller

This theory intends to describe the physical adsorption of a gas particle on a solid surface and provides the base for an essential chemical analysis method for the measurement of the SSA (Specific surface area). The results from this technique commonly mentioned as physical adsorption. The BET method applies to a system of multilayer adsorption and usually utilizes probing gas as Nitrogen which does not interact with the material surface as adsorbate to quantify specific surface area. BET assessment is carried out at the boiling temperature of N_2 (77K) for nano adsorbent AC, GO, and AC-GO.

3.5 Experimental Procedure

The adsorption performance of nonabsorbent Activated carbon (AC), Graphene Oxide (GO), and Activated carbon -Graphene Oxide (AC-GO) for removal of pharmaceutical drugs namely Tetracycline (TC) and Doxycycline (DC) was being investigated in this experimental work. A systematic approach has been incorporated in this work to report different concentration as per experiments requirement.

The following steps have been followed throughout an experiment. A series of a conical flask of capacity 250 ml were used throughout the batch adsorption experiment. A fresh stock solution of 500 mg/l of TC(Tetracycline) and 400 mg/l of DC (Doxycycline)had been prepared by dissolving 500 mg of TC and 400 mg DC in 1L of DI water in the volumetric flask. The batch adsorption experiment was carried out for concentration range of (10,50,100,200,400,500). The conical flask washed properly with DI water and dried properly before use. With the proper dilution of stock solutions (TC, DC), all the conical flask filled with 50 ml with desired concentration and the initial pH recorded of the solution was 4.1 to 4.2. 0.01g of nano adsorbent AC (activated carbon), GO (Graphene Oxide), and AC-GO (Activated Carbon-Graphene oxide) were added to solutions prepared based on tentative experiments and previous studies. Conical flasks were labelled and covered with paraffin film. Solutions were placed in an Incubator shaker at temperature 303 K,313 K, and 323 K with an rpm speed of 200 for 24 h. After 24 h conical flasks were removed from the shaker for filtration. With help of a vacuum gas pump, beaker, funnel and filter paper, solutions were filtered out and analyzed for absorbance of a pharmaceutical drug through UV-Vis at 365 nm for TC and 346 nm for DC.

For the kinetic experiment, 50mg/l and 100 mg/l concentration were used based on a literature review for pharmaceutical drugs TC and DC. In detail, 50ml of TC and DC solution added to a conical flask with the addition of 0.01 g nonabsorbent AC, GO, and AC-GO. The conical flasks were placed in the Incu shaker for a time frame of 2 min to 90 min. Samples were removed from the shaker at appropriate time intervals as mentioned before at 303 K, 313 K, and 323 K. Samples were filtered and evaluated through UV-vis at 365 nm (TC) and 346 nm (DC) same as the batch experiment. To understand the pH effect, 0.1 M HCl and 0.5 M NaOH had been added to the solution of TC and DC of 50 mg/l to adjust the initial pH of the solution (4.1 to 4.2). The pH range of 3 to 10.5 had been tested to analyze how raising and decreasing pH will impact the adsorption capacity of nano adsorbent AC, GO and AC-GO.

To analyze the effect of adsorbent dose on the adsorption process, four different sets of adsorbent dosage had been investigated. The number of adsorbent doses taken was 3 mg, 5 mg, 10 mg, and 15 mg for a concentration of 50 mg/l TC and DC pollutant at a temperature of 303 K for 1h.

3.6 Adsorption Equilibrium:

The utilization of adsorption isotherms is exceptionally valuable to represent the relationship between the adsorbate and the adsorbent for the related process [98]. Modelling of isotherm provides parameter which helps to gather important information to analyze and design adsorption isotherm. There are many adsorption isotherms that have been developed over time, in order to understand the specific system of adsorption in an environmental system. The most common isotherms used for the description of adsorption of tetracycline are listed in Table 6. Langmuir adsorption is based on an assumption of

monolayer adsorption and there is no interaction of molecules with the adjacent site. Freundlich isotherm is assuming that there is multi-layer adsorption is taking place for the adsorption system. In Temkin isotherm, the model assumes that the molecular heat is decreased with coverage increase in the active site of adsorbent and adsorption is characterized by binding energy is distributed uniformly. Elovich model based on the principle that the adsorption process is taking because of the chemical reaction between adsorbate and adsorbent. The Dubinin-Radushkevich equilibrium isotherm was based on the theory that the adsorption process was taking place with a Gaussian energy distribution on a heterogeneous surface. This model helps to find the energy of the adsorption process.

Table 5: Common Equilibrium Isotherm Models Used for Analysis

Isotherm models	Equations	Ref.
Langmuir	$q_e = \frac{q_{max} * K_L * C_e}{1 + K_L * C_e}$	[99]
Freundlich	$q_e = K_F * C_e^{\frac{1}{n}}$	[99]
Temkin	$q_e = \frac{RT}{BT} \ln(KT * C_e)$	[100]
Elovich	$q_e/q_m = K_E * C_e * \exp(-q_e/q_m)$	[100]
Dubinin - Radushkevich	$q_e = q_m * \exp \left[-B \left(R * T * \ln \left(1 + \frac{1}{C_e} \right) \right)^2 \right]$	[102]

Where,

q_e : Adsorption capacity (mg/g)

q_{max} : Maximum monolayer Langmuir adsorption capacity (mg/g)

K_L : Langmuir constant,

C_e : Equilibrium concentration (mg/l)

k_F and n : Freundlich constant

B_T and K_T = Temkin constant

R = Universal gas constant (8.314 J/mol/K)

T = Temperature (K)

q_m = theoretical isotherm saturation capacity (mg/g)

K_E = Elovich isotherm constant

B = Dubinin – Radushkevich isotherm constant

$$q_e = (C_o - C_e) * \frac{V}{1000 * W} \quad [20]$$

$$q_t = (C_o - C_t) * \frac{V}{1000 * W} \quad [21]$$

Where,

C_o = Initial TC and DC concentration (mg/l)

C_e = TC and DC concentration at equilibrium (mg/l)

V = Volume of solution (ml)

W = adsorbent mass in (mg)

C_t = Concentration of TC and DC at different time interval (mg/l)

3.7 Adsorption Kinetics

In order to establish the relationship between the rate of adsorption with the adsorption time, the adsorption kinetic of the whole process was studied. Kinetic models based on chemical reaction have been used to describe the adsorption process. Among these models, the pseudo-first-order, second-order kinetic, Elovich model, and intraparticle diffusion had been employed to describe the adsorption of Tetracycline (TC) and Doxycycline (DC).

The pseudo-first-order model based on the theory that it is not a first-order reaction naturally, but it is made first order by increasing or decreasing the concentration of one or

another reactant. The pseudo-second-order reaction model stated that adsorption capacity is directly proportional to the number of active sites occupied on the adsorbent. The third model used for adsorption kinetic was Elovich which based on assumption that the rate of adsorption of adsorbent decreases exponentially as the amount of adsorbed adsorbent increases and the final model used was intraparticle diffusion, assumed that the adsorption process existed through the diffusion of adsorbate molecule into pores of adsorbent material. The Intraparticle model was described by Weber and Morris. The kinetic isotherms are listed below in Table 14.

Table 6: Common Kinetic Model Used in Analysis

Kinetics models	Equations	Ref.
Pseudo first order	$\ln(q_t - q_e) = \ln(q_e) - K_1 * t$	[101]
Pseudo second order	$\frac{t}{q_t} = \frac{1}{K_2 * q_e} + \frac{t}{q_e}$	[101]
Elovich model	$q_t = \frac{\ln * a_e * b_e}{b_e} + 1 * \ln * \frac{t}{b_e}$	[102]
Intraparticle Diffusion	$q_t = k_{id} * \frac{t^1}{2} + C_i$	[103]

Where,

K_1 : Adsorption rate constant,

t : Adsorption time,

K_2 : Adsorption rate constant,

q_t : capacity at time t ,

a_e : Initial adsorption rate (g/h),

b_e surface coverage and activation energy for chemisorption (g/mg),

qt: adsorption capacity,

qe: Equilibrium capacity,

K_{id} , C_i = Intraparticle diffusion constant

qe and qt are described by the equation given below:

$$q_e = (C_o - C_e) * \frac{V}{1000 * W} \quad [22]$$

$$q_t = (C_o - C_t) * \frac{V}{1000 * W} \quad [23]$$

Where,

C_o = Initial TC and DC concentration (mg/l)

C_e = TC and DC concentration at equilibrium (mg/l)

V= Volume of solution (ml)

W= adsorbent mass in (mg)

C_t = Concentration of TC and DC at different time interval (mg/l)

CHAPTER 4: RESULTS AND DISCUSSION

The objective of the work is to examine the adsorption capacity of several nano adsorbents including AC (Activated Carbon), GO (Graphene Oxide), AC-GO (Activated carbon - Graphene Oxide) for the removal of pharmaceutical drugs under batch operation mode. The selected contaminants are Tetracycline (TC) and Doxycycline (DC). The nano adsorbent namely, AC (commercial powdered activated carbon), synthesized GO and AC-GO, characterized through several techniques includes X-Ray Diffraction (XRD), Scanning Electron microscope (SEM), Transmission Electron Microscopy (TEM), Fourier Transformed Infrared Spectroscopy (FT-IR), Energy Dispersive X-ray Spectroscopy (EDX), Brauner EmmettTeller Analysis (BET).

There are several factors that affect the adsorption equilibrium isotherm process of TC and DC includes: 1) Temperature 2) initial concentration and 3) pH of the solution. For adsorption equilibrium isotherm, numerous isotherms were tested namely, 1) Langmuir 2) Freundlich 3) Temkin 4) Elovich and 5) Dubinin-Radushkevich The factor affecting adsorption kinetics of TC and DC include 1) Effect of contact time. For kinetic adsorption, many isotherms were tested to understand the fitting efficiency of experimental data includes 1) Pseudo first order 2) Pseudo second order and 3) Elovich. Studies on the Intraparticle diffusion model was carried out to understand that, this particular phenomenon was not the only driving force for the adsorption process.

To understand the effect of temperature on the adsorption process, thermodynamics studies were carried out. Comparison of all the three adsorbents (AC, GO, and AC-GO), on contaminant TC and DC, were carried out to understand which adsorbent is having maximum adsorption capacity.

4.1 Characterisation of Nano Adsorbent

4.1.1 X-Ray Diffraction

4.1.1.1. Activated Carbon (AC)

X-ray diffraction profile of activated carbon is given in Figure 19. indicated that AC was a predominantly amorphous structure. Activated carbon exhibited two broad peaks at $2\theta = 26$, and at $2\theta = 40$. The presence of the peak at about 24° , was because of activation temperature (700°C) indicated an improving symmetry of crystalline formation, which will lead to a better layer configuration.

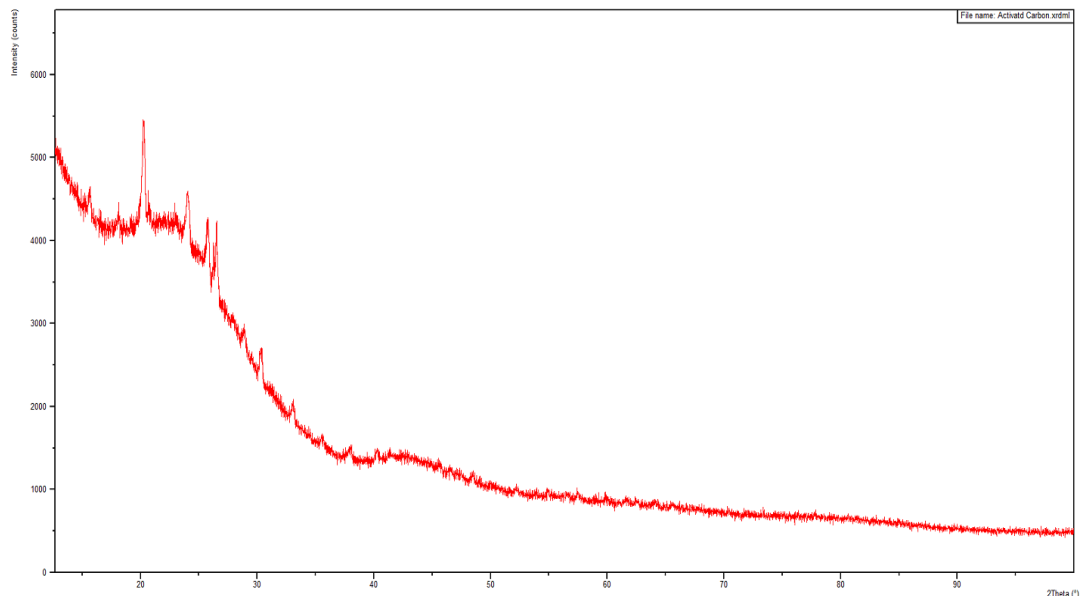


Figure 20: XRD image of Commercial Powdered AC

4.1.1.2. Graphene Oxide (GO)

Oxidation of graphite is a method of adding oxygen groups to the graphite layer. As a result of this process, the force of repulsion between layers increases and space between layers also broaden. The XRD spectra measured in the range of 2θ from 5° to 80° show sharp peak

at $2\theta = 9.98$ for graphene oxide, suggesting the difference between graphene layers and diffraction peak at $2\theta = 42.26$ suggesting a short-range order in the stacked graphene layer.

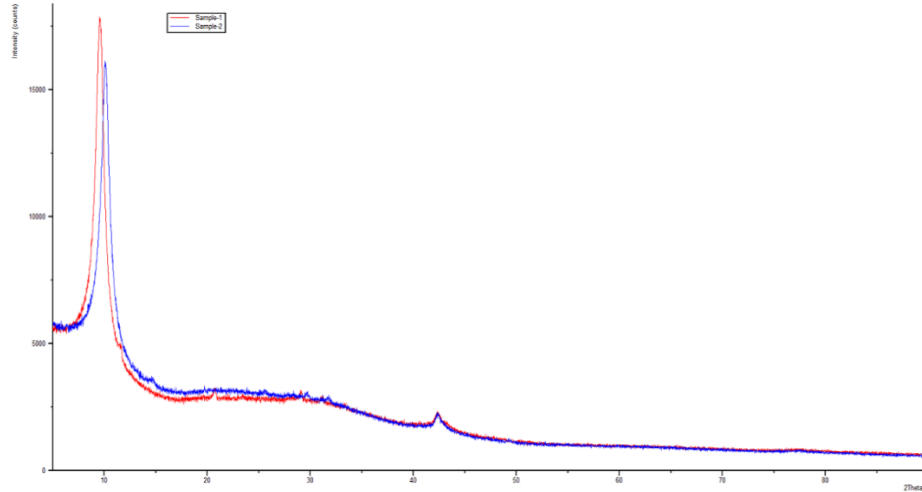


Figure 21: XRD Image of Synthesized Nano adsorbent GO.

4.1.1.3. Activated carbon – Graphene oxide (AC-GO)

The XRD spectra of nano adsorbent composite AC-GO, measured in the range of 2θ from 5° to 80° shows sharp peak at $2\theta = 9.50$. This peak is indicating that the graphene layers are well-organized with an interlayer spacing of 0.93nm. Additionally, the key peak of GO could be used as a sign of the occurrence of extremely planned inter-layered assembly. Furthermore, the XRD pattern of nano adsorbent AC-GO shows a weak wide-ranging peak at $2\theta = 25^\circ$ with three subordinate peaks of milled-AC. Discussed pattern indicating that there is a disappearance of the GO and m-AC peaks and presence of new broad peak could be a sign of formation of the nonabsorbent composite AC-GO[95].

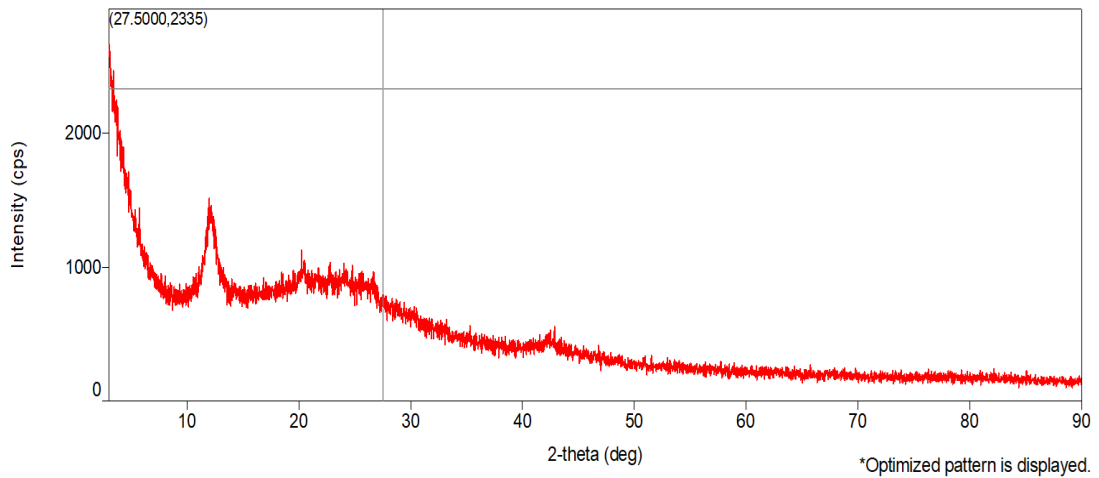
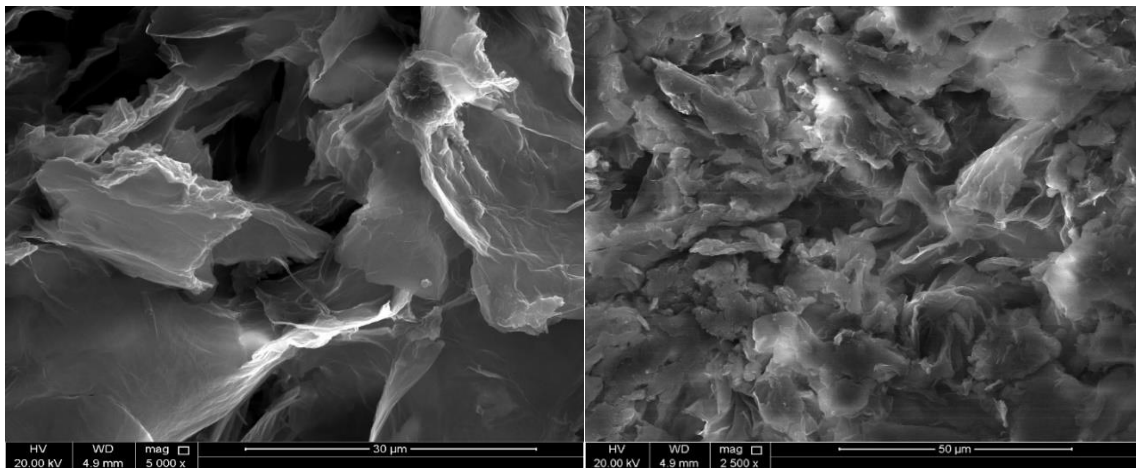


Figure 22: XRD Image of Synthesized Nano adsorbent AC-GO

4.1.2 Scanning Electron microscopy

4.1.2.1 Graphene oxide (GO)

SEM images of GO at different magnifications are presented below in the figure. Images of GO suggesting that graphite is a flake structure while Graphene Oxide possesses monolayer formation. Furthermore, at increased magnification morphology of each layer becomes clearer. Significantly, SEM images representing that, graphite flakes converted to GO monolayer because of the oxidation process.



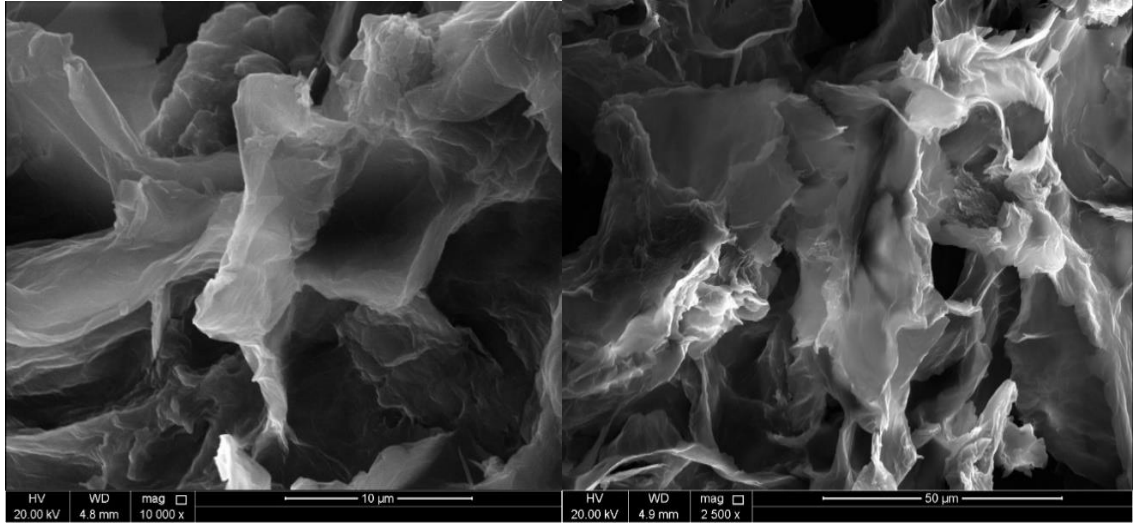
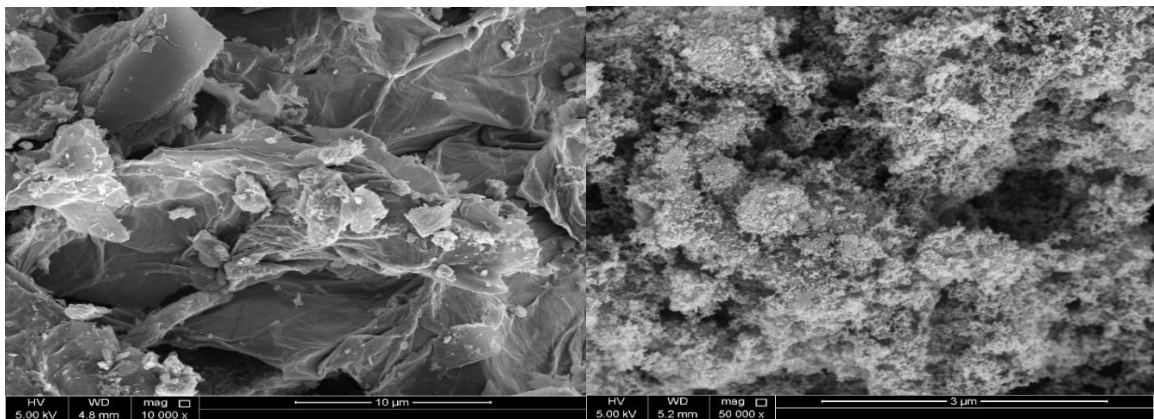


Figure 23: SEM Images of GO at 30μm, 50μm, 10 μm, 50 μm

4.1.2.2 Activated carbon-Graphene oxide (AC-GO)

The synthesized nano adsorbent possesses a flattened type structure of GO single layer and staking of AC particles had been observed on the surface through SEM images. SEM images also suggested that the prepared nano adsorbent composite had a heterogeneous surface structure as well as irregular surface morphology. This type of arrangement possibly indicates that the prepared composite will provide good adsorption and trapping of TC (Tetracycline) and DC (Doxycycline).



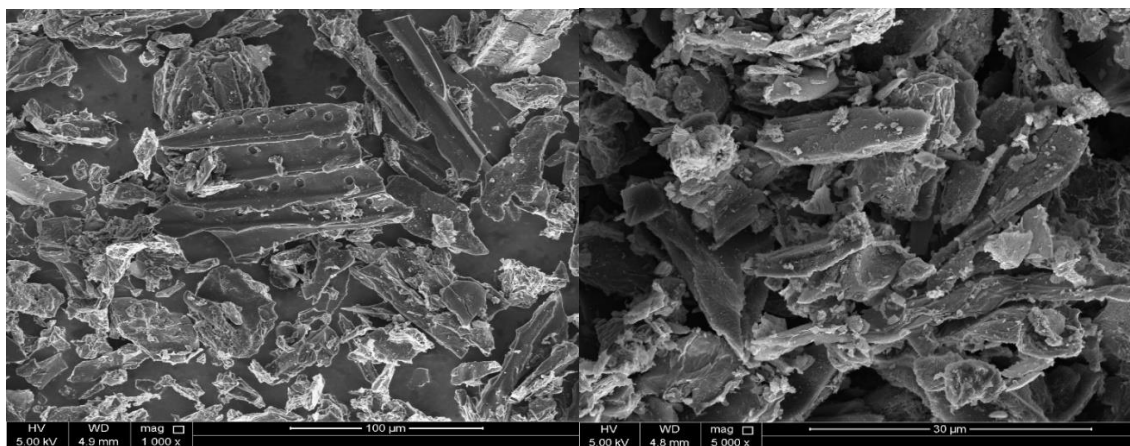


Figure 24: SEM Images of AC-GO at 10 μm, 3 μm, 100 μm, 30 μm

4.1.3 Transmission Electron Microscopy

4.1.3.1. Activated Carbon (AC)

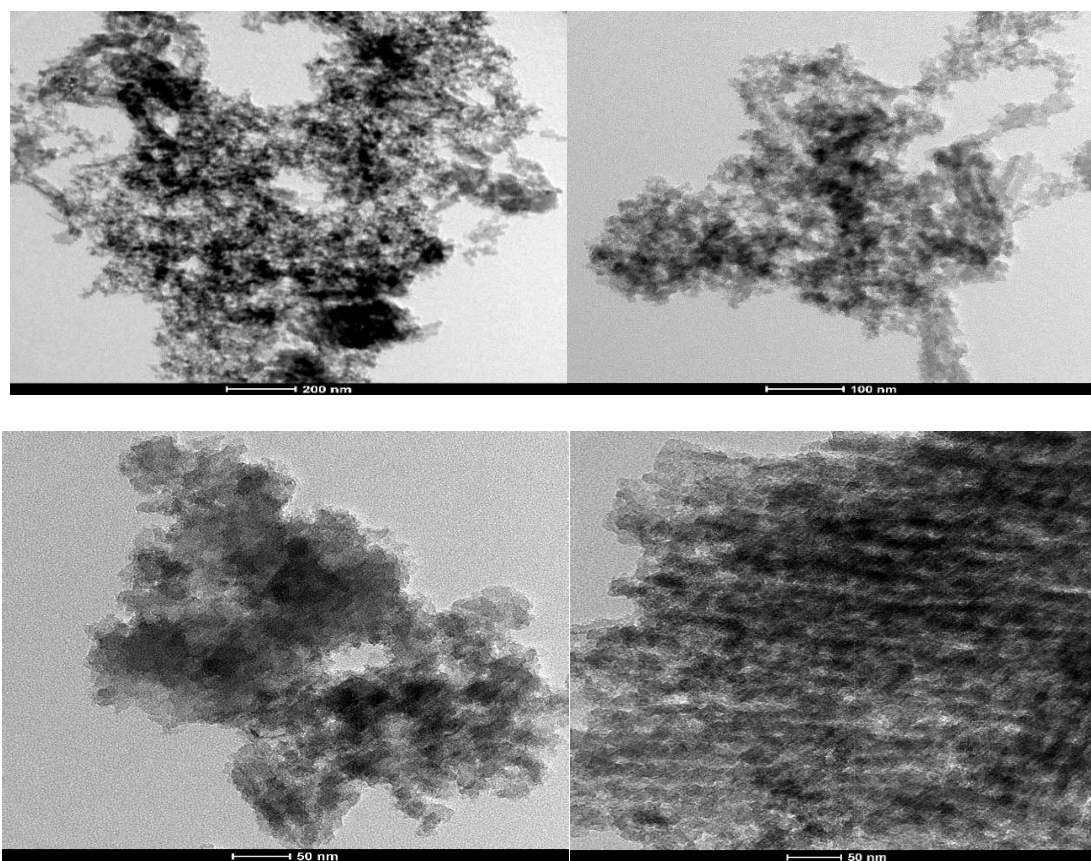


Figure 25: TEM Images of AC at 200nm, 100 nm,50 nm, 50 nm

4.1.3.2. Graphene oxide (GO)

TEM images suggesting GO palates show sheet-like morphology with diverse transparencies of the examined area of about $2 \times 2 \mu\text{m}$ (Scale: $1 \mu\text{m}$). Dark area signifying the stacking of numerous graphene oxide or graphene layer with some oxygen-containing functional group. Transparent areas of images indicating that a very thinner layer of limited graphene oxide is present resulted from stacking of nanomaterial exfoliation.

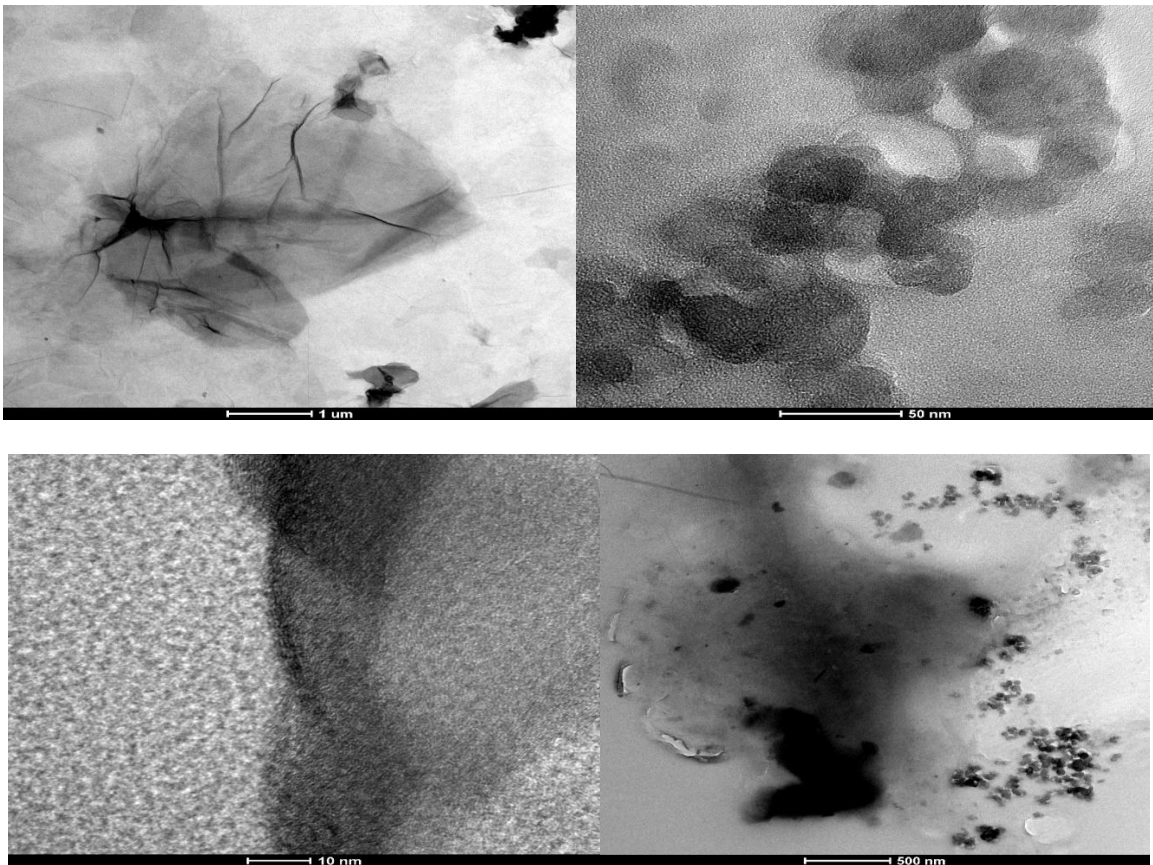


Figure 26: TEM Images of GO at $1 \mu\text{m}$, 50 nm , 10 nm , 500 nm .

4.1.3.3. Activated carbon-Graphene oxide (AC-GO)

TEM images of composite GO-AC were observed dark spots of well-arranged spherical activated carbon particle of the normal size of (65 nm) over the surface of single-layer GO. Images indicating that the prepared nanocomposite was having a sheet-like structure with

a transparent and dark area. The dark coloured area shows the presence of activated carbon particle, while the transparent area is a result of GO.

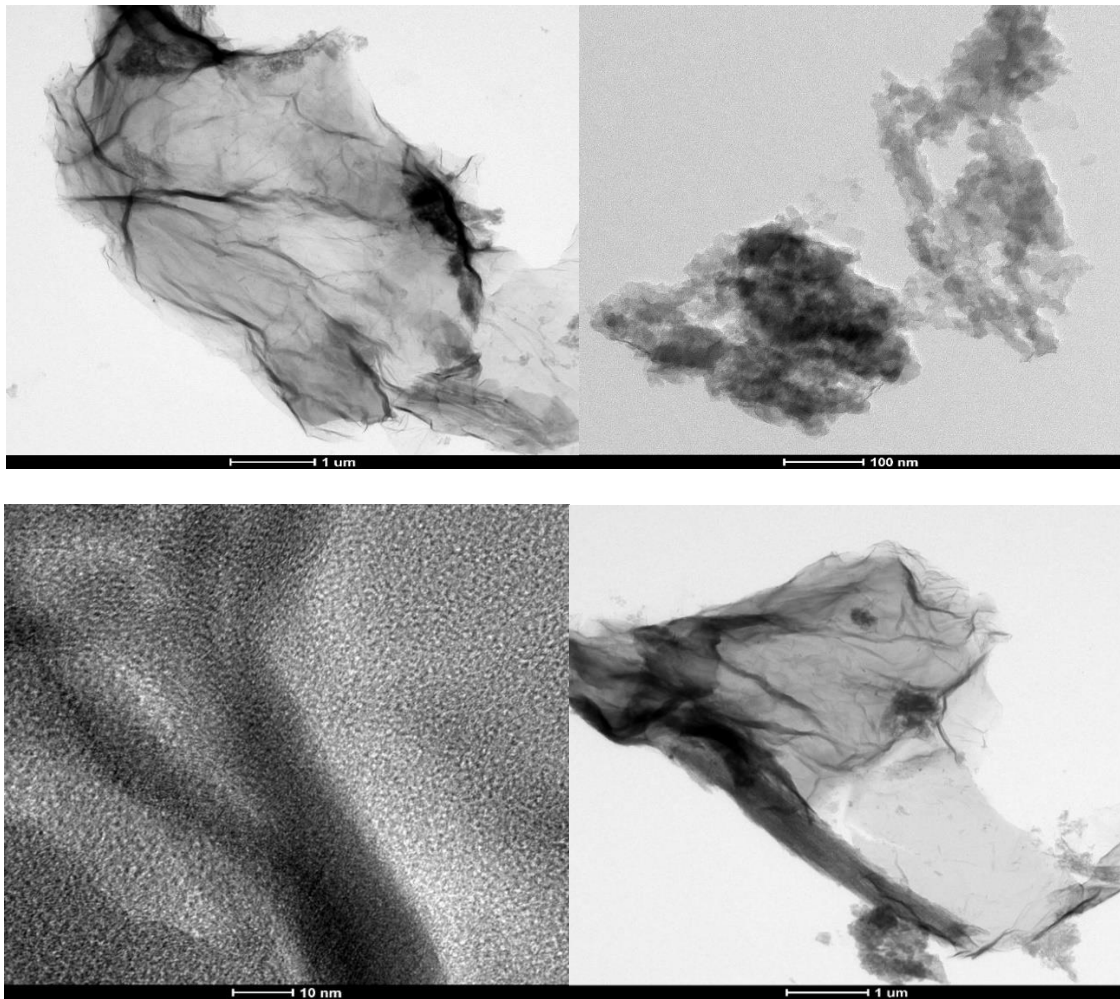


Figure 27: TEM Images of AC-GO at 1 μm, 100 nm, 10 nm, 1 μm

4.1.4 Fourier Transform -Infrared Spectroscopy

4.1.4.1 Activated Carbon (AC)

As shown in Figure 27, below the FTIR spectrum of AC. The AC displays a broad-spectrum peak at 3327cm^{-1} conforming to OH enlarging of water molecule absorbed onto the AC. A peak was observed at 1636cm^{-1} was because of the stretching of carboxylic acid ($\text{C}=\text{O}$), present at AC [95].

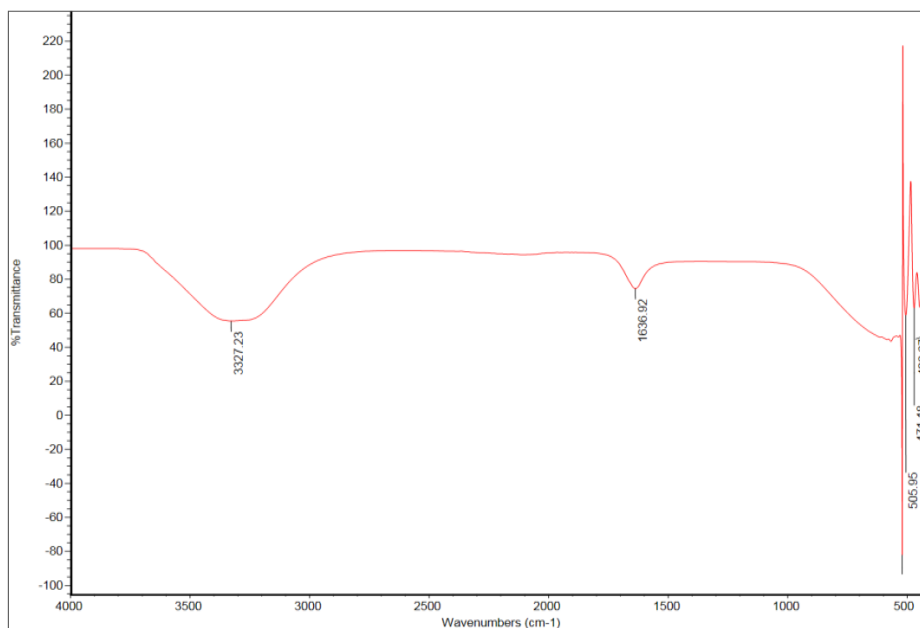


Figure 28: FTIR Image of Nano adsorbent AC

4.1.4.2 Graphene Oxide (GO)

FTIR analysis was carried out to find out which functional groups exist as well as the structure of GO. FTIR spectrum of GO is shown below in Figure 28. The GO displays a broad-spectrum peak at 3397cm^{-1} conforming to C-O stretching of carboxylic acid (C=O), and the O-H group present at GO. Furthermore, a broad-spectrum was observed at 1618cm^{-1} , because of the stretching of an aromatic group (C=C). The absorption peaks at 1108cm^{-1} was related to the enlargement of an epoxy group (C-O) as well as the alkoxy group (C-O). The existence of oxygen attached functional group made sure that the graphite was effectively oxidized to GO [101].

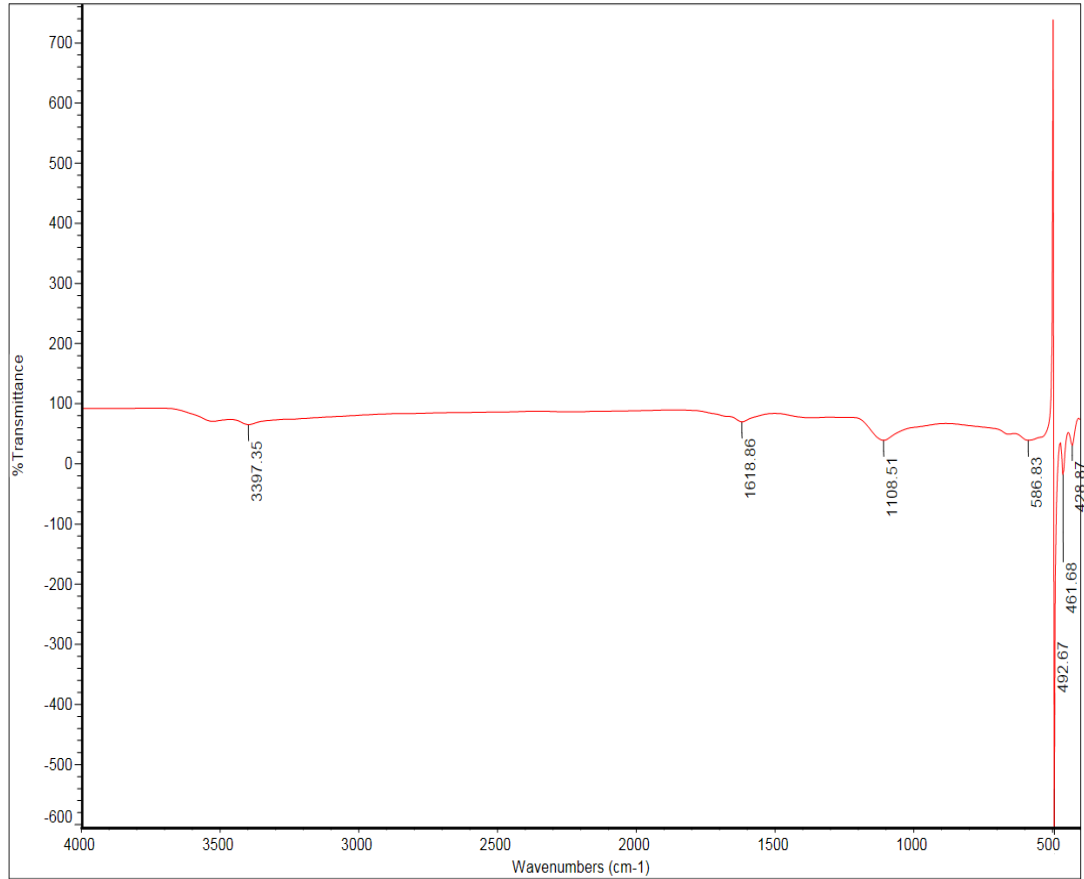


Figure 29: FTIR Image of Nano adsorbent GO

4.1.4.3 Activated carbon-Graphene oxide (AC-GO)

FTIR spectra of the AC-GO composite are shown in Figure 29. their-pattern of the composite show absorption peaks display at 3345, 1664, 1586, and 1068 cm^{-1} correspond to the conjugation between two components namely, GO and m-AC [95]. Remarkably, it is detected that the nano adsorbent composite has shifted bends, while others were disappeared, related to the initial components of the composite. This is the indication the composite GO, and m-AC was connected successfully via the link as shown in the figure.

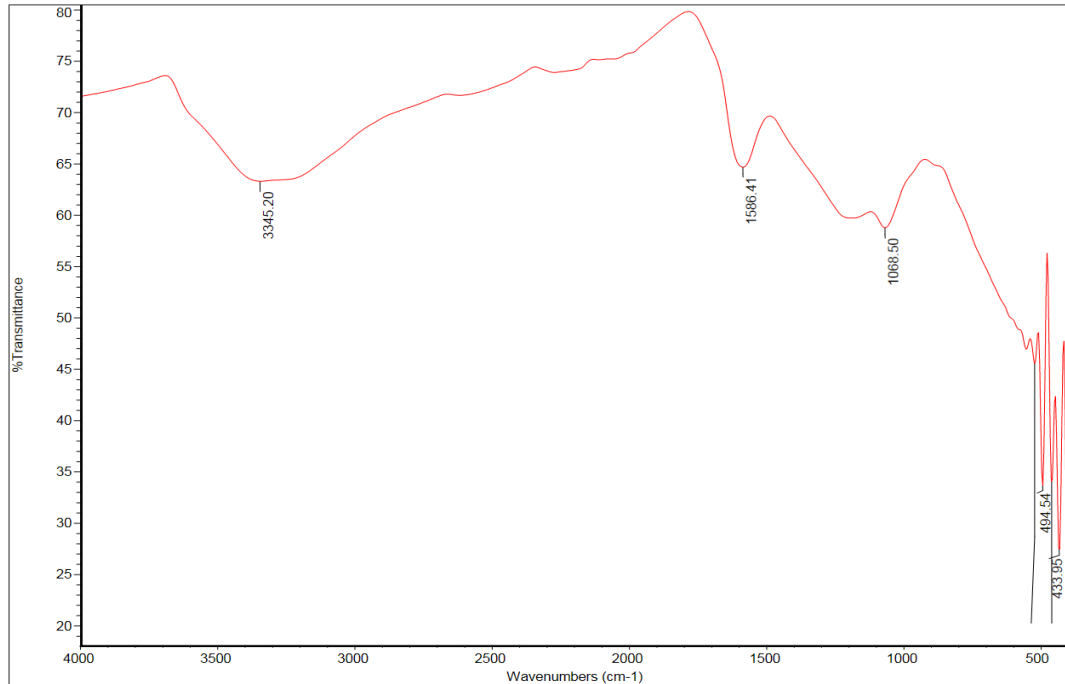
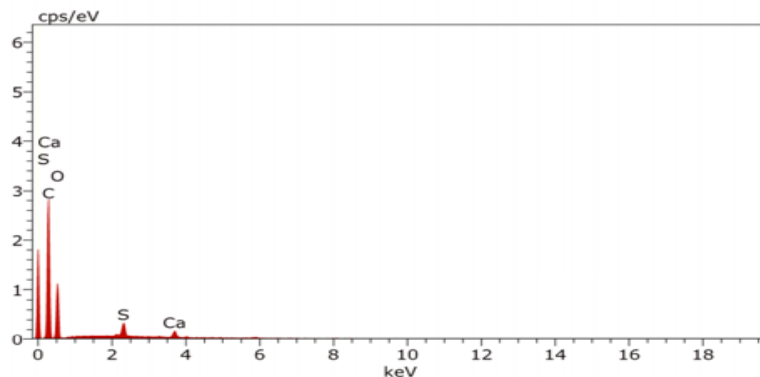


Figure 30: FTIR Image of Nano adsorbent GO

4.1.5 Energy Dispersive X-Ray Spectroscopy

4.1.5.1 Graphene Oxide (GO)

EDX spectrum of GO thin film shows sharp peaks for Carbon, Oxygen, Sulphur, and Calcium. Sulphur was present because of the addition of H_2SO_4 , which was used during the synthesis of GO as an oxidizing agent. While calcium (Ca) was from the substrate. This is an approval that graphene oxide was formed successfully.



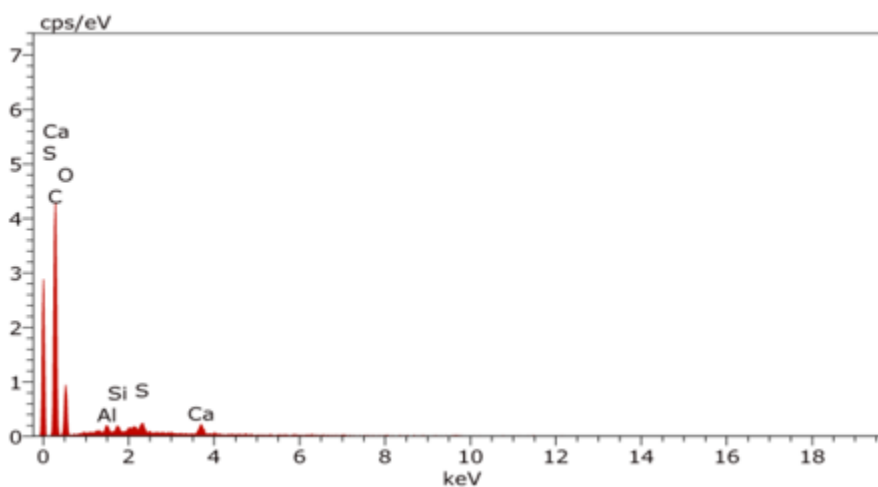
Spectrum: 1.spx

El	AN	Series	unn. C [wt.%]	norm. C [wt.%]	Atom. C [at.%]	Error (1 Sigma) [wt.%]
C	6	K-series	79.04	79.04	83.77	1.98
O	8	K-series	19.95	19.95	15.87	1.18
S	16	K-series	0.52	0.52	0.21	0.05
Ca	20	K-series	0.48	0.48	0.15	0.05
Total:			100.00	100.00	100.00	

Figure 31: EDX Image of GO

4.1.5.2. Activated carbon -Graphen oxide (AC-GO)

EDX spectrum of AC- GO thin film shows sharp peaks for Carbon and Oxygen. Additionally, peaks of Sulphur, Calcium, Silicon, and Aluminum can be observed from EDX images. Sulphur was present because of the addition of GO (H_2SO_4 was used while synthesizing GO as an oxidizing agent) during the synthesis of AC -GO. While Silicon was present because of the addition of tetra orthosilicate ($SiC_8H_2OO_4$). Spectra showed peaks for Aluminum (Al) and Calcium (Ca) were coming from the substrate. The presence of Carbon, Oxygen, Silicon, and Sulphur indicate that a nano adsorbent composite AC-GO was ready to be made.



Spectrum: 1-B.spx

El	AN	Series	unn. C [wt.%]	norm. C [wt.%]	Atom. C [at.%]	Error (1 Sigma) [wt.%]
C	6	K-series	85.53	85.53	89.08	2.95
O	8	K-series	13.52	13.52	10.57	2.81
Al	13	K-series	0.11	0.11	0.05	0.04
Si	14	K-series	0.09	0.09	0.04	0.03
S	16	K-series	0.24	0.24	0.09	0.04
Ca	20	K-series	0.51	0.51	0.16	0.05
Total:			100.00	100.00	100.00	

Figure 32: EDX Image of AC-GO

4.1.6 Brunauer–Emmett–Teller

The findings of specific surface area (SSA) and pore structure of Activated carbon (AC), Graphene Oxide (GO), and Activated carbon -Graphene Oxide (AC-GO) from BET analysis is shown below in Table 5. The Table contains SSA (specific Surface Area m^2/g), Total Pore Volume V_{TOT} (cm^3/g), Volume of micropore V_{micro} (cm^3/g), Volume of mesopore V_{meso} (cm^3/g), and Average pore size L (nm). The average pore size L (nm) of all three adsorbents ranging between 2nm-50nm, means nano adsorbents are mesoporous material [87].

Table 7: BET Analysis of AC, GO, AC-GO

Nano adsorbent	S_{BET} (m^2/g)	V_{TOT} (cm^3/g)	V_{micro} (cm^3/g)	V_{meso} (cm^3/g)	L (nm)
AC	2709.14	2.55	1.203	1.347	10.8
GO	46.52	0.07	0.025	0.045	11.0
AC-GO	1268.60	1.28	0.593	0.687	26.0

4.2 Adsorption Equilibrium

4.2.1 Analyses

Determination of Tetracycline Concentration

Five standard solutions (5,4,3,2,1 mg/L) of Tetracycline (TC) were prepared by dissolving TC powder (≥ 99 wt%, 444.435 g/mol.) into deionized water. Such solutions were then analyzed by a UV-Vis detector at wavelength 365 nm. The UV-Vis absorption of five TC standard solutions was illustrated in Table 7. All the measurements were done in triplicate. The obtained calibration curve had a high correction coefficient $R^2 = 0.9977$ and was used for the TC adsorption experiment

Table 8: Absorption/Concentration Data for Calibration Curve of Tetracycline (TC)

Abs	Concentration (ppm)	Wavelength (nm)
0.20	5	365
0.16	4	365
0.13	3	365
0.11	2	365
0.08	1	365

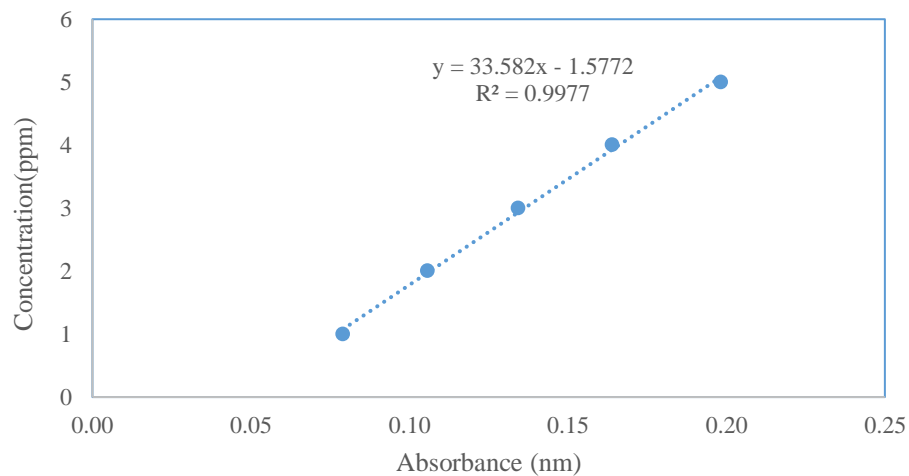


Figure 33: Calibration Curve for Tetracycline (Abs vs Conc)

Determination of Doxycycline Concentration

Five standard solutions (5,4,3,2,1 mg/L) of Doxycycline (DC) were prepared by dissolving DC powder (≥ 99 wt%, 444.435 g/mol.) into deionized water. Such solutions were then analyzed by a UV-Vis detector at 346 nm. The UV absorption of five standard DC solutions is illustrated in Table 8 below. All the measurements were done in triplicate. With a high value of R^2 equals (0.9952), The obtained calibration curve has a high correction coefficient R^2 equals (0.9952) and was applied for the DC adsorption experiments.

Table 9: Absorption/Concentration Data for Calibration Curve of Doxycycline (DC)

ABS (absorption)	Concentration (ppm)	Wavelength (nm)
0.1979	5	346
0.1670	4	346
0.1329	3	346
0.1018	2	346
0.0795	1	346

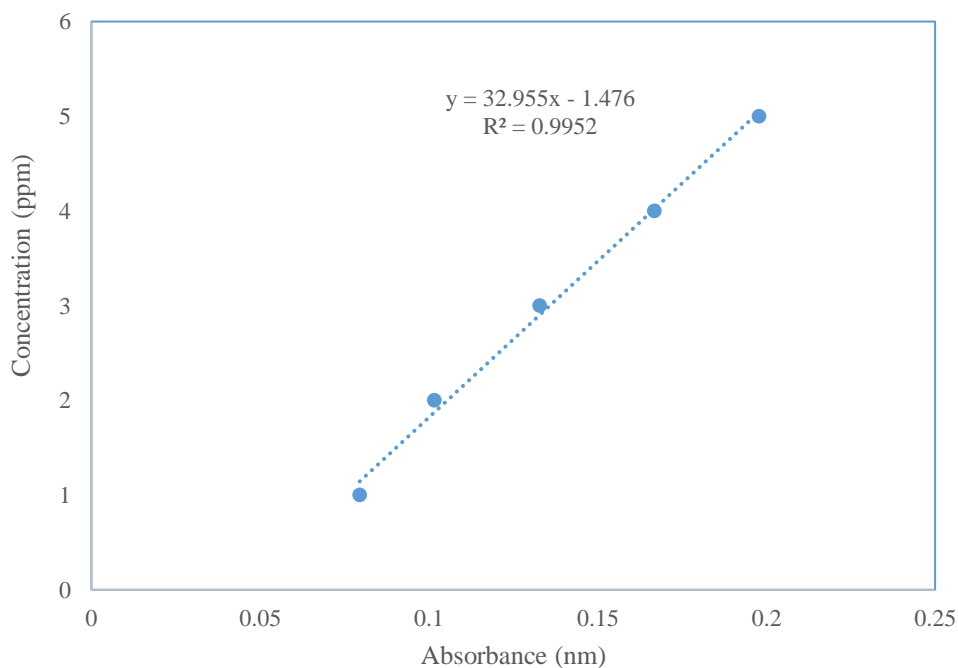


Figure 34: Calibration Curve for Doxycycline (Abs vs Conc)

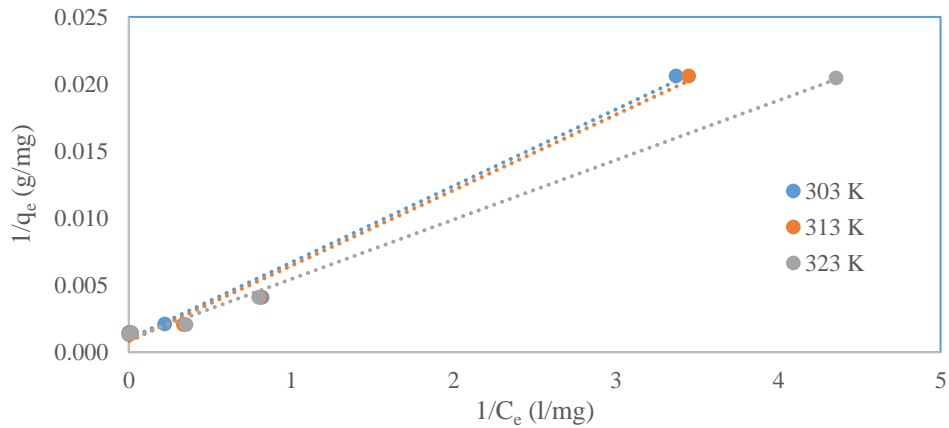
4.2.2 Adsorption of Tetracycline on Activated carbon, Graphene oxide, and Activated carbon-Graphene oxide

4.2.2.1 Effect of Temperature

As a critical environment parameter, temperature influences the adsorption process. A systematic study on the characteristics of the TC adsorption process including isotherms with respect to temperature has been performed in this section. The respective knowledge is important for understanding the mechanisms of TC adsorption by nano adsorbent AC, GO, and AC-GO. The TC adsorption isotherms of AC, GO and AC-GO at 303K, 313K, and 323K are illustrated in Figure(34,35,36). The equilibrium TC adsorption capacities of AC, GO and AC-GO, increased as the temperature was increased, which revealed that the adsorption of TC on AC, GO and AC-GO was an endothermic process. The Langmuir, Freundlich, Temkin, Elovich, and Dubinin – Radushkevich isotherm model [99-102], were analyzed to examine the fitting efficiencies of experimental data with the corresponding isotherms. Among the tested models, Freundlich, Elovich and Dubinin-Radushkevich with lower determination coefficients ($R^2 = 0.730-0.790$) indicated that these isotherms were not justifying the experimental data (Appendix-A) and thus not a good fit. Langmuir and Temkin's isotherms were the best fit for equilibrium data with a high determination coefficient ($R^2 = 0.97-0.94$). The obtained values for q_m , K_L , and $1/K_L q_m$ at 303 K, 313 K, and 323 K were shown in Tables 9- 11. The values of q_{max} and K_L of Langmuir isotherm were increasing with increase in temperature suggested that increasing temperature and increasing initial concentration was conducive for all the three nanoadsorbents. The isotherm model results suggested that adsorption of TC on AC, GO and AC-GO was monolayer adsorption and chemical in nature.

Table 10: Parameters of Adsorption Isotherm Model of TC Adsorption of AC

Temperature (K)		303	313	323
Langmuir	q_{\max} (mg/g)	1024.70	1233.05	1379.31
	K_L (L/mg)	0.124	0.144	0.163
	$1/K_L q_m$	0.007	0.006	0.004
	R^2	0.988	0.989	0.997
Freundlich	kf	5.037	5.091	5.115
	n	3.280	3.250	3.190
	R^2	0.730	0.763	0.739
Temkin	B	87.129	93.717	97.874
	$B \ln A$	235.78	250.42	259.06
	R^2	0.909	0.914	0.939
Elovich	q_m (mg/g)	147.06	158.73	161.13
	K_E	3.86	3.76	4.29
	R^2	0.735	0.735	0.792
Dubinin-Radushkevich	q_m (mg/g)	578.25	607.89	607.89
	Bo	-1.93E-07	-1.80E-07	-1.33E-07
	R^2	0.945	0.935	0.911



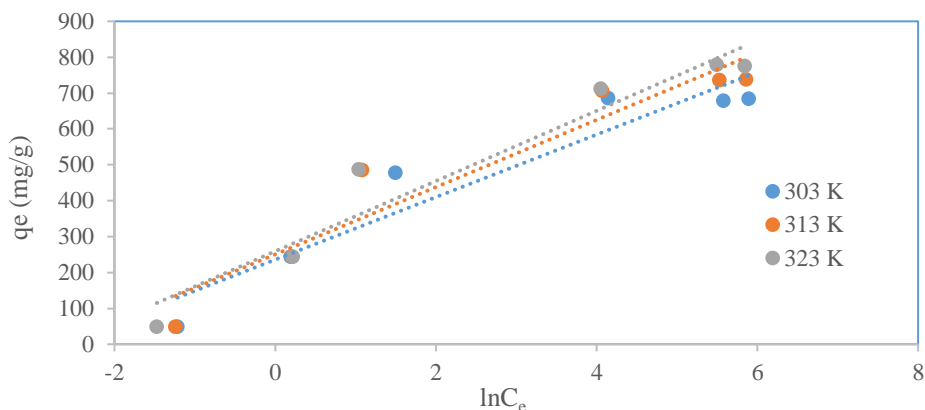


Figure 35: Adsorption Isotherm Langmuir (1) and Temkin (2) of TC on AC

Table 11: Parameters of Adsorption Isotherm Model of TC Adsorption of GO

Temperature (K)		303	313	323
Langmuir	q_{\max} (mg/g)	295.68	344.00	377.22
	K_L (L/mg)	0.037	0.104	0.224
	$1/K_L q_m$	0.090	0.028	0.012
	R^2	0.994	0.992	0.992
Freundlich	kf	3.358	3.818	4.204
	n	2.28	2.72	2.96
	R^2	0.882	0.960	0.950
Temkin	B	62.551	58.219	61.093
	$B \ln A$	36.903	9.201	62.729
	R^2	0.976	0.975	0.990
Elovich	q_m (mg/g)	116.28	93.46	92.59
	K_E	0.16	0.52	1.41
	R^2	0.873	0.979	0.990
Dubinin-Radushkevich	q_m (mg/g)	257.24	270.43	327.01
	B_0	-4.92E-06	-9.72E-07	-.318E-07
	R^2	0.909	0.861	0.879

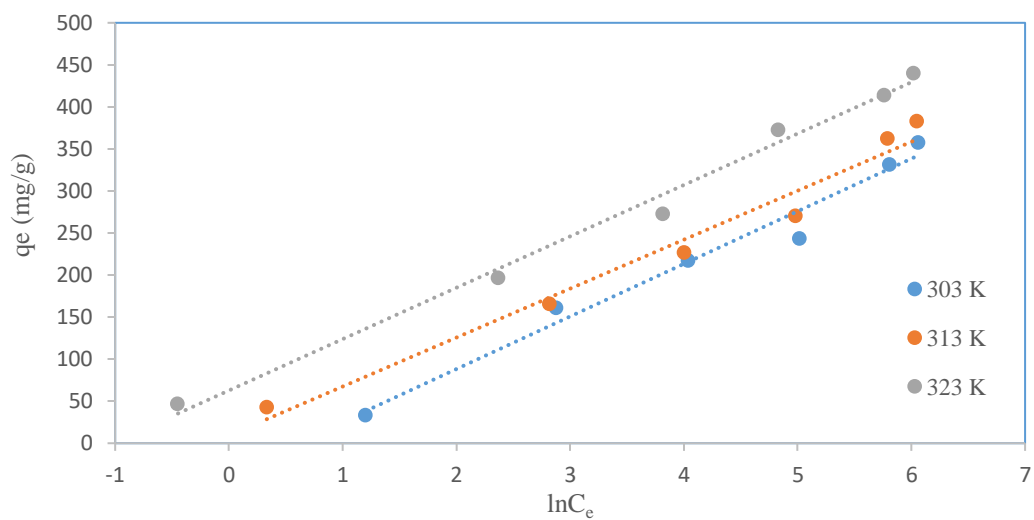
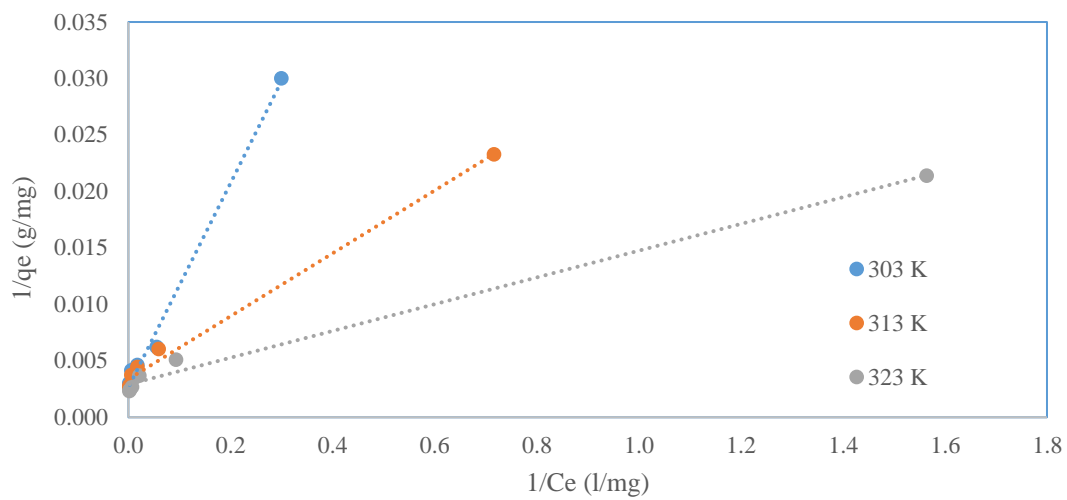
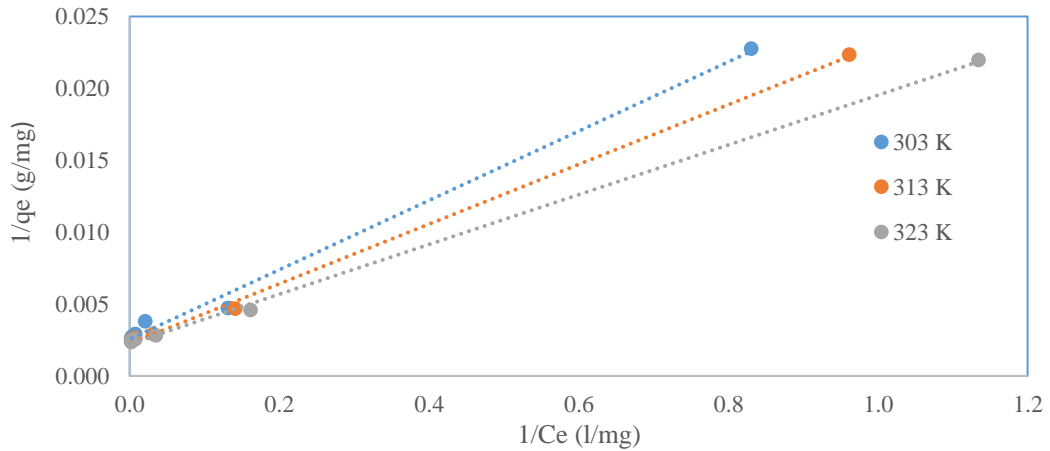


Figure 36: Adsorption Isotherm Langmuir (1) and Temkin (2) of TC on GO

Table 12: Parameters of Adsorption Isotherm Model of TC Adsorption of AC-GO

Temperature (K)		303	313	323
Langmuir	q_{\max} (mg/g)	389.56	443.26	449.64
	K_L (L/mg)	0.101	0.109	0.129
	$1/K_L q_m$	0.024	0.021	0.017
	R^2	0.995	0.998	0.999
Freundlich	kf	4.201	4.362	4.158
	n	3.02	3.11	3.04
	R^2	0.805	0.800	0.835
Temkin	B	55.217	59.470	59.148
	$B \ln A$	60.426	81.587	94.767
	R^2	0.966	0.933	0.927
Elovich	q_m (mg/g)	88.50	101.01	100.00
	KE	1.20	1.19	1.47
	R^2	0.856	0.779	0.774
Dubinin-Radushkevich	q_m (mg/g)	314.19	350.72	357.81
	B_0	-8.88E-07	-7.01E-07	-5.22E-07
	R^2	0.941	0.941	0.941



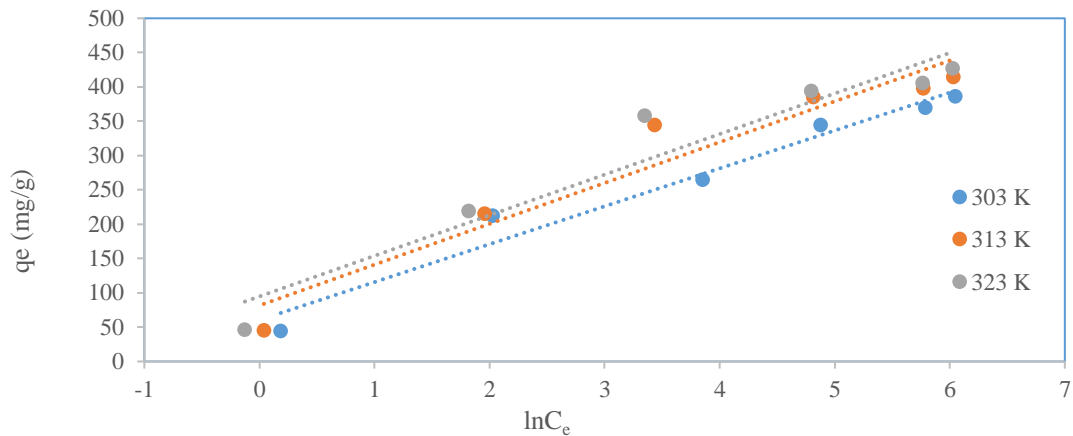


Figure 37: Adsorption Isotherm Langmuir (1) and Temkin (2) of TC on AC- GO

4.2.2.2 Effect of Solution pH

Presence of three function groups within TC molecule can result in TC molecule being charged either positively ($\text{pH} < 3.32$), neutrally ($3.3 < \text{pH} < 7.8$), or negatively ($\text{pH} > 7.8$)[100]. In this process, pH_{pcz} plays a major role and adsorbents with lower pH values than pH_{pcz} possess a positive surface charge. Therefore, positively charged AC contribute to the higher adsorption capacity of TC.

A diminished amount of TC adsorption could be potentially attributed to electrostatic repulsion between AC & TC due to their surface being negatively charged at pH 10. & 313 K. Increased rates of adsorption was witnessed between pH 3.0 to pH 7.0 as compared to pH range of 8-10 due to the fact that AC surface was positively charged & TC surface being neutral. The effect of solution pH on TC adsorption was examined by varying the pH from 3.0 to 10.5 ± 0.05 (final pH) at an initial TC concentration of 50 mg/L and 303 K. Figure 37, shows that as solution pH was increased from 3.0 to 6.0, TC adsorption increased, then decreased when solution pH was continuously increased to 10.5 ± 0.05 .

From solution pH examination, it can be concluded that AC is working efficiently to eliminate TC for the initial solution pH range of 4.05-4.10. Among the tested pH values, pH 5.00 ± 0.03 had the highest % removal of 93.52 %.

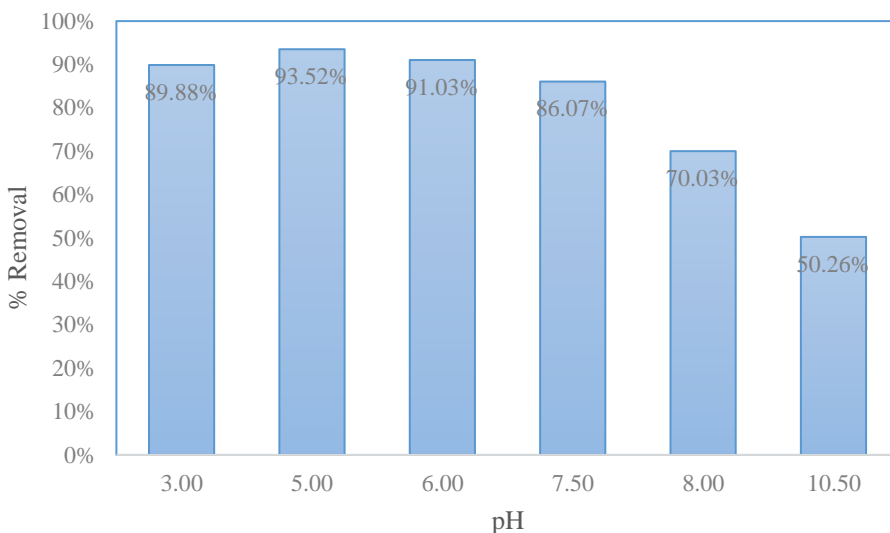


Figure 38: Effect of pH on Adsorption of TC onto AC

The effect of solution pH on TC adsorption was examined by varying the pH from 3.0 to 10.5 ± 0.05 (final pH) at an initial TC concentration of 50 mg/L and 303 K. The adsorption capacity of nano adsorbent GO, was highest at pH 3.0 as shown in Figure 38, and then it starts decreasing as pH solution was increased in the range of 3.0 to 10.5. At pH 3.0, TC molecules were positively charged. The synthesized graphene oxide was negatively charged under the same pH value. Therefore, there was a strong electrostatic attraction between synthesized GO and TC. When solution pH was 5.0, TC molecules existed as zwitterionic species (molecule's net charge was negative). At this pH, GO was still negative. Therefore, electrostatic repulsion between TC and GO made the TC adsorption rate reduction. When the pH value of the solution was higher than 5.0, TC molecules

occurred in the form of anions and GO was still negatively charged. The electrostatic repulsion between TC and GO was further enhanced, which caused the adsorption rate of TC to decrease further.

From solution pH examination, it can be concluded that GO is working efficiently to eliminate TC for acidic solution pH range of 3.0 to 5.0. Among the tested pH values, pH 3.0 ± 0.03 had the highest % removal of 57.04 %.

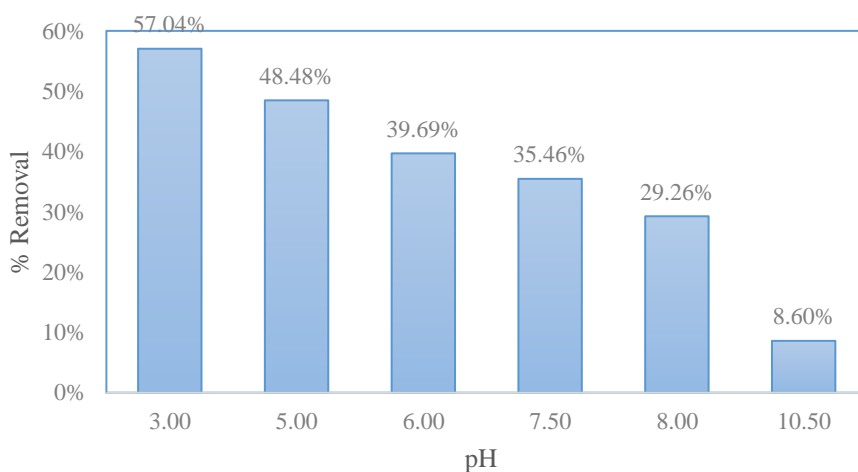


Figure 39: Effect of pH on Adsorption of TC onto GO

The effect of solution pH on TC adsorption was examined by varying the pH from 3.0 to 10.0 ± 0.05 (final pH) at an initial TC concentration of 50 mg/L and 303 K. The adsorption capacity of nano adsorbent AC-GO, was highest at pH 3.0 as shown in Figure 39, and then it starts decreasing as pH solution was increased in the range of 3.0 to 10.0. As this nano adsorbent is a composite of AC and GO, it has also gone through similar phenomena of electrostatic attraction and repulsion which AC and GO experienced when the pH of the solution increased or decreased. From solution pH examination, it can be concluded that

AC-GO was working efficiently to eliminate TC for acidic solution pH range of 3.0 to 5.0. Among the tested pH values, pH 3.0 ± 0.03 had the highest removal 70.10%.

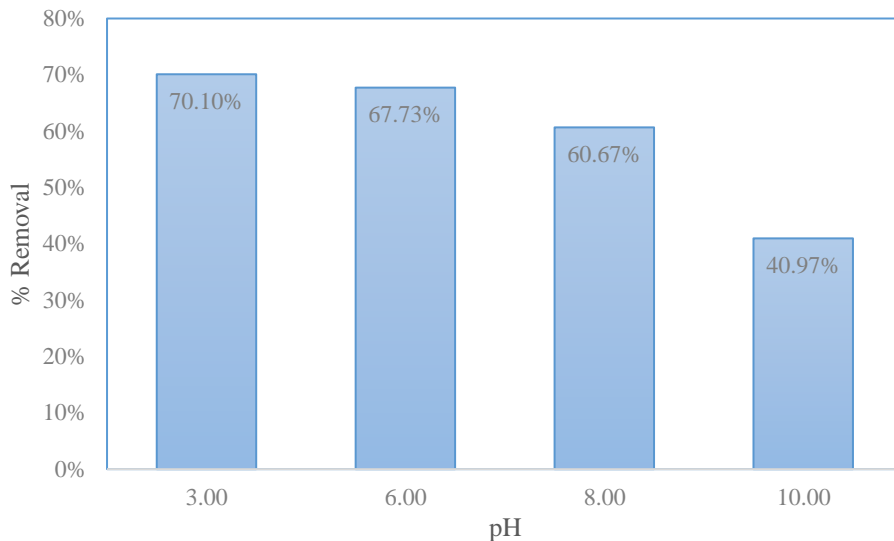


Figure 40: Effect Of pH on Adsorption of TC onto AC-GO

4.2.2.3 Effect of Initial Concentration

The following observations have been reported from the literature that, initial concentration plays a significant role to find out when the adsorption process become saturated. Different antibiotics have their different removal capacity to reach equilibrium. So, in general, the rise in the concentration of adsorbate will lead to a reduction of removal capacity, and the same pattern was observed during adsorption of TC on AC, GO and AC-GO. The removal % of TC onto AC is reduced from 97.03 % to 27.36 % for the concentration range of 10-500 mg/l at temperature 303 K. A similar adsorption pattern was observed for adsorbent GO, removal % decreased from 66 % to 14.29 % for a concentration range of 10-500 mg/l. For AC-GO the maximum % removal obtained was 87.97 % for 10 mg/l concentration and it reduced to 15.44 % for the concentration of 500 mg/l. This experimental result suggested that with increased concentration adsorption capacity diminished.

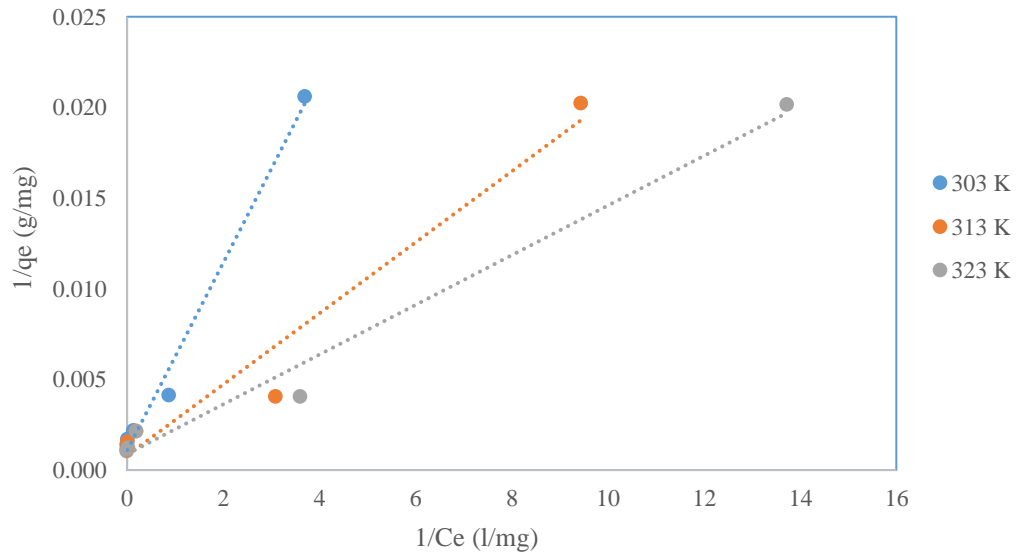
4.2.3 Adsorption Doxycycline on Activated carbon, Graphene oxide, and Activated carbon-Graphene oxide

4.2.3.1 Effect of temperature

The DC adsorption isotherms of AC, GO, and AC-GO at 303 K, 313 K, and 323 K are illustrated in Figure(40,41,42). The equilibrium DC adsorption capacities of AC, GO, and AC-GO increased as the temperature was increased, which revealed that the adsorption of DC on AC was an endothermic process. The Langmuir, Freundlich, Temkin, Elovich, and Dubinin – Radushkevich isotherm model [83-86], were analyzed to examine the fitting efficiencies of experimental data with the corresponding isotherms. Among the tested models, Freundlich, Elovich and Dubinin-Radushkevich with lower determination coefficients ($R^2 = 0.730-0.790$) indicated that these isotherms were not justifying the experimental data (Appendix-B) and thus not a good fit. Langmuir and Temkin's isotherm were best fit for equilibrium data with a high determination coefficient ($R^2 = 0.989$). The isotherm model results suggested that adsorption of DC on AC, GO, and AC-GO was monolayer and chemical in nature based on Langmuir model. The values of q_{max} and K_L of Langmuir isotherm was increasing with increase in temperature suggested that increasing in temperature and initial concentration was conducive for adsorption process.

Table 13: Parameters of Adsorption Isotherm of DC Adsorption of AC

Temperature (K)		303	313	323
Langmuir	q_{\max} (mg/g)	933.71	1246.26	1345.35
	K_L (L/mg)	0.207	0.409	0.543
	$1/K_L q_m$	0.005	0.002	0.001
	R^2	0.989	0.961	0.983
Freundlich	k_f	4.968	5.277	5.349
	n	2.93	3.19	2.91
	R^2	0.795	0.813	0.862
Temkin	B	93.58	98.92	119.94
	$B \ln A$	214.73	307.92	365.21
	R^2	0.972	0.976	0.980
Elovich	q_m (mg/g)	151.52	151.52	188.68
	K_E	3.56	9.55	8.07
	R^2	0.842	0.897	0.933
Dubinin-Radushkevich	q_m (mg/g)	533.79	651.97	713.37
	B_0	-1.68E-07	-7.25E-08	-5.43E-08
	R^2	0.945	0.964	0.943



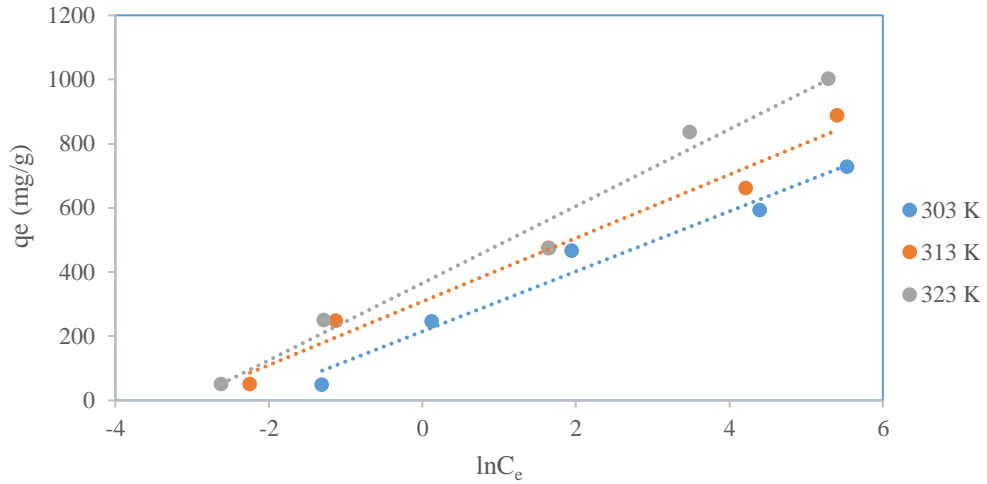


Figure 41: Adsorption Isotherm Langmuir (1) and Temkin (2) of DC on AC

Table 14: Parameters of Adsorption Isotherm Model of DC Adsorption of GO

Temperature (K)		303	313	323
Langmuir	q_{\max} (mg/g)	358.22	465.55	478.24
	K_L (L/mg)	0.027	0.024	0.045
	$1/K_L q_m$	0.103	0.089	0.046
	R^2	0.999	0.999	0.993
Freundlich	k_f	2.964	3.072	3.434
	n	1.71	1.75	1.97
	R^2	0.950	0.983	0.945
Temkin	B	90.572	92.361	88.165
	$B \ln A$	102.46	96.671	59.632
	R^2	0.977	0.978	0.950
Elovich	q_m (mg/g)	217.39	212.77	188.68
	K_E	0.06	0.07	0.11
	R^2	0.930	0.950	0.988
Dubinin-Radushkevich	q_m (mg/g)	275.89	284.29	292.95
	B_0	-5.78E-06	-4.55E-06	-1.83E-06
	R^2	0.858	0.855	0.822

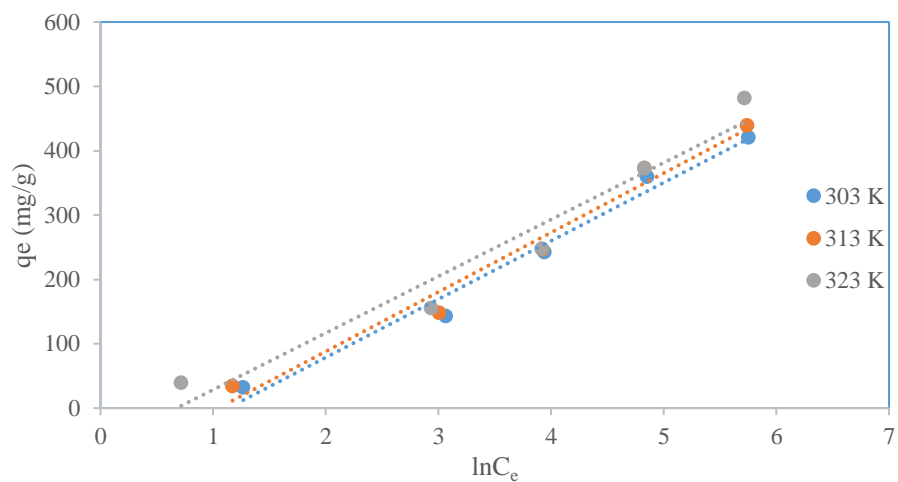
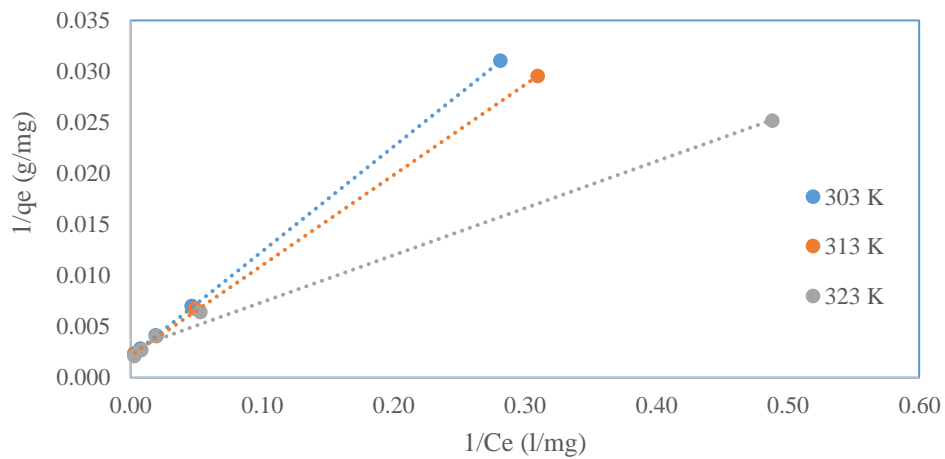
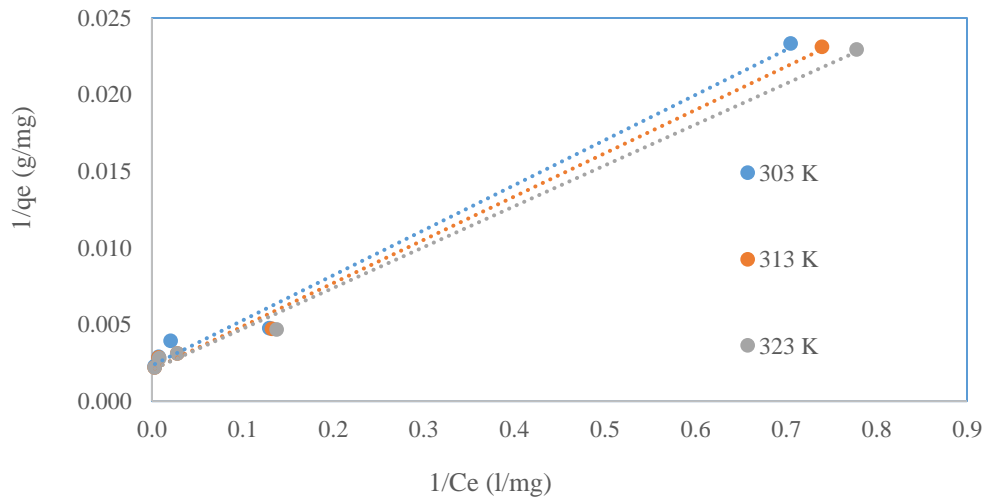


Figure 42: Adsorption Isotherm Langmuir (1) and Temkin (2) of DC on GO

Table 15: Parameters of Adsorption Isotherm Model of DC Adsorption of AC- GO

Temperature (K)		303	313	323
Langmuir	q_{max} (mg/g)	423.19	488.52	487.80
	K_L (L/mg)	0.0718	0.0723	0.077
	$1/K_L q_m$	0.032	0.028	0.027
	R^2	0.990	0.994	0.995
Freundlich	k_f	4.075	4.099	4.019
	n	2.54	2.55	2.63
	R^2	0.847	0.839	0.843
Temkin	B	63.891	70.454	70.782
	$B \ln A$	38.726	44.333	47.454
	R^2	0.967	0.959	0.973
Elovich	q_m (mg/g)	111.11	125.00	123.46
	K_E	0.60	0.58	0.63
	R^2	0.834	0.823	0.838
Dubinin-Radushkevich	q_m (mg/g)	304.90	333.62	333.62
	Bo	-1.14E-06	-1.03E-06	-9.01E-07
	R^2	0.935	0.938	0.937



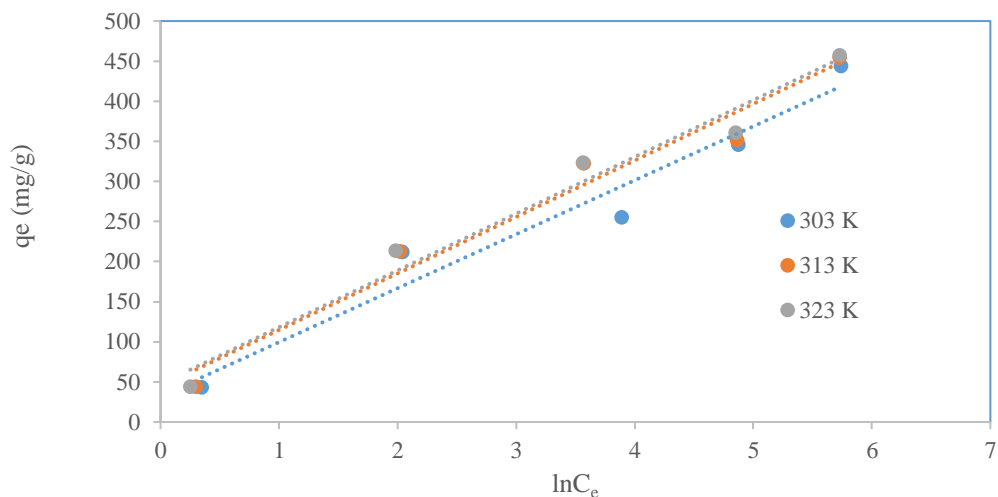


Figure 43: Adsorption Isotherm Langmuir (1) and Temkin (2) of DC on AC -GO

4.2.3.2 Effect of Solution pH

The effect of solution pH on DC adsorption was examined by varying the pH from 3.0 to 10.5 ± 0.05 (final pH) at an initial DC concentration of 50 mg/L and 303 K. The adsorption capacity of nano adsorbent AC, was highest at pH 5.0, as shown in Figure 43, and then it starts decreasing as pH solution was increased in the range of 3.0 to 10.5. In this process, pH_{pcz} plays a major role and adsorbents AC with lower pH values than pH_{pcz} possess a positive surface charge. Therefore, positively charged AC contribute to the higher adsorption capacity of DC. Electrostatic repulsion and attraction play a significant role in this process. When molecule DC and nano adsorbent AC were negatively charged, electrostatic repulsion decreased the adsorption capacity. When the adsorbent is positively charged and the DC molecule is a zwitterion, that case adsorption capacity was increased due to electrostatic attraction. From solution pH examination, it can be concluded that AC is working efficiently to eliminate DC for acidic solution pH range of 3.0 to 5.0 (AC was

positively charged, and DC was negatively charged and the case of electrostatic attraction).

Among the tested pH values, pH 5.0 ± 0.03 had the highest % removal of 94.15 %.

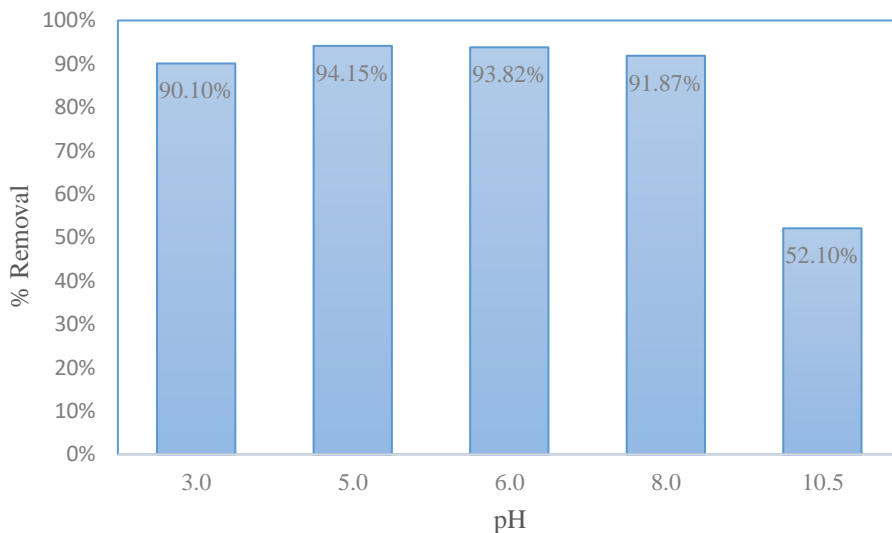


Figure 44: Effect of pH on Adsorption of DC onto AC

The adsorption capacity of nano adsorbent GO, was highest at pH 3.0 (The synthesized GO was negatively charged, and molecule DC was positively charged so, electrostatic attraction helped to raise adsorption capacity) as shown in Figure 44, and then it starts decreasing as pH solution was increased in the range of 3.0 to 10.5 (GO was still negatively charged and DC molecule was also in an anionic form which caused to decrease the adsorption capacity).

From solution pH examination, it can be concluded that GO is working efficiently to eliminate DC for acidic solution pH range of 3.0 to 5.0. Among the tested pH values, pH 3.0 ± 0.03 had the highest % removal of 58.59 %, and afterwards adsorption capacity starts decreasing as pH increase.

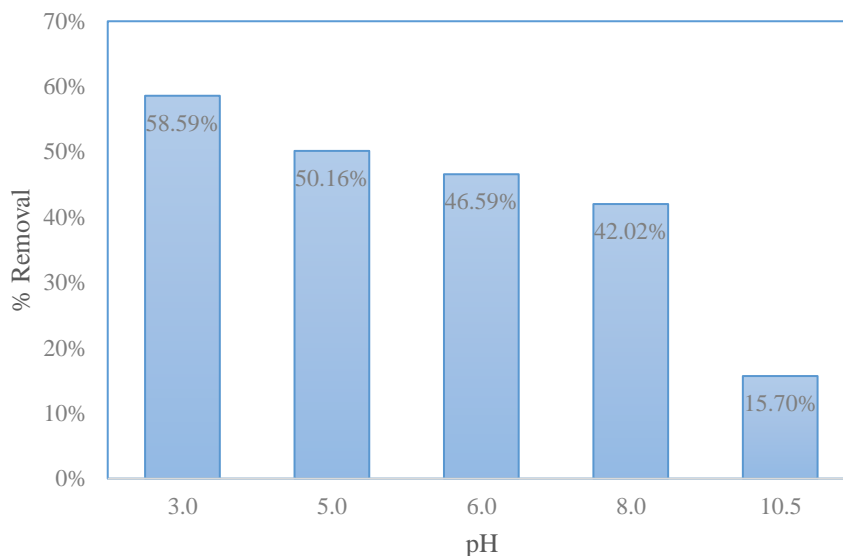


Figure 45: Effect of pH on Adsorption of DC onto GO

The effect of solution pH on DC adsorption was examined by varying the pH from 3.0 to 10.0 ± 0.05 (final pH) at an initial TC concentration of 50 mg/L and 303 K. The adsorption capacity of nano adsorbent AC-GO, was highest at pH 3.0, as shown in Figure 45, and then it starts decreasing as pH solution was increased in the range of 3.0 to 9.0. As this nano adsorbent is a composite of AC and GO, it has also gone through similar phenomena of electrostatic attraction and repulsion which AC and GO experienced when the pH of the solution increased or decreased. From solution pH examination, it can be concluded that AC-GO was working efficiently to eliminate DC for acidic solution pH range of 3.0 to 5.0. Among the tested pH values, pH 3.0 ± 0.03 had the highest removal 73.39 %.

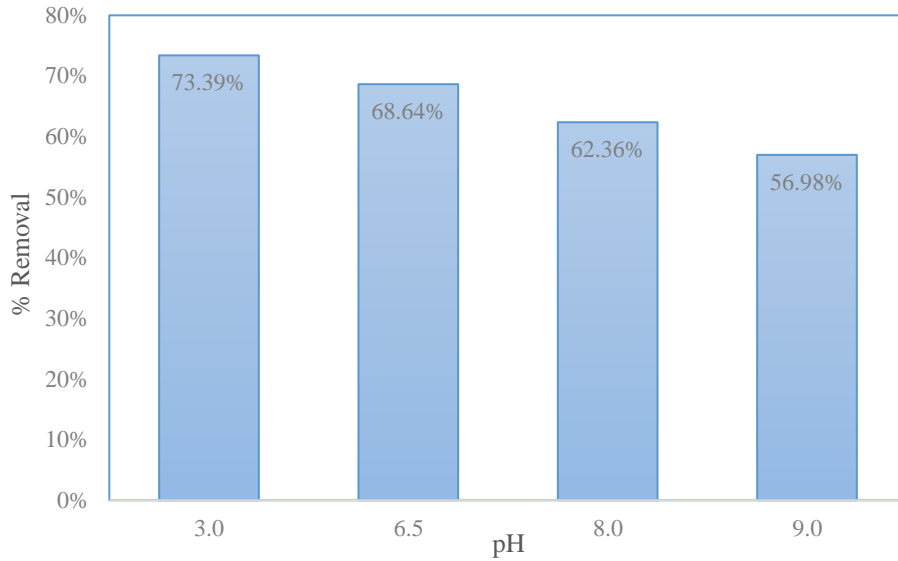


Figure 46: Effect of pH on Adsorption of DC onto AC-GO

4.2.3.3 Effect of Initial Concentration

In general, the rise in the concentration of adsorbate will lead to a reduction of removal capacity, and the same pattern was observed during adsorption of DC on AC, GO and AC-GO. The removal % of DC onto AC is reduced from 97.29 % to 36.23 % for the concentration range of 10-400 mg/l at temperature 303K. A similar adsorption pattern was observed for adsorbent GO, removal % decreased from 64.50 % to 21.06 % for a concentration range of 10-400 mg/l. For AC-GO the maximum % removal obtained was 85.83 % for 10 mg/l concentration and it reduced to 20.85 % for the concentration of 400 mg/l. This experimental result suggested that with increased concentration adsorption capacity diminished.

4.3 Adsorption Kinetics

4.3.1 Adsorption of Tetracycline on Activated carbon ,Graphene oxide, Activated carbon -Graphene oxide

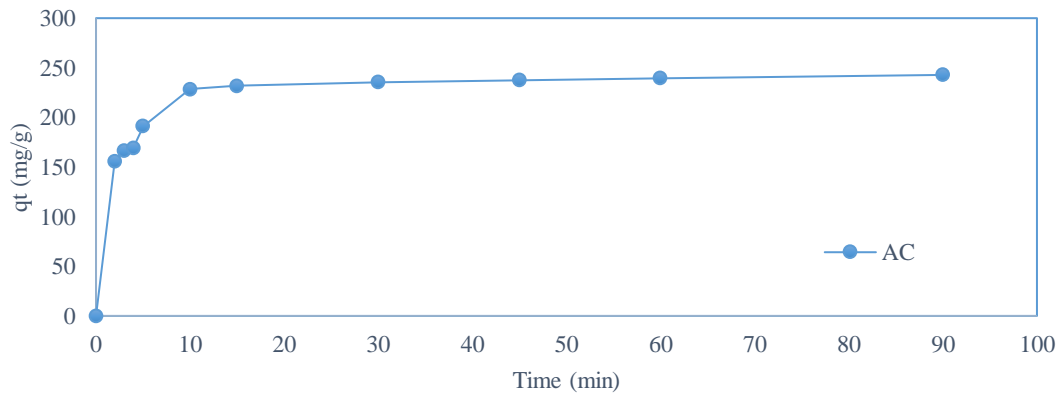
4.3.1.1 Effect of Time

Adsorption kinetics is of importance to affect the adsorption. Figure (46,47,48) demonstrates the effect of contact time on TC adsorption by nano adsorbent AC, GO and AC-GO at an initial TC concentration of 50 mg/l. The adsorption of TC was observed between the time frame of 2min to 90min. From the investigation, it revealed that the rate of adsorption increases as time increases initially and then after 60min it almost becomes stagnant means the adsorption process reached equilibrium. The adsorption process was very quick initially and then followed by slower adsorption. The early rapid adsorption may be because the process was taking place at an exterior surface of the adsorbent and when the exterior surface was saturated by contaminant then followed by a reduced internal diffusion. Among the tested kinetic isotherm, pseudo-second-order well fitted with experimental data with high determination coefficient (R^2) = 0.999 and maximum adsorption capacity achieved for AC was 237.92 mg/g. For nano, adsorbent GO, the kinetic analysis showed that pseudo-second-order and Elovich models were well fitted with experimental data with a high determination coefficient (R^2) = 0.998 and 0.966 and maximum adsorption capacity achieved was 140.84 mg/g at temperature 303K which was very close to the experimental value of q_e 139.73 mg/g. was 139.73 mg/g. For AC-GO, the kinetic analysis suggested that pseudo-second-order and Elovich models were well fitted with experimental data. The determination coefficient (R^2) from Pseudo second order was 0.988 while from Elovich was 0.970. Maximum adsorption capacity achieved from

Pseudo second order was 192.31 mg/g at temperature 303K which was very close to the experimental value of q_e 190.55 mg/g. This proved that Pseudo second order is the best fit for experimental data with high accuracy values of q_e and R^2 .

Table 16: Parameters of Adsorption Kinetic Model of TC Adsorption of AC

Temperature (K)		303	313	323
Experimental	q_e (mg/g)	237.92	238.66	239.08
	C_o (mg/l)	50	50	50
Pseudo First order	q_e (mg/g)	35.26	53.81	53.54
	K_1 (min ⁻¹)	0.053	0.046	0.047
	R^2	0.750	0.901	0.906
Pseudo Second order	q_e (mg/g)	238.09	243.90	243.90
	K_2	0.0032	0.0031	0.0032
	R^2	0.999	0.999	0.999
Elovich	α	17631.45	17287	18508
	β	0.044	0.044	0.044
	R^2	0.874	0.878	0.882



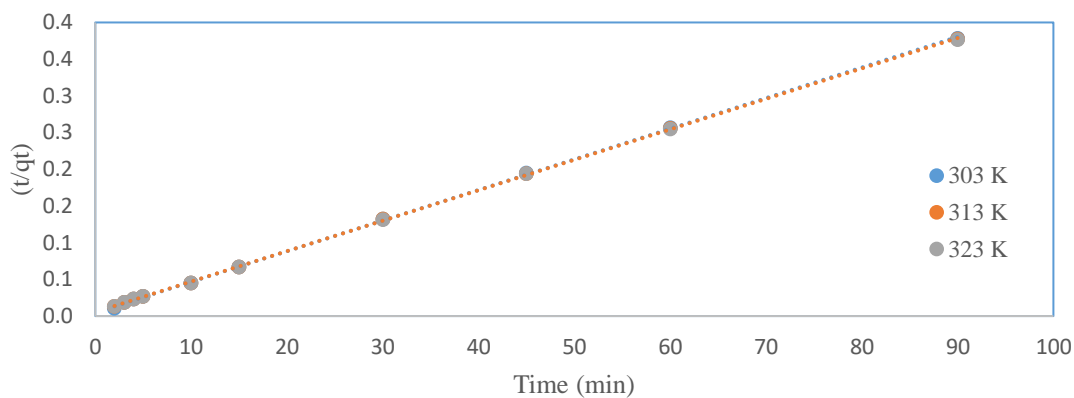


Figure 47: Analysis Models for Adsorption of TC on AC

Table 17: Parameters of Adsorption Kinetic Model of TC Adsorption of GO

Temperature (K)		303	313	323
Experimental	q_e (mg/g)	139.73	145.81	150.27
	C_o (mg/l)	50	50	50
Pseudo First order	q_e (mg/g)	42.55	43.31	41.14
	K_1 (min ⁻¹)	0.039	0.042	0.039
	R^2	0.913	0.946	0.936
Pseudo Second order	q_e (mg/g)	140.84	142.85	144.92
	K_2	0.003	0.003	0.003
	R^2	0.998	0.997	0.997
Elovich	α	13384.41	7832.17	4791.357
	β	0.081	0.075	0.068
	R^2	0.952	0.940	0.966

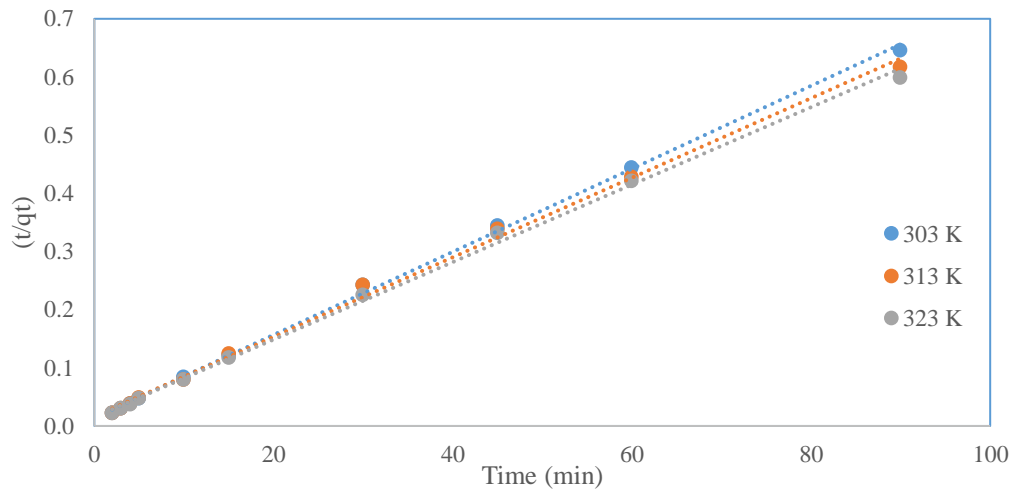
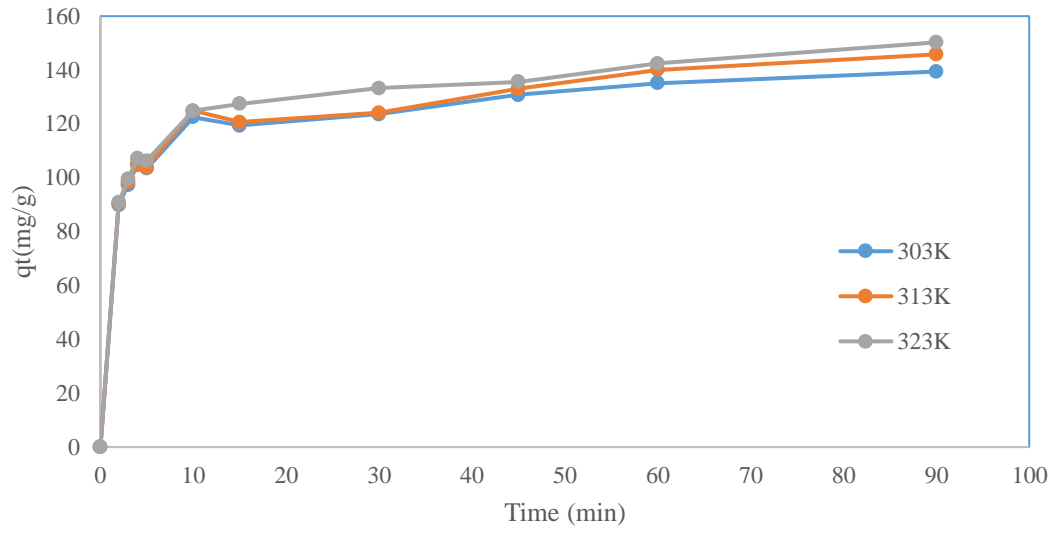


Figure 48: Analysis Models for TC on GO

Table 18: Parameters of Adsorption Kinetic Model of TC Adsorption of AC-GO

Temperature (K)		303	313	323
Experimental	q_e (mg/g)	190.55	192.00	195.37
	C_o (mg/l)	50	50	50
Pseudo First order	q_e (mg/g)	137.26	132.67	134.64
	$K1$ (min ⁻¹)	0.045	0.045	0.047
	R2	0.895	0.898	0.926
Pseudo Second order	q_e (mg/g)	192.31	192.30	196.07
	K2	0.0008	0.0008	0.0008
	R2	0.988	0.988	0.989
Elovich	α	154.21	167.19	188.94
	β	0.033	0.032	0.034
	R2	0.972	0.959	0.970

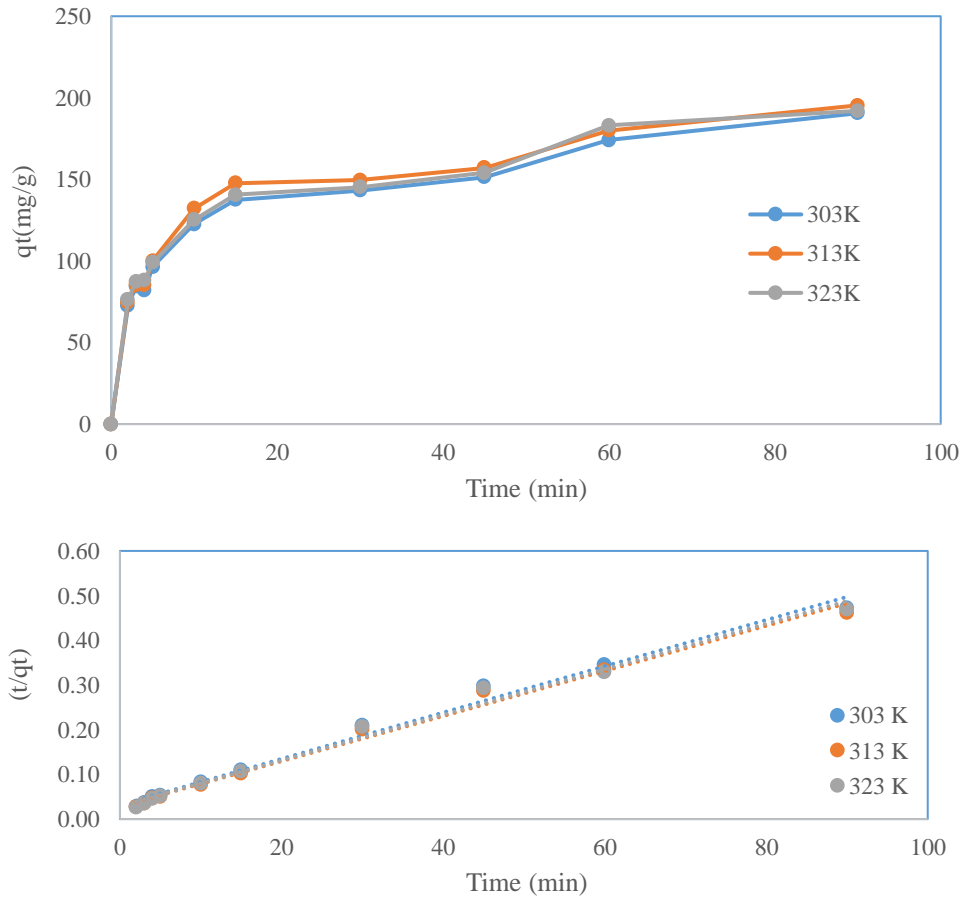


Figure 49: Analysis Models for Adsorption of TC on AC-GO

4.3.2 Adsorption of Doxycycline Activated carbon, Graphene oxide, and Activated carbon-Graphene oxide

4.3.2.1 Effect of Time

The effect of contact time on Doxycycline (DC) adsorption by AC, GO, and AC-GO at an initial DC concentration of 50 mg/l, is demonstrated in Figure (49,50,51). The adsorption process was taken for the time frame of 2 min to 90 min. The adsorption process was very quick initially and then followed by slower adsorption. The early rapid adsorption may be because the process was taking place at the exterior surface of the adsorbent and when the exterior surface was saturated by contaminant then followed by a reduced internal diffusion. Among the tested kinetic isotherm, pseudo-second-order well fitted with experimental data with a high determination coefficient (R^2) = 0.999 and maximum adsorption capacity achieved for AC was 243.90 mg/g at temperature 303K which is very close to the experimental value of q_e . For GO, the pseudo-second-order and Elovich model fitted well with experimental data with a high determination coefficient (R^2) = 0.999-0.950 and maximum adsorption capacity achieved was 144.92 mg/g at temperature 303K which is very close to the experimental value of q_e = 144.58 mg/g. For AC-GO, the kinetic analysis indicated that pseudo-second-order and Elovich models were well fitted with experimental data. The determination coefficient (R^2) from Pseudo second order was 0.988 while from Elovich was 0.970. Maximum adsorption capacity achieved from Pseudo second order was 175.43 mg/g at temperature 303K which was very close to the experimental value of q_e 174.83 mg/g. This proved that Pseudo second order is the best fit for experimental data with high accuracy values of q_e and R^2 .

Table 19: Parameters of Adsorption Kinetic Model of DC Adsorption of AC

Temperature (K)		303	313	323
Experimental	q_e (mg/g)	242.80	246.09	248.73
	C_o (mg/l)	50	50	50
Pseudo First order	q_e (mg/g)	52.175	53.303	53.887
	K_1 (min ⁻¹)	0.047	0.047	0.047
	R^2	0.866	0.881	0.903
Pseudo Second order	q_e (mg/g)	243.90	243.90	250.00
	K_2	0.0031	0.0031	0.0029
	R^2	0.999	0.999	0.0999
Elovich	α	11446.47	10887.04	11112.92
	β	0.041	0.041	0.041
	R^2	0.858	0.869	0.879

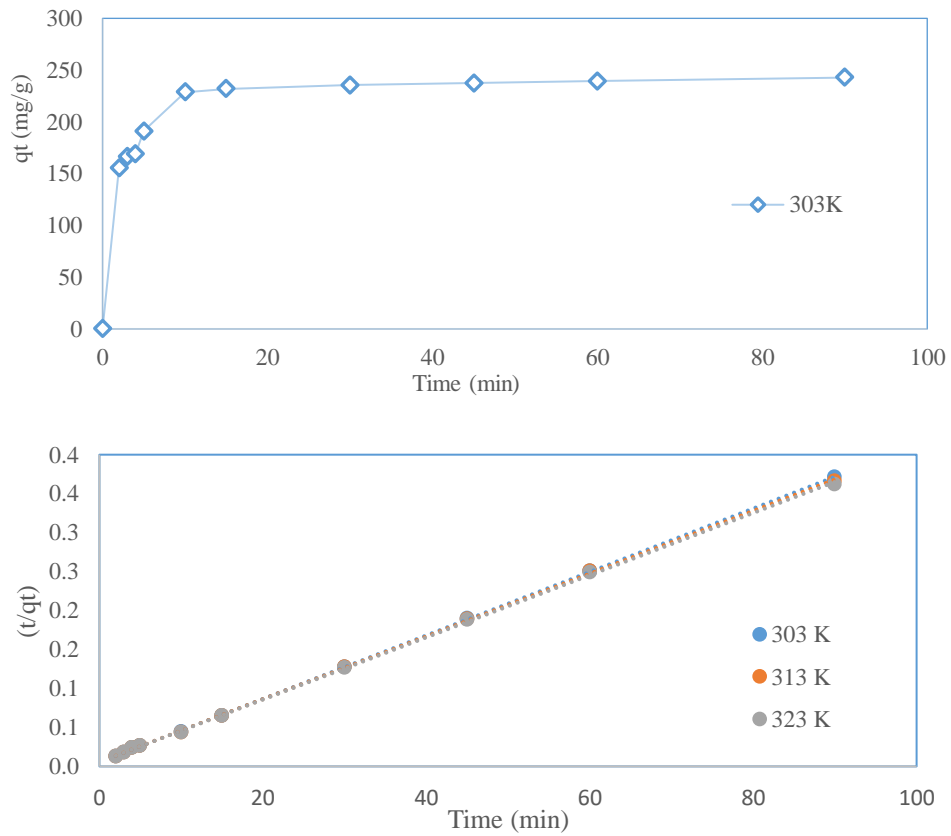
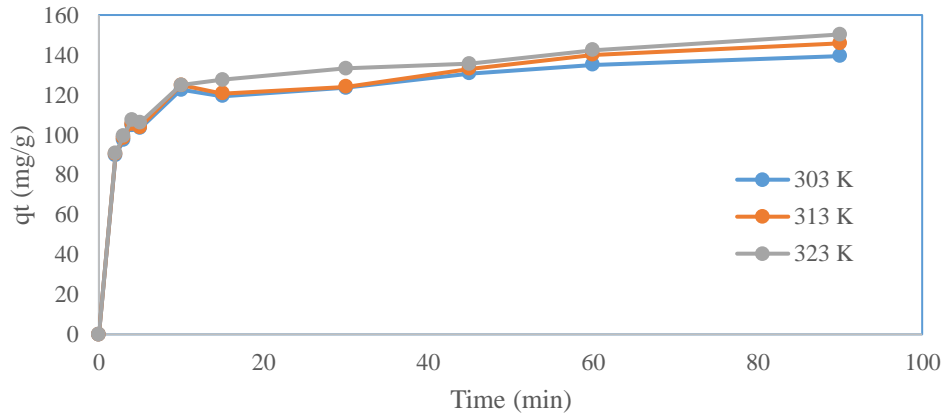


Figure 50: Analysis Models for Adsorption of DC on AC

Table 20: Parameters of Adsorption Kinetic Model of DC Adsorption of GO

Temperature (K)		303	313	323
Experimental	q_e (mg/g)	144.58	145.55	151.38
	C_o (mg/l)	50	50	50
Pseudo First order	q_e (mg/g)	48.80	48.57	46.39
	K_1 (min ⁻¹)	0.0390	0.0372	0.0394
	R^2	0.942	0.934	0.902
Pseudo Second order	q_e (mg/g)	144.92	144.92	147.05
	K_2	0.003	0.003	0.003
	R^2	0.998	0.998	0.996
Elovich	α	6842.25	6308.24	7163.95
	β	0.071	0.073	0.074
	R^2	0.964	0.965	0.961



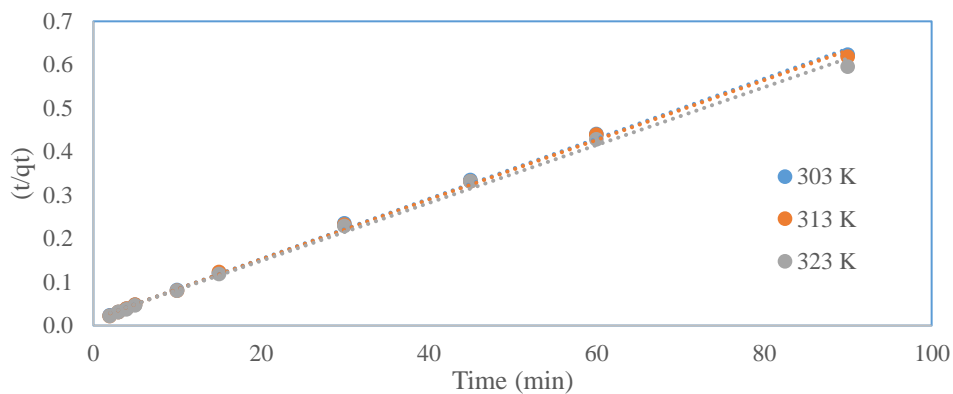
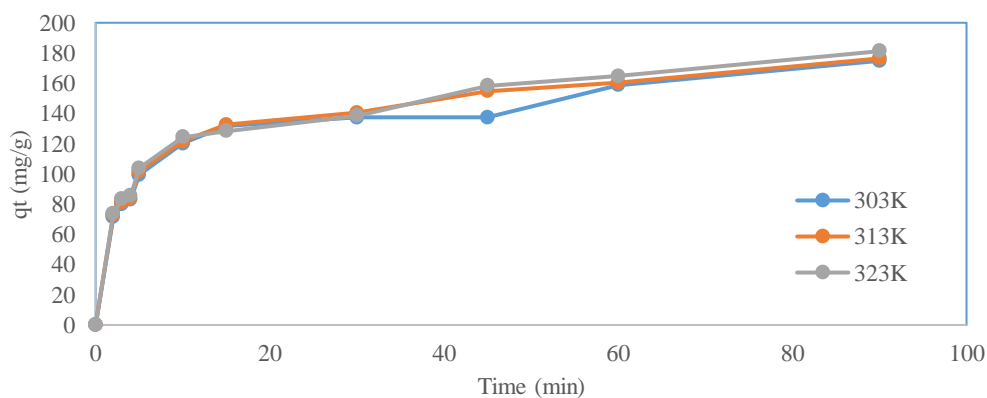


Figure 51: Analysis Models for Adsorption of DC on GO

Table 21: Parameters of Adsorption Kinetic Model of DC Adsorption of AC-GO

Temperature (K)		303	313	323
Experimental	q_e (mg/g)	174.83	176.39	181.17
	C_o (mg/l)	50	50	50
Pseudo First order	q_e (mg/g)	113.05	110.56	110.07
	K_1 (min ⁻¹)	0.043	0.044	0.045
	R^2	0.878	0.919	0.918
Pseudo Second order	q_e (mg/g)	175.43	178.57	178.57
	K_2	0.001	0.001	0.001
	R^2	0.988	0.995	0.993
Elovich	α	214.67	200.78	198.11
	β	0.039	0.037	0.036
	R^2	0.961	0.984	0.982



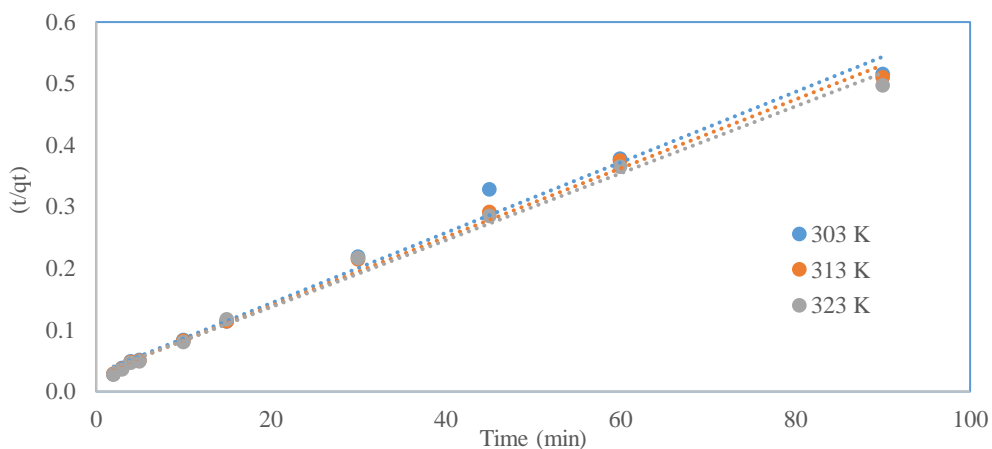


Figure 52: Analysis Models for Adsorption of DC on AC- GO

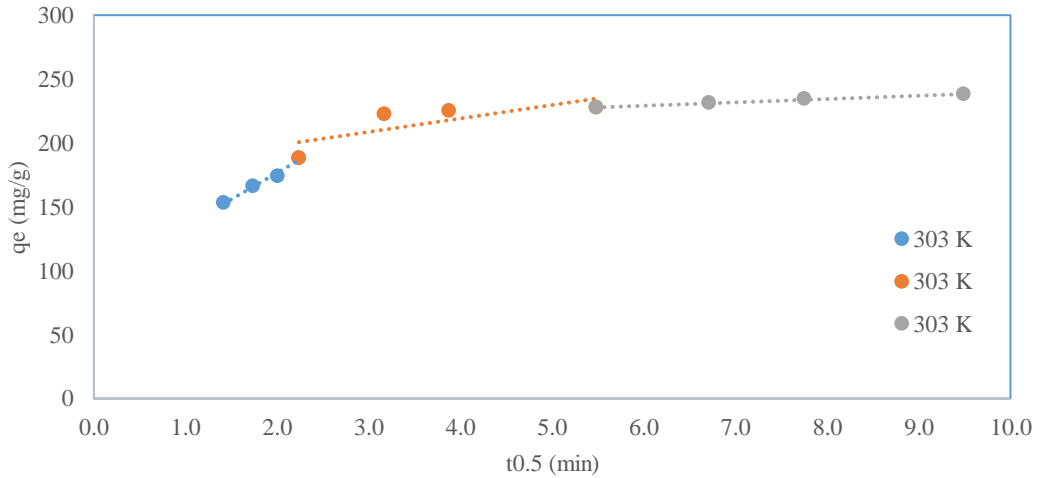
4.4 Intraparticle Diffusion Studies of Tetracycline and Doxycycline adsorption on Activated Carbon, Graphene Oxide, and Activated carbon-Graphene oxide

Values of qt versus $t^{1/2}$ are plotted and shown in Figure (52,53). Table 21 depicts the data of k_{id} , C_i , and R^2 . The concentration of TC and DC was kept at 50 mg/l for adsorption studies at temperature 303 K for a time frame of 2 min-90 min. The linear-line slope corresponds to the intra-particle diffusion constant i.e., k_{id} . While the intercept represents C_i , provides the thickness of the boundary layer. Adsorption is considered to be only progressing due to intra-particle diffusion when entire data sets in a linear segment pass through the origin. If not, the involvement of additional mechanisms exists along with intraparticle diffusion [99]. It is evident from Figure (52,53) all graphs are divided into three linear segments representing three different phases. Phase one is associated with the diffusion of TC and DC onto the external surface of AC, GO and AC-GO. The high adsorption rate can be validated by the high k_{id} value of phase one. While during phase two, slow adsorption is being attributed to intraparticle diffusion which is the rate-limiting step. During phase three, due to extremely low concentration of TC & DC intra-particle

diffusion starts to slow down and accordingly resulting in lower K_{id} values compared to the first phase. Moreover, as during phase two and phase three the data sets are not passing through the origin, representing that intraparticle diffusion is not the only driving factor for adsorption. [99]

Table 22: Intraparticle Diffusion Data of Adsorption of TC and DC on AC, GO, AC-GO

Adsorbate	Adsorbent	Temp(K)	$K_{id}(\text{mg g}^{-1}\text{min}^{-1/2})$			$C_i(\text{mg g}^{-1})$			R^2		
			K_{id1}	K_{id2}	K_{id3}	C_{i1}	C_{i2}	C_{i3}	R1	R2	R3
TC	AC	303	41.44	2.21	2.13	93.78	215.96	217.7	0.98	0.97	1.0
	GO	303	18.86	5.22	3.88	64.03	98.29	103.61	0.95	0.67	0.95
	AC-GO	303	25.14	13.84	12.47	37.33	73.85	73.08	0.82	0.81	0.96
DC	AC	303	39.25	11.99	1.83	98.19	177.53	225.34	0.87	0.63	0.99
	GO	303	20.16	6.28	3.92	61.38	96.67	107.14	0.97	0.73	0.97
	AC-GO	303	31.31	11.23	10.22	25.58	80.62	76.79	0.89	0.83	0.90



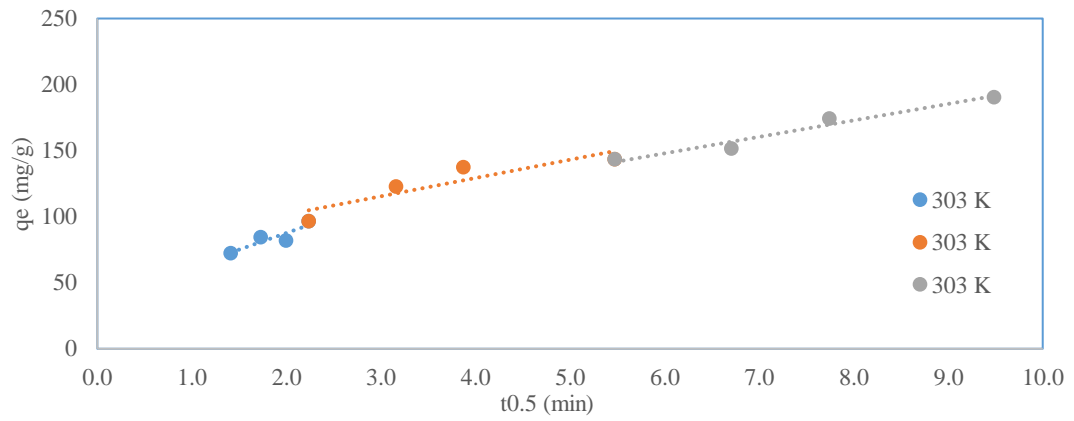
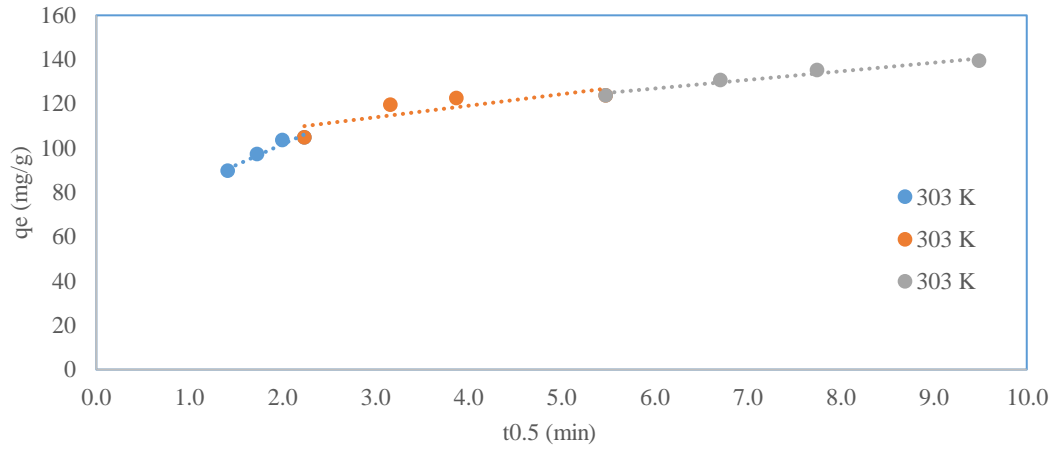
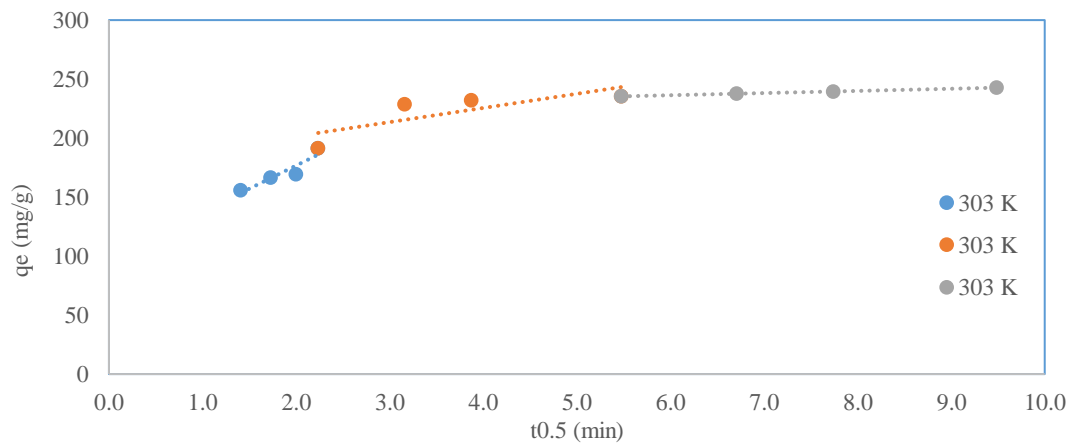


Figure 53: Intraparticle Diffusion Model Analysis of TC on AC (1), GO (2), AC-GO (3)



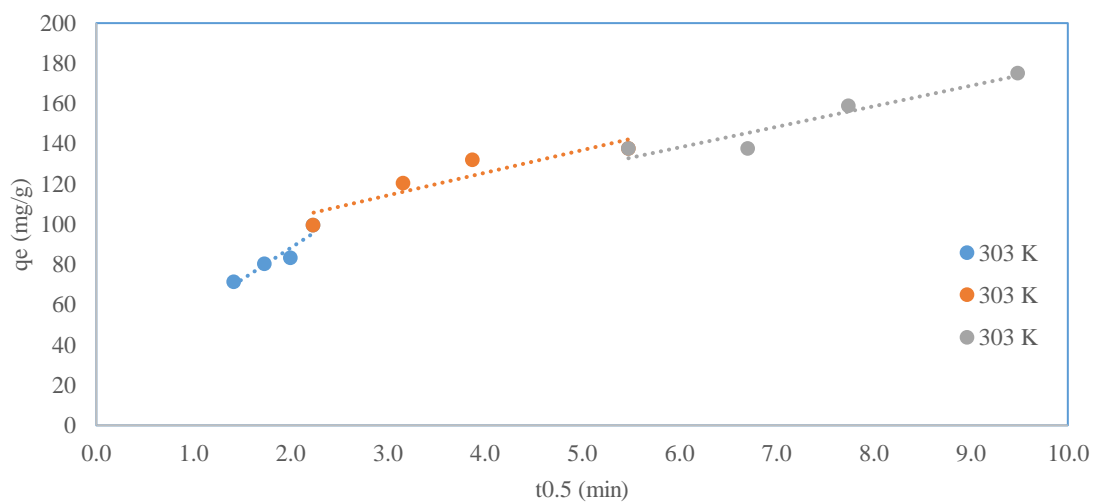
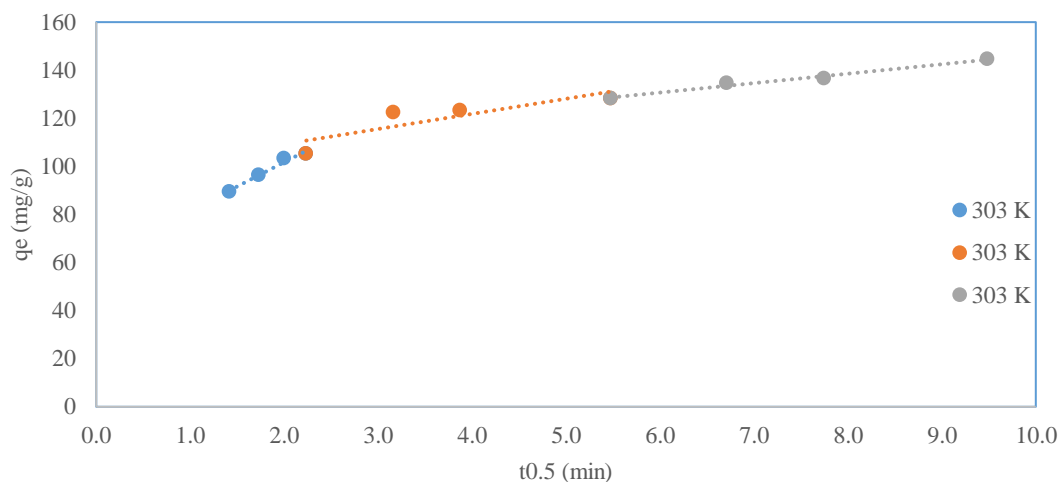


Figure 54: Intraparticle Diffusion Model Analysis of DC on AC (1), GO (2), AC-GO (3)

4.5 Thermodynamic Study

To understand the effect of temperature on the adsorption process, parameters like Gibbs free energy (ΔG°), enthalpy (ΔH°) and entropy (ΔS°) are vital. The following Gibbs energy equation was used to calculate the thermodynamic parameters [106]

$$\Delta G^\circ = -R * T * \ln K \quad [24]$$

Where,

R = Universal gas constant 8.314 J/mol K

T = Temperature (K)

$\ln K = q_e/C_e = (\Delta S^\circ/R - \Delta H^\circ/RT)$

ΔS° = Slope of the graph (1/T Vs $\ln K$)

ΔH° = Intercept of the graph (1/T Vs $\ln K$)

4.5.1 Thermodynamics Study of Adsorption of Tetracycline and Doxycycline on Activated Carbon, Graphene Oxide, and Activated carbon-Graphene oxide

The graph between T^{-1} and $\ln K$ ($\ln q_e/C_e$) was plotted as shown in Figure(54,55) below. The values of ΔS° and ΔH° were taken from the plotted graph as slope and intercept. The values of ΔG° , ΔH° , and ΔS° for TC and DC were calculated and presented in Table 22, below. The values of calculated Gibb's energy (ΔG°) <0 means, process of adsorption on nano adsorbent AC, GO, and AC-GO was spontaneous and appropriate. Furthermore, enthalpy change (ΔH°) possesses a positive value, specify that the adsorption process is endothermic, while entropy (ΔS°) with a positive value indicating that there is a rise in the randomness at the boundary of solid solute during the process of adsorption.

Table 23: Thermodynamic Data of Adsorption of TC and DC on AC, GO, AC-GO

Adsorbent	Adsorbate	Temp(K)	1/T	$\ln K$ = $\ln(q_e/C_e)$	ΔG° KJ/mol	ΔH° KJ/mol	ΔS° JK/mol	R^2
AC	TC	303	3.03	4.31	-10.85	4.30	49.94	0.952
		313	3.19	4.34	-10.93			
		323	3.10	4.41	-11.11			
	DC	303	3.03	4.73	-11.92	8.43	67.04	
		313	3.19	4.80	-12.09			
		323	3.10	4.94	-12.44			
GO	TC	303	3.03	1.77	-4.46	4.89	30.92	0.965
		313	3.19	1.85	-4.67			
		323	3.10	1.89	-4.76			
	DC	303	3.03	22.70	-4.52	0.96	18.07	
		313	3.19	22.62	-4.54			
		323	3.10	22.79	-4.58			
AC-GO	TC	303	3.03	2.44	-6.15	7.16	43.98	0.980
		313	3.19	2.55	-6.43			
		323	3.10	2.62	-6.59			
	DC	303	3.03	2.16	-5.44	2.99	27.82	
		313	3.19	2.19	-5.51			
		323	3.10	2.24	-5.63			

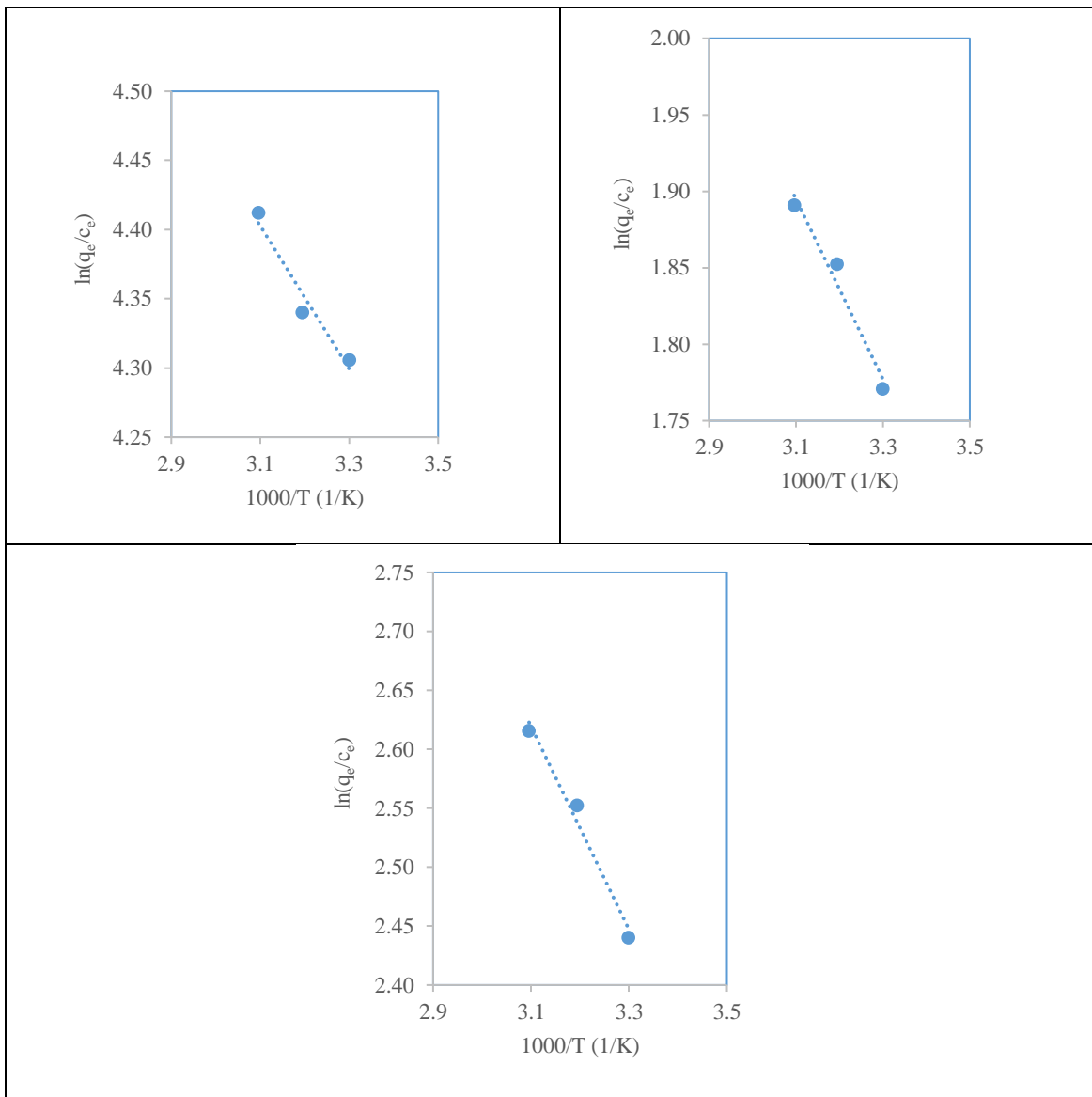


Figure 55: Thermodynamic Analysis of TCon AC (1), GO(2), and AC-GO (3)

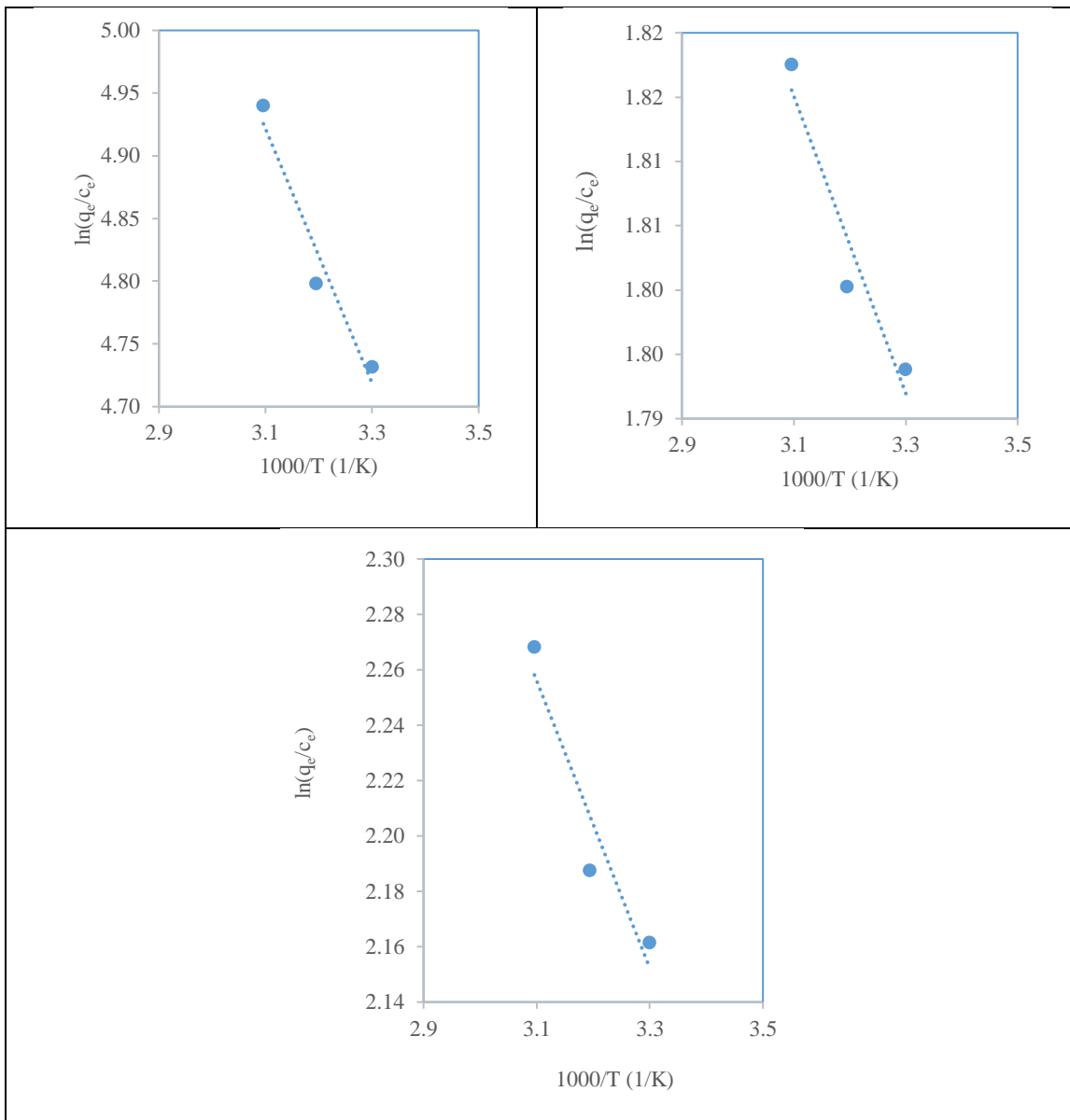
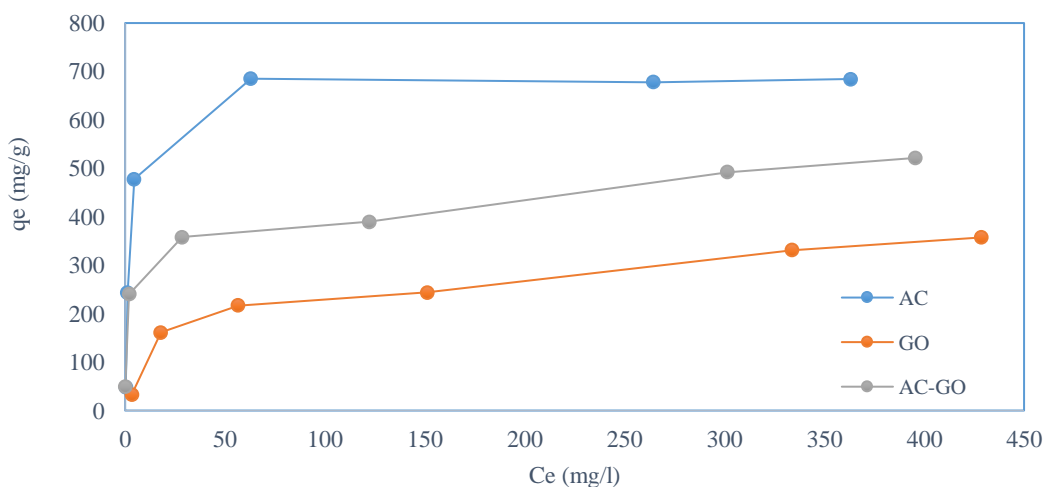


Figure 56: Thermodynamic Analysis of DC on AC (1), GO(2), and AC-GO (3)

4.6 Comparative Study of Tetracycline and Doxycycline on Activated Carbon, Graphene Oxide and Activated carbon-Graphene oxide

4.6.1 Adsorption Isotherm

The adsorption isotherms of TC and DC at initial solution pH of 4.10 ± 0.03 is presented in Figure (56,57). The isotherms were obtained at an initial TC and DC concentration range of 10–500 mg/L. It is visible that TC molecules were more favourably adsorbed onto nano adsorbent AC, GO, and AC-GO, its adsorption capacity attained 684.11 mg/g at an initial concentration of 500 mg/l. The adsorption capacities were obtained for GO was 357.35 mg/l and 385.90 mg/l for nano adsorbent AC-GO for the same set of the experimental condition of time 24 h and at temperature 303 K. A similar adsorption pattern was noticed in the adsorption DC and obtained values for maximum adsorption capacity (q_e mg/g) were 726.43 mg/g for AC, 357.35 mg/g for GO and 417.07 mg/g. As discussed in previous sections, among the tested equilibrium isotherm models, Langmuir and Temkin's models were fitting well with experimental data obtained for pharmaceutical drugs TC and DC. The isotherm model results suggested that TC and DC adsorption on the tested set of nano adsorbents was monolayer and adsorption sites were in a homogenous pattern.



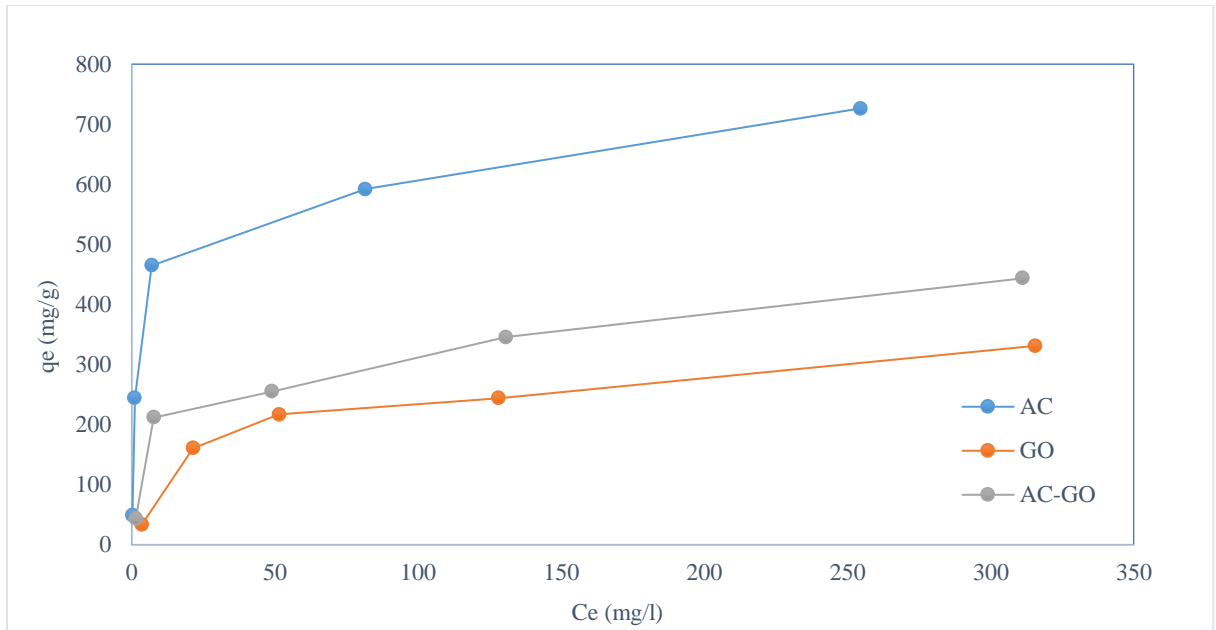


Figure 57: Adsorption Isotherms of TC (1) and DC (2) on AC, GO, AC-GO at 303 K

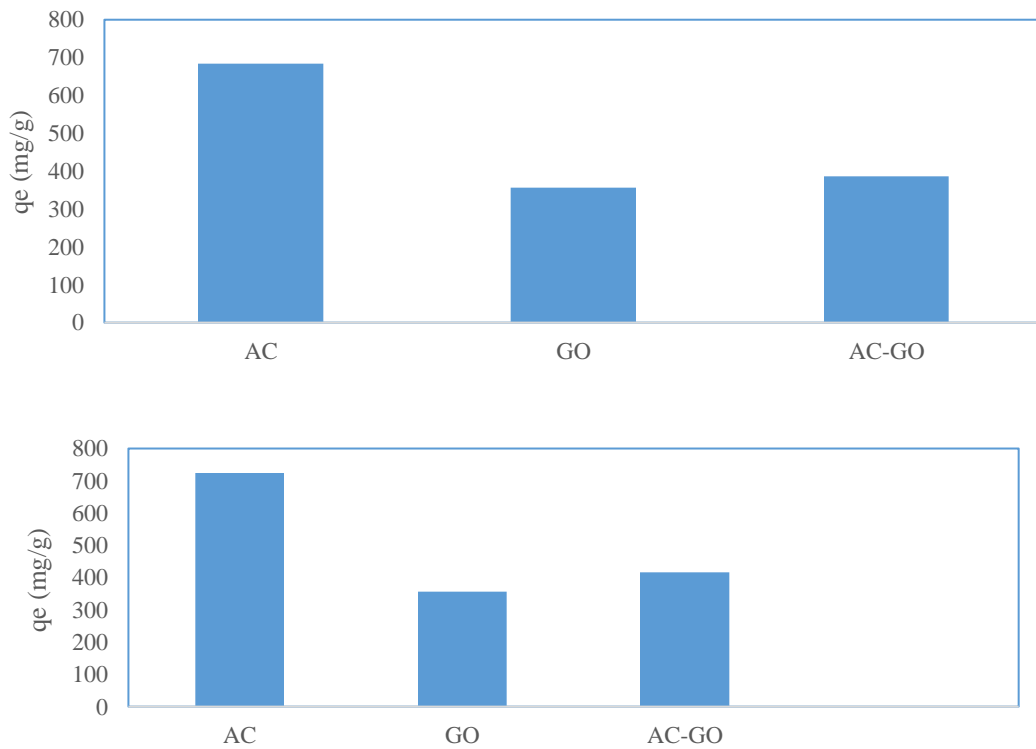
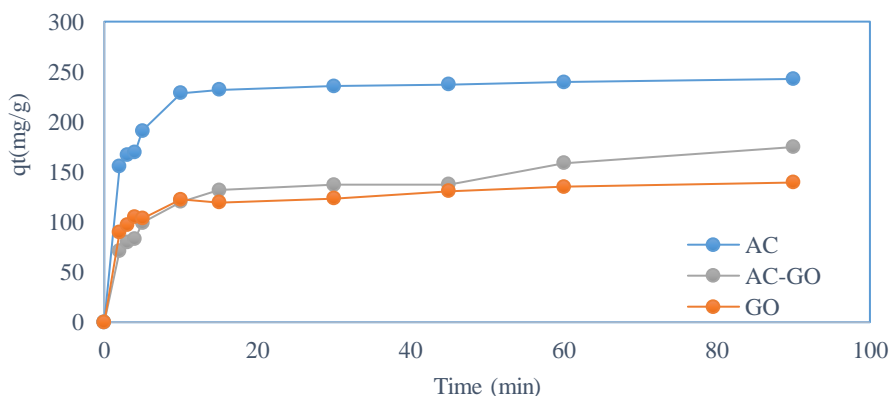


Figure 58: Comparative Maximum Adsorption capacity of TC (1) and DC (2) on AC, GO, AC-GO

4.6.2 Adsorption Kinetics

To estimate the effectiveness of the adsorbents AC, GO, and AC-GO, the plots of the quantity of TC and DC adsorbed, q_t , as a function of the time is plotted in Figure(58,59). The initial adsorption process was quick for all adsorbents, because of the adsorption of the particle on the exterior surface. The subsequent stage of the adsorption was slow. It is credited to that TC and DC molecule diffuse slowly into inner walls of the porous structure of the adsorbent because available exterior sites of adsorbent became saturated in the initial phase. The nano adsorbent AC has the highest adsorption capacity in comparison with the other two nano adsorbent because AC possessed the highest specific surface area(SSA) 2709.14 m²/g. The nano adsorbent composite AC-GO also possessed a higher removal rate of TC and DC because the composite made from m-AC and graphite oxide, which also possessed high SSA 1268.60 (m²/mg). The nano adsorbent GO had the lowest adsorption capacity on TC and DC because it had the lowest SSA 46.52 m²/g in comparison to another nano adsorbent. The liner plot of t vs t/q_e was plotted shown below in the figure. The high determination coefficient value ($R^2 = 0.99$) of pseudo-second-order and the calculated value of q_e from isotherm was well fitted with experimental data, suggested that kinetic modelling of TC and DC for the tested nano adsorbents fit pseudo-second-order model.



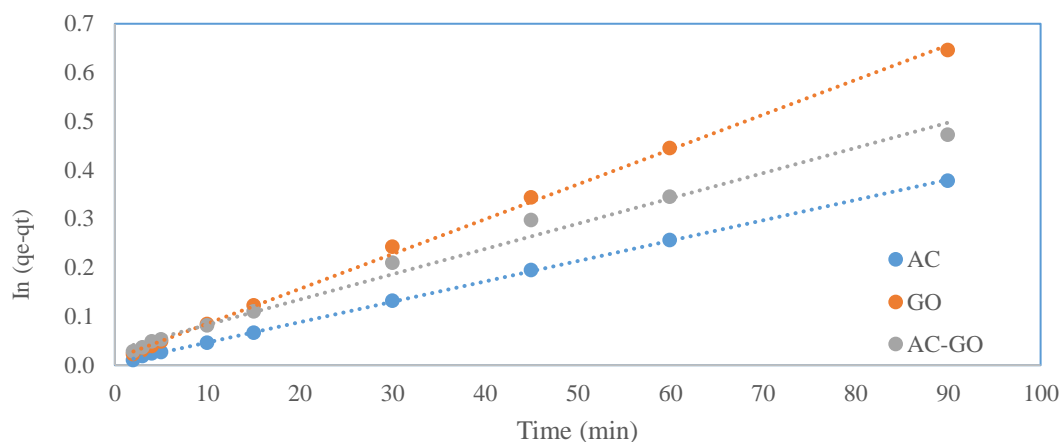


Figure 59: Analysis Models of TC on AC, GO, AC-GO

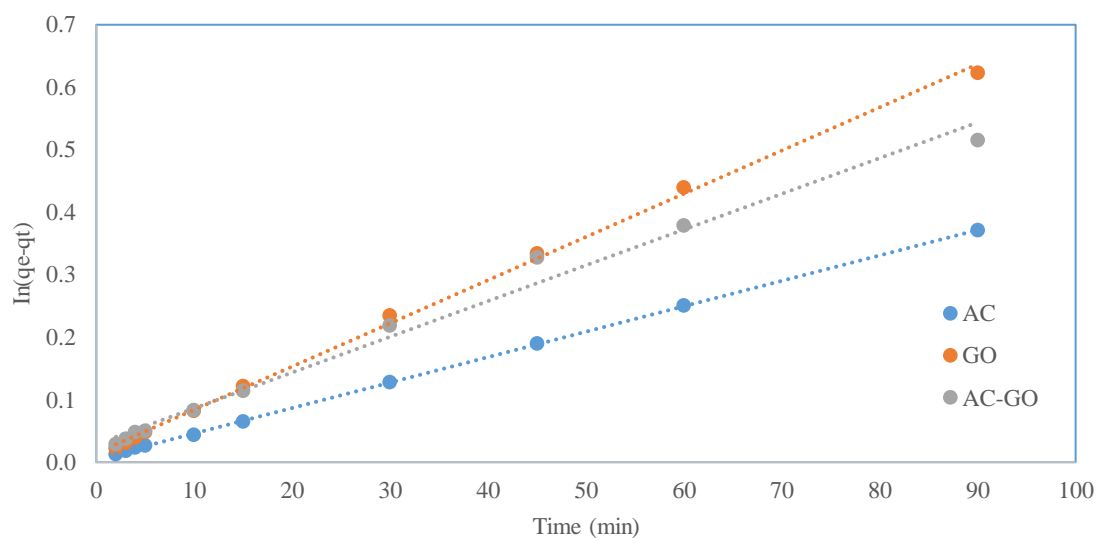


Figure 60: Pseudo Second-Order Model of DC on AC, GO, AC-GO

4.7 Adsorption Mechanism

The highest adsorption capacities of three nano adsorbents followed an order of AC > AC-GO > GO as shown in Figure 57 above. The justification that AC adsorbs much more TC and DC than the other two nanomaterials are most probably associated with the reality that it has the greatest specific surface area (SSA m²/g).

To recognize the adsorption systems of TC and DC more in-depth, onto AC, GO, and AC-GO, FTIR, and XRD analyses were conducted out on the samples before and after the adsorption. The XRD results of TC and DC loaded AC, GO, AC-GO confirmed that the peak intensities were decreased after the process of adsorption because TC and DC molecules got adsorbed on mentioned nano adsorbent surface[101]. The surface of AC, GO, and AC-GO was graphitized (XRD analysis) after adsorption, which can behave as π donor during the $\pi - \pi$ electron donor-acceptor interaction. The presence of benzene ring in TC and DC, combined more conveniently with AC, GO and AC-GO, suggesting the presence of $\pi - \pi$ EDA interaction among them.

The FTIR results revealed that the peak intensities were improved at 3427 and 1637 per centimetre, related to -OH & C=C correspondingly, due to adsorption of TC and DC molecules on AC. The FTIR analysis indicated that the hydrogen bonding interaction affected the process of adsorption as phenol, amine, hydroxyl & enone moieties can produce hydrogen bonding with functional group carboxyl & hydroxyl of AC [101]. FTIR spectra of GO indicated that there was numerous oxygen-containing functional group existed which would likely make hydrogen bonding with the -OH group of the TC molecule [101].

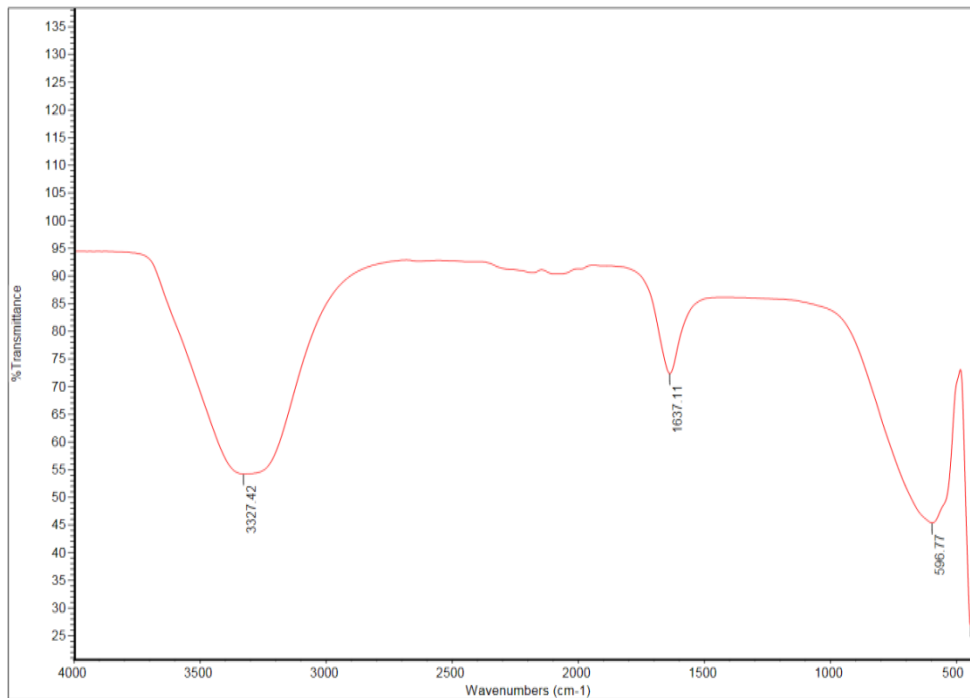


Figure 61: FTIR Spectra of AC After Adsorption of TC

Furthermore, the FTIR spectra for GO-AC shows peaks at (1586, 1541, 1068 cm^{-1}). While during adsorption of TC, previous peaks shifted to (1585, 1415, 1065 per centimetre). Based on which it can be concluded that adsorption has progressed via the combination of the negative active groups of adsorbents and the positive active group of the adsorbate. Outcomes of solution pH effect & ionic strength demonstrate electrostatic attraction and repulsion interactions exist between TC and DC molecules on nano absorbent viz. AC, GO, and AC-GO. Nevertheless, additional forces over and above the electrostatic interactions were present supporting adsorption. Accordingly, the adsorption was mostly affected by available surface area, π - π Electron Donor Acceptance, Hydrogen bonds interaction & electro-static interaction [104].

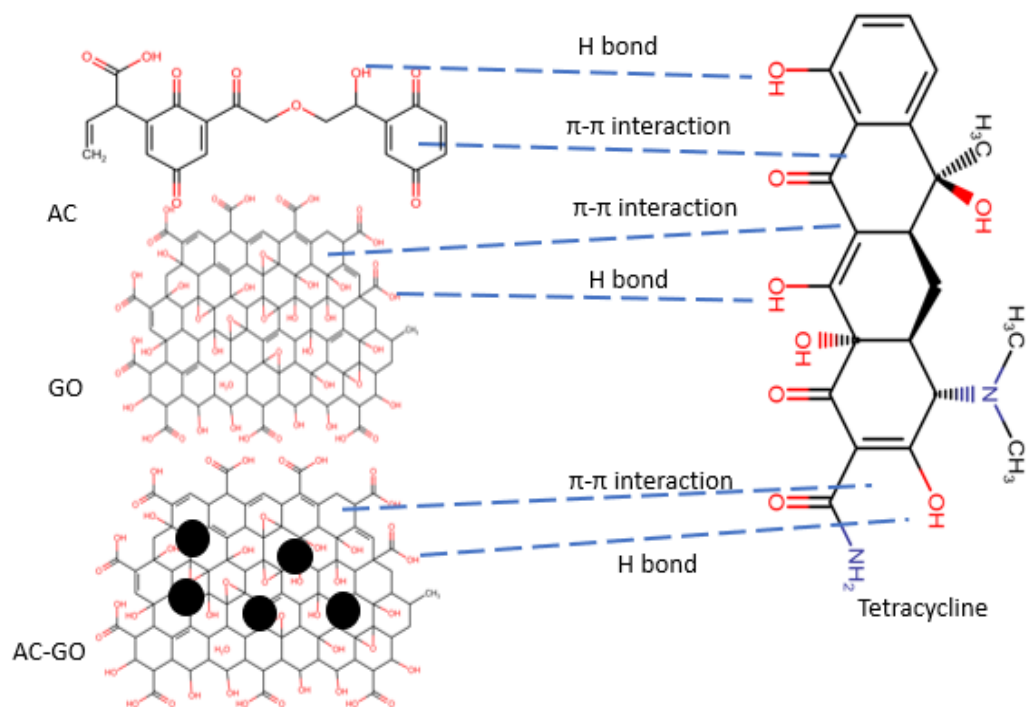


Figure 62: Adsorption Mechanism of Tetracycline on AC, GO, and AC-GO

4.8 Reusability of Nano Adsorbent Composite Activated carbon-Graphene oxide

The reusability is a key parameter for the commercial use of adsorbents. In this research, the utilized nano adsorbent AC- GO was rinsed with deionized water (DI water) and oven-dried overnight for regeneration and reuse. The adsorption-desorption test was reiterated 3 times in 50 mg/L TC and DC solution at 303 K and $\text{pH} = 4.10 \pm 0.03$, 1.5 h. As shown in Figure 62, the regenerated adsorbent's adsorption capability after three sets of adsorption-desorption cycles. The adsorption quantity reduced by 2–4% in each cycle, this may be due to the loss of irretrievable activity of incomplete-adsorption sites [98]. The percentage of removal of TC decreased from 95.7 % in the first cycle to 87.05 % in the third cycle, while in the case of DC it reduced from 93.20 % to 86.9 % from the first to third cycle. The regeneration results indicated that the adsorption capacity of TC and DC onto AC-GO had

reduced by 7 % after three cycles. The nano adsorbent showed higher removal capacity even after three successive cycles of regeneration, representing the great reusability ability and constancy of AC-GO for TC and DC removal.

Table 24:Regeneration Data of TC and DC onto AC-GO

Adsorbent	Adsorbate	Cycle	% Removal
AC-GO	TC	1	95.7
		2	91.7
		3	87.1
	DC	1	93.2
		2	90.6
		3	86.9

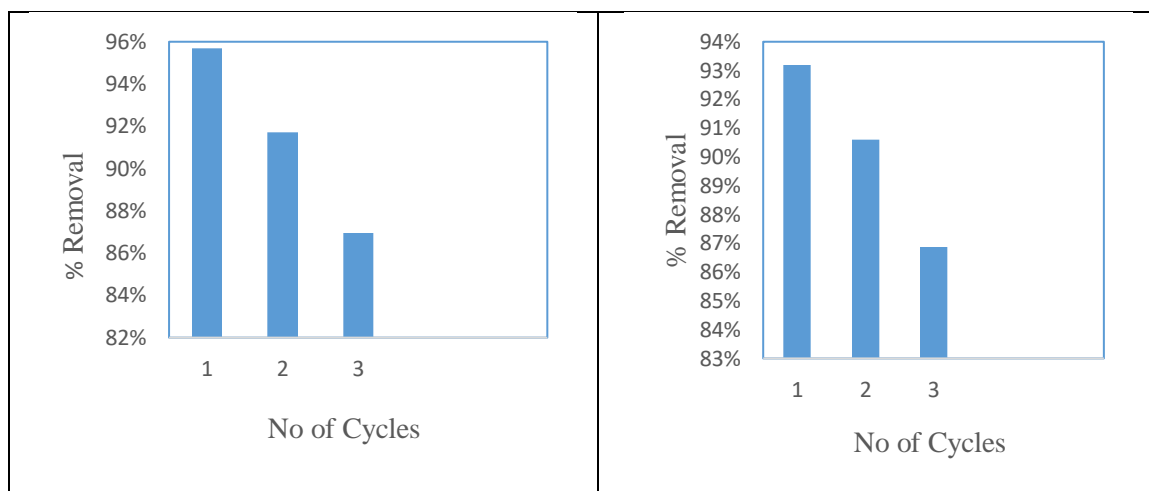


Figure 63: Regeneration Capacity of TC (1) and DC (2) onto AC-GO

4.9 Reproducibility of Results

The accuracy of the data is influenced by the following measured quantities: Tetracycline and Doxycycline solution concentration before and after the experiment, the temperature of shaker (sometimes fluctuating due to ambient condition), amount of adsorbent measured

on analytical balancing. An assessment of the data reproducibility was executed to determine which particular analysis gives the greatest error. It was found that error determination while making solution concentration and fluctuating temperature of the shaker to adjust with the ambient condition was the greatest. However, it was estimated that the error in the overall analysis was less than 7 %.

CHAPTER 5: CONCLUSION AND RECOMMENDATION

5.1 Conclusion

The nano adsorbent AC (Commercial grade), GO (synthesized by modified hummer method), Composite AC-GO (synthesized by conjugation of AC and GO) utilized in this work for the removal of Tetracycline and Doxycycline. The Nano adsorbents were characterized by several techniques includes XRD, SEM TEM, EDX, FTIR, and BET. The BET analysis suggested that the specific surface area (SSA) of AC was highest in comparison with GO and AC-GO.

The equilibrium and kinetic isotherm models best suited with experimental data were Langmuir, Temkin, Pseudo second order, and Elovich, correspondingly. Tetracycline and Doxycycline were capably removed from the solution by AC, GO, and AC-GO in a broad range of solution pH (3.0-10.5). Adsorption of TC and DC on AC, GO, and AC-GO was an endothermic and spontaneous process. The experimental TC and DC adsorption capacity of AC (684 mg/g, 726.43 mg/g at pH 4.10±0.05, 303 K, 24 h) were much higher than in comparison with the other two nano adsorbent.

The adsorption capacity of TC on AC, GO, and AC-GO were 684, 357, 414 mg/g respectively and followed the order AC > AC-GO > GO. The adsorption capacity of DC on AC, GO and AC-GO were 726, 421, 443 mg/g respectively and followed similar order same as TC. The normalized adsorption capacity by the BET SSA of TC on AC, GO and AC-GO were 0.37, 8.10, and 0.30 mg/m² correspondingly, representing that adsorption of TC on nano adsorbent was owing not only to the larger surface area but also due to π -EDA (electron donor-acceptor interactions), hydrogen bonding, and electrostatic attraction-

repulsion theory between positively charged TC molecule and negatively charged adsorbents.

However, the plots of intraparticle diffusion possessed straight lines with good correlation co-efficient, but they were not passing through origin in each case, suggested the pore diffusion was not the only driving mechanism for adsorption of TC and DC on mentioned nano adsorbent. This recommends that the adsorption process is complex with more than one mechanism limiting the rate of adsorption. The regeneration data of AC-GO demonstrated a high-percentage removal capability even after three cycles which suggested that nano adsorbent has excellent recycle ability.

5.2 Future Work and Recommendation

Nano adsorbent discussed above demonstrated high adsorption capacities for TC and DC, whether nano adsorbents work for other antibiotics (e.g., β -lactams, sulfonamides, and fluoroquinolones) needs to be investigated. Although the adsorption kinetics in this work was investigated by the pseudo-second-order kinetic model that is built on chemical reaction, the mass transfer in the adsorption process should be studied. π EDA interactions and hydrogen-bond were proposed as one of the mechanisms in the adsorption of TC and DC antibiotics on nano adsorbent. However, in an aquatic system, processes like EDA interactions, and electrostatic attraction may concurrently operate for the adsorption of TC and DC antibiotics on nonabsorbent. Thus, further investigations on the binding strengths of EDA interactions, electrostatic attraction, hydrogen bonding interaction, and other interactions are required. The initial concentrations of antibiotics were at ppm level (mg/L) for experimental analysis, while most of the reported antibiotic concentrations in water

bodies and water streams were at ppb level ($\mu\text{g/L}$) and even at ppt level (ng/L). More works should be done at such low concentrations.

Cost-benefit analysis of different nano adsorbent (waste derived activated carbon and graphene-based material) for their production as well as an application at pilot and industrial scale. Developing an integrated system for removal of tetracycline and other pharmaceutical drugs using different removal techniques with consideration of important factors. Increasing adsorption efficiency of different adsorbent, by modifying the surface properties of adsorbent. Multiple or mixture of adsorbate could have experimented with for better removal performance. A maximum number of the adsorption studies are limited to the lab only. Adsorption should be carried in an actual complex wastewater condition, to understand the efficiency of adsorbent material.

REFERENCES

- [1] U. WHO, "Meeting the MDG drinking water and sanitation target: the urban and rural challenge of the decade," *World Health Organization & UNICEF*, 2006.
- [2] W. H. Organization and UNICEF, "Global water supply and sanitation assessment 2000 report," World Health Organization (WHO), 2000.
- [3] J. Olinger, *Transforming Our World: The 2030 Agenda for Sustainable Development*. HUMAN, 2015.
- [4] M.Davoudi, S.Samieirad, H.R, Mottaaghi,A.R Safadoost. " The main source of wastewater and sea contamination in the south pars natural gas processing plant: Prevention and recovery".*J.of.Natu.Gas Scien and Engin*, pp,137-146,2014.
- [5] C. Xinchun,W.Mengyang.,G.Xianping,Z.Yalian."Assesssing water scarcity in agricultural production system based on the generalized water resources and water footprint framework". *J. Scien.Tot.Envir.*,pp 587-597,2017.
- [6] S. Sengupta, M. K. Chattopadhyay, and H. P. Grossart, *Front. Microbiol.*, vol. 4, p. 47, 2013.
- [7] L. Du and W. J. A. f. s. d. Liu, "Occurrence, fate, and ecotoxicity of antibiotics in agro-ecosystems. A review," vol. 32, no. 2, pp. 309-327, 2012.
- [8] V. Homem and L. Santos, "Degradation and removal methods of antibiotics from aqueous matrices – A review," *Journal of Environmental Management*, vol. 92, no. 10, pp. 2304-2347,2011.
- [9] N. Kemper, "Veterinary antibiotics in the aquatic and terrestrial environment," *Ecological Indicators*, vol. 8, no. 1, pp. 1-13,2008.
- [10] A. Naquin, A. Shrestha, M. Sherpa, R. Nathaniel, and R. J. B. t. Boopathy,

- "Presence of antibiotic resistance genes in a sewage treatment plant in Thibodaux, Louisiana, USA," vol. 188, pp. 79-83, 2015.
- [11] Daghrrir, R., Drogui, P. "Tetracycline antibiotics in the environment: a review". *Environ.Chem. Lett.* 11, pp.209–227, 2013.
- [12] Miao, X.S., Bishay, F., Chen, M. and Metcalfe, C.D. "Occurrence of antimicrobials in the final effluents of wastewater treatment plants in Canada". *Environmental Science & Technology*, 38(13), pp. 3533-3541, 2014.
- [13] Deblonde, T., Cossu-Leguille, C. and Hartemann, P. "Emerging pollutants in wastewater: A review of the literature". *International Journal of Hygiene and Environmental Health*, 214(6), pp. 442-448, 2011.
- [14] Sköld, O., 2011. "Antibiotics and Antibiotics Resistance". Wiley, New Jersey, pp. 207.
- [15] Owens Jr, R.C. and Ambrose, P.G. "Clinical use of the fluoroquinolones. *Medical Clinics of North America*" 84(6), pp. 1447-1469, 2000.
- [16] Bouyarmane, H., El Hanbali, I., El Karbane, M., Rami, A., Saoiabi, A., Saoiabi, S., Masse, S., Coradin, T. and Laghzizil, A. "Parameters influencing ciprofloxacin, ofloxacin, amoxicillin and sulfamethoxazole retention by natural and converted calcium phosphates". *Journal of Hazardous Materials*, 291, pp. 38-44, 2015.
- [17] Gao, L., Shi, Y., Li, W., Liu, J. and Cai, Y. "Occurrence and distribution of antibiotics in urban soil in Beijing and Shanghai, China". *Environmental Science and Pollution Research*, 22(15), pp. 11360-11371, 2015.
- [18] Leal, R.M.P., Alleoni, L.R.F., Tornisielo, V.L. and Regitano, J.B. "Sorption of fluoroquinolones and sulfonamides in 13 Brazilian soils". *Chemosphere*, 92(8), pp.

979-985, 2013.

- [19] Yiruhan, Wang, Q.J., Mo, C.H., Li, Y.W., Gao, P., Tai, Y.P., Zhang, Y., Ruan, Z.L. and Xu, J.W. "Determination of four fluoroquinolone antibiotics in tap water in Guangzhou and Macao". *Environmental Pollution*, 158(7), pp. 2350-2358, 2010.
- [20] Appelbaum, P.C. and Hunter, P.A. "The fluoroquinolone antibacterial: Past, present and future perspectives". *International Journal of Antimicrobial Agents*, 16(1), pp. 5-15, 2000.
- [21] Ambrose, P.G., Owens, R.C., Quntilian, R. and Nightingale, C.H. "New generations of quinolones: With particular attention to levofloxacin". *Connecticut Medicine*, 61(5), pp. 269-272, 1997.
- [22] Khan, G.A., Berglund, B., Khan, K.M., Lindgren, P.-E. and Fick, J. "Occurrence and abundance of antibiotics and resistance genes in rivers, canal and near drug formulation facilities: A study in Pakistan", 2013.
- [23] Bu, Q., Wang, B., Huang, J., Deng, S. and Yu, G. "Pharmaceuticals and personal care products in the aquatic environment in China: A review". *Journal of Hazardous Materials*, 262, pp. 189-211, 2013.
- [24] Gu, C. and Karthikeyan, K.G. "Sorption of the antimicrobial ciprofloxacin to aluminum and iron hydrous oxides". *Environmental Science & Technology*, 39(23), pp. 9166-9173, 2015.
- [25] Pan, B., Qiu, M., Wu, M., Zhang, D., Peng, H., Wu, D. and Xing, B.S. "The opposite impacts of Cu and Mg cations on dissolved organic matter-ofloxacin interaction". *Environmental Pollution*, 161, pp. 76-82, 2012.

- [26] Wormser, G.P. and Keusch, G.T. "Drugs five years later: Trimethoprim-sulfamethoxazole in the united states". *Annals of Internal Medicine*, 91(3), pp. 420-429, 1979.
- [27] Peng, X., Wang, Z., Kuang, W., Tan, J. and Li, K."A preliminary study on the occurrence and behavior of sulfonamides, ofloxacin and chloramphenicol antimicrobials in wastewaters of two sewage treatment plants in Guangzhou, China". *Science of The Total Environment*, 371(1), pp. 314-322, 2016.
- [28] Peng, X., Tan, J., Tang, C., Yu, Y. and Wang, Z. "Multiresidue determination of fluoroquinolone, sulfonamide, trimethoprim, and chloramphenicol antibiotics in urban waters in China". *Environmental Toxicology and Chemistry*, 27(1), pp. 73-79, 2008.
- [29] Dmitrienko, S.G., Kochuk, E.V., Apyari, V.V., Tolmacheva, V.V. and Zolotov, Y.A." Recent advances in sample preparation techniques and methods of sulfonamides detection: A review". *Analytical Chemical Acta*, 850, pp. 6-25, 2014.
- [30] Van Doorslaer, X., Dewulf, J., Van Langenhove, H. and Demeestere, K. "Fluoroquinolone antibiotics: An emerging class of environmental micropollutants". *Science of The Total Environment*, 500-501, pp. 250-269, 2014.
- [31] I. Rafraf. I.Lekunberri,A.S. Melsio,M.Aouni,C.M.Borrego, J.L.Balcazer." Abundance of antibiotic resistance genes in five municipal wastewater treatment plants in the monastir governorate, Tunisia".*J. Enviro. Pollu*, pp. 353-358, 2016.

- [32] Kümmerer, K., Al-Ahmad, A. and Mersch-Sundermann, V. "Biodegradability of some antibiotics, elimination of the genotoxicity and affection of wastewater bacteria in a simple test". *Chemosphere*, 40(7), pp. 701-710, 2000.
- [33] E.L.Terechova,G.Zhang,J.Chen,N.A.Sosnina,F.Yang." Combined chemical coagulation- Flocculation/Ultraviolet photosynthesis treatment for anionic surfactants in laundry wastewater". *J. Enviro. Chemi.Eng.* pp. 2111-2119,2014.
- [34] U. J. W. r. Von Gunten, "Ozonation of drinking water: Part II. Disinfection and by-product formation in presence of bromide, iodide or chlorine," vol. 37, no. 7, pp. 1469-1487, 2003.
- [35] V. K. Sharma, "Oxidative transformations of environmental pharmaceuticals by Cl₂, ClO₂, O₃, and Fe(VI): Kinetics assessment," *Chemosphere*, vol. 73, no. 9, pp. 1379-1386, 2008.
- [36] I. Akmehtmet Balcıoğlu and M. Ötker, "Treatment of pharmaceutical wastewater containing antibiotics by O₃ and O₃/H₂O₂ processes," *Chemosphere*, vol. 50, no. 1, pp. 85-95,2003.
- [37] M. M. Huber et al., "Oxidation of Pharmaceuticals during Ozonation of Municipal Wastewater Effluents: A Pilot Study," *Environmental Science & Technology*, vol. 39, no. 11, pp. 4290-4299,2005.
- [38] F. J. Beltrán, A. Aguinaco, J. F. García-Araya, and A. Oropesa."Ozone and photocatalytic processes to remove the antibiotic sulfamethoxazole from water," *Water Research*, vol. 42, no. 14, pp. 3799-3808,2008.

- [39] Fink, L., Dror, I. and Berkowitz, B. "Enrofloxacin oxidative degradation facilitated by metal oxide nanoparticles". *Chemosphere*, 86(2), pp.144-149, 2012.
- [40] Petrovic, M., Radjenovic, J. and Barcelo, D." Advanced oxidation processes (AOPs) applied for wastewater and drinking water treatment: Elimination of pharmaceuticals". *The Holistic Approach to Environment* 1(2), pp. 63-74, 2011.
- [41] Keen, O.S. and Linden, K.G. "Degradation of antibiotic activity during UV/H₂O₂ advanced oxidation and photolysis in wastewater effluent". *Environmental Science & Technology* 47(22), pp.13020-13030, 2013.
- [42] H. J. H. Fenton, "LXXIII.—Oxidation of tartaric acid in presence of iron." *Journal of the Chemical Society, Transactions*, 10.1039/CT8946500899 vol. 65, no. 0, pp. 899-910, 1894.
- [43] S. Wang and J. Wang, "Trimethoprim degradation by Fenton and Fe(II)-activated persulfate processes," *Chemosphere*, vol. 191, pp. 97-105, 2018.
- [44] N. Wang, T. Zheng, G. Zhang, and P. Wang, "A review on Fenton-like processes for organic wastewater treatment," *Journal of Environmental Chemical Engineering*, vol. 4, no. 1, pp. 762-787,2016.
- [45] J. Wang and Z. Bai."Fe-based catalysts for heterogeneous catalytic ozonation of emerging contaminants in water and wastewater," *Chemical Engineering Journal*, vol. 312, pp. 79-98,2017.
- [46] C. Comninellis, "Electrocatalysis in the electrochemical conversion/combustion of organic pollutants for wastewater treatment," *Electrochimica Acta*, vol. 39, no. 11, pp. 1857-1862,1994.

- [47] C. A. Martínez-Huitle and E. Brillas, "Decontamination of wastewaters containing synthetic organic dyes by electrochemical methods: A general review," *Applied Catalysis B: Environmental*, vol. 87, no. 3, pp. 105-145, 2009.
- [48] C. A. Martínez-Huitle and S. Ferro, "Electrochemical oxidation of organic pollutants for the wastewater treatment: Direct and indirect processes," *Chemical Society Reviews*, Review vol. 35, no. 12, pp. 1324-1340, 2006.
- [49] O. Simond, V. Schaller, and C. Comninellis, "Theoretical model for the anodic oxidation of organics on metal oxide electrodes," *Electrochimica Acta*, vol. 42, no. 13, pp. 2009-2012, 1997.
- [50] D. W. Kirk, H. Sharifian, and F. R. Foulkes, "Anodic oxidation of aniline for wastewater treatment," *Journal of Applied Electrochemistry*, Article vol. 15, no. 2, pp. 285-292, 1985.
- [51] J. S. Do and W. C. Yeh, "Paired electrooxidative degradation of phenol within situ electrogenerated hydrogen peroxide and hypochlorite," *Journal of Applied Electrochemistry*, Article vol. 26, no. 6, pp. 673-678, 1996.
- [52] L.-C. Chiang, J.-E. Chang, and T.-C. Wen, "Indirect oxidation effect in electrochemical oxidation treatment of landfill leachate," *Water Research*, vol. 29, no. 2, pp. 671-678, 1995.
- [53] B. Subedi, K. Balakrishna, D. I. Joshua, and K. Kannan, "Mass loading and removal of pharmaceuticals and personal care products including psychoactives, antihypertensives, and antibiotics in two sewage treatment plants in southern India," *Chemosphere*, vol. 167, pp. 429-437, 2017.
- [54] S. J. Judd, "The status of industrial and municipal effluent treatment with

- membrane bioreactor technology," *Chemical Engineering Journal*, vol. 305, pp. 37-45, 2016.
- [55] T.-T. Nguyen, X.-T. Bui, V.-P. Luu, P.-D. Nguyen, W. Guo, and H.-H. Ngo, "Removal of antibiotics in sponge membrane bioreactors treating hospital wastewater: Comparison between hollow fiber and flat sheet membrane systems". *Bioresource Technology*, vol. 240, pp. 42-49, 2017.
- [56] Liu, M.K., Liu, Y.K., Bao, D.D., Zhu, G., Yang, G.H., Geng, J.F. and Li, H.T. "Effective removal of tetracycline antibiotics from water using hybrid carbon membranes". *Scientific Reports* 7, pp. 43717, 2017.
- [57] Boparai, H.K., Joseph, M. and O'Carroll, D.M. "Kinetics and thermodynamics of cadmium ion removal by adsorption onto nano zerovalent iron particles", *Journal of Hazardous Materials*, 186(1), pp. 458-465, 2011.
- [58] Sun, Y., Yang, S., Chen, Y., Ding, C., Cheng, W. and Wang, X. "Adsorption and desorption of U(VI) on functionalized graphene oxides: A combined experimental and theoretical study". *Environmental Science & Technology*, 49(7), pp. 4255-4262, 2015.
- [59] S.Tyagi, D Ratwani, N.Khatri, M.Tharmavarm." Strategies for nitrate removal from aqueous environment using nanotechnology: A review". *J.Water.Proc.Eng*, pp. 84-95, 2018.
- [60] Hong B.H., J.P., Purewal, M. S, Mullokandav, A., M.Y., Wang, F. Lee, J.Y., "Extracting sub nanometer single shells from ultralong multiwalled carbon nanotubes " *National Academy Science U.S.A.* 102, pp. 14155-14158, 2005.

- [61] Wang, C., Li, H., Liao, S., Zheng, H., Wang, Z., Pan, B., Xing, B." Coadoption, desorption hysteresis and sorption thermodynamics of sulfamethoxazole and carbamazepine on graphene oxide and graphite. *Carbon*, 65, pp. 243-351, 2013.
- [62] Zhao, L., Xue, F., Yu, B., Xie, J., Zhang, X., Wu, R., Wang, R., Hu, Z., Yang, S.-T., Luo, J. " TiO₂ - graphene sponge for removal of tetracycline". *Journal of nanoparticle resources*,17, pp. 1-9, 2015
- [63] Iijima, S." Helical microtubules of graphitic carbon". *Nature*, pp.354-568 1991.
- [64] Iijima, S., Ichihashi, T." Single-shell Carbon Nanotubes of 1-nm Diameter", 1993.
- [65] Ajayan, P. "Nanotubes from carbon". *Chem. Rev.* 99, pp.1787-1800, 1999.
- [66] Aksu, Z., Tunç, Ö. "Application of biosorption for penicillin G removal: comparison with activated carbon". *Process Biochem.* 40 (2), pp. 831–847,2005.
- [67] Guo, S., Peng, J., Li, W., Yang, K., Zhang, L., Zhang, S. "Effects of CO₂ activation on porous structures of coconut shell-based activated carbons". *Appl.Surf. Sci.* pp.255, 8443–8449,2009.
- [68] Pavagadhi, S., Tang, A.L., Sathishkumar, M., Loh, K.P., Balasubramanian, R."Removal of microcystin-LR and microcystin-RR by graphene oxide, adsorption, and kinetic experiments". *J. of Water Res.* 47, pp. 4621–4629,2013.
- [69] Tang, Y., Guo, H., Xiao, L., Yu, S., Gao, N., Wang, Y. "Synthesis of reduced graphene oxide/magnetite composites and investigation of their adsorption performance of fluoroquinolone antibiotics". *J. Colloids Surf. A, Physicochem. Eng. Aspects* 424, pp. 74–80, 2013.

- [70] Yuanxiu Yang, Xinjiang Hu, Yunlin Zhao, Lihua Cui, Zhujian Huang, Jianliang Long, Jiawen Xu, Jianbin Deng, Cuiyu Wu, Wenwei Liao. “Decontamination of tetracycline by thiourea-dioxide–reduced magnetic graphene oxide: Effects of pH, ionic strength, and humic acid concentration”. *J.Col.Int.Sci.*495, pp. 68-77.
- [71] Yuan Zhuang, Fei Yu, Jie Ma, Junhong Chen. “Enhanced adsorption removal of antibiotics from aqueous solutions by modified alginate/graphene double network porous hydrogel”. *J.Col.Int.Sci.*507, pp .250-259,2017.
- [72] Yan Kong, Yuan Zhuang, Kun Han, Baoyou Shi. “Enhanced tetracycline adsorption using alginate-graphene-ZIF67 aerogel”. *J. Col.and sur A.*588, pp. 124-360,2020.
- [73] Jiahe Miao, Fenghe Wang, Yajun Chen, Yezhi Zhu, Yan Zhou, Shengtian Zhang. “The adsorption performance of tetracyclines on magnetic graphene oxide: A novel antibiotics absorbent”. *J.App.Sur.Sci.*475,pp .579-558.,2019.
- [74] S.A.C. Carabineiroa, T. Thavorn-amornsri , M.F.R. Pereira, P. Serp, J.L.Figueiredo. “Comparison between activated carbon, carbon xerogel and carbon nanotubes for the adsorption of the antibiotic ciprofloxacin”. *J.of Cataly.Today*,186, pp.29-34,2012.
- [75] L. Zhang, X. Song, X.Liu, L.Yang, F. Pan, Junna Lv. “Studies on the removal oftetracycline by multi-walled carbon nanotubes. *Chem.Eng.*178, pp. 26-33,2011.
- [76] Teixeira, S., Delerue-Matos, C., Santos, L. “Application of experimental design methodologyto optimize antibiotics removal by walnut shell based activated carbon”. *J. Sci.Total Environ.* 646, pp.168–176, 2019.

- [77] Lawal, I.A., Lawal, M.M., Akpotu, S.O., Okoro, H.K., Klink, M., Ndungu, P. “Noncovalent Graphene Oxide Functionalized with Ionic Liquid: Theoretical, Isotherm, Kinetics, and Regeneration Studies on the Adsorption of Pharmaceuticals”. *J.Ind. Eng.Chem. Res.* 59, pp. 4945–4957, 2020.
- [78] Yadav, S., Goel, N., Kumar, V., Singhal, S. “Graphene oxide as proficient adsorbent for the removal of harmful pesticides: Comprehensive experimental cum DFT investigations”. *J. Anal. Chem. Lett.* 9,pp. 291–310, 2019.
- [79] H. Fu,X. Li, J. Wang,P. Lin,C. Chen,X. Zhang, I.H. (Mel) Suffet. “Activated carbon adsorption of quinolone antibiotics in water: Performance, mechanism, and modeling”. *J.Enviro.Science*,56, pp.145-152,2017
- [80] F. Yu ,Y. Li, S. Han a, J. Ma. “Adsorptive removal of antibiotics from aqueous solution using carbon materials”. *J. Chemosphere*,153, pp. 365-385,2016.
- [81] Ncibi, M.C., Sillanpaa, M. “Optimized removal of antibiotic drugs from aqueous solutions using single, double and multi-walled carbon nanotubes”. *J. Hazard. Mater.* 298, pp.102-110, 2015.
- [82] W. Yang, Y. Lua, F. Zhenga, X. Xue, Na Li , D. Liu. “Adsorption behavior and mechanisms of norfloxacin onto porous resins and carbon nanotube”. *J.Chem. Eng.Jour*, 179 pp.112-118, 2012.
- [83] W. Zhao, Y.Tian, X. Chu, L. Cui, H. Zhang,M, Li, P.Zhao. “Preparation and characteristics of a magnetic carbon nanotube adsorbent: Its efficient adsorption and recoverable performances”. *J.Sep.and Puri.Tech*,257, pp.117-917,2021.

- [84] T.Pérez, J., Gérente, C., Andrés, Y. “Sustainable Activated carbons from agricultural residues dedicated to antibiotic removal by adsorption”. *J.Chem. Eng.* 20, pp.524–529 , 2012.
- [85] Acosta, R., Fierro, V., de Yuso, A.M., Nabarlatz, D., Celzard, A. “Tetracycline adsorption onto activated carbons produced by KOH activation of tyre pyrolysis char”. *J.Chemo.*149, pp. 168–176,2016.
- [86] Martins, A.C., Pezoti, O., Cazetta, A.L., Bedin, K.C., Yamazaki, D.A.S., Bandoch,G.F.G.Asefa, T., Visentainer, J.V., Almeida, V.C. “Removal of tetracycline by NaOH-activated carbon produced from macadamia nut shells: kinetic and equilibrium studies”. *J.Chem. Eng.* 260, pp.291–299 , 2015.
- [87] Saygılı, H., Güzel, F. “Effective removal of tetracycline from aqueous solution using activated carbon prepared from tomato (*Lycopersicon esculentum* Mill.) industrial processing waste”. *Ecotoxicol. Environ. Saf.* 131, pp. 22–29, 2016.
- [88] Wang, B., Jiang, Y. Song, Li, F. Yun, Yang, D. Yue. “Preparation of biochar by simultaneous carbonization, magnetization, and activation for norfloxacin removal in water”. *Bioresour. Technol.* 233, pp. 159–165, 2017.
- [89] Wan, J., Deng, H.P., Shi, J., Zhou, L., Su, T. “Synthesized magnetic manganese ferrite nanoparticles on activated carbon for sulfamethoxazole removal”. *Clean - Soil, Air, Water* 42, pp. 1199–1207, 2014.
- [90] A.Xie, J.Cui, Y.Chen, J.Lang,C.Li, Y.Yan,J.Dai. “Simultaneous activation and magnetization toward facile preparation of auricularia-based magnetic porous carbon for efficient removal of tetracycline”. *J.Alloy& Comp.*784, pp. 76-87,2019.

- [91] W. Xiong, G. Zeng, Z. Yang, Y. Zhou, C. Zhang, M. Cheng. "Adsorption of tetracycline antibiotics from aqueous solutions on nanocomposite multi-walled carbon nanotube functionalized MIL-53 (Fe) as new adsorbent". *J.Scienc.of Tot.Enviro*, 627, pp. 235-244, 2018.
- [92] J.R.Utrilla, C.V.Gomez, M.S.Polo, J.J.Lopez, R.O.Perez. "Tetracycline removal from water by adsorption/bioadsorption on activated carbons and sludge-derived adsorbents". *J.Envior.Manag.* 131, pp. 16-24, 2013.
- [93] K.Li, M.Zhou, L.Liang, L.Jiang, W.Weng. Ultrahigh-surface-area activated carbon aerogels derived from glucose for high-performance organic pollutants adsorption. *J.Collo. and Int. Scien.* 546, pp. 333-343, 2019.
- [94] N.I. Zabba, K.L. Foo., U. Hashim, S.J. Tan., Wei-Wen Liu., C.H. Voon. "Synthesis of graphene oxide using modified hummer method: Solvent influence". *Adv.in mate. &proc. tech.conf 184*, pp. 469-477, 2017.
- [95] A.I. Abd-Elhamid, Elbadawy A. Kamoun, Ahmed A. El-Shanshory, Hesham M.A. Soliman, H.F. Aly. "Evaluation of graphene oxide-activated carbon as effective composite adsorbent toward the removal of cationic dyes: Composite preparation, characterization and adsorption parameters". *Joun.of Mole.Liqu* 279, pp. 530-539, 2019.
- [96] S.L. Upstone, "Ultraviolet/Visible Light Absorption Spectrophotometry in Clinical Chemistry". (2000)
- [97] A.I. Abd-Elhamid, H.F. Aly, Hesham A.M. Soliman, Ahmed A. El-Shanshory. "Graphene oxide: follow the oxidation mechanism and its application in

- water treatment”. *J. Mol. Liq.* 265 , pp. 226–237, 2018.
- [98] Jang, H.M., Yoo, S., Choi, Y., Park, S., Kan, E. “Adsorption isotherm, kinetic modelling, and mechanism of tetracycline on Pinus taeda-derived activated biochar”. *Bioresour. Technol.* 259, pp. 24–31,2018.
- [99] Zhang, D., Yin, J. Zhao J., Zhu, H. Wang, C.”Adsorption and removal of tetracycline from water by petroleum coke derived highly porous activated carbon”. *J.Enviro.Chem.Eng.*3, pp. 1504-1512, 2015.
- [100] Z. Li, L. Schulz, C. Ackey, N. Fenske.“Adsorption of tetracycline on kaolinite withpH-dependent surface charges”. *J. Colloid Interface Sci.* 351, pp. 254–260,2010.
- [101] Lin-ling Yu , Wen Cao , Shi-chuan Wu , Cao Yang , Jian-hua Cheng. “Removal oftetracycline from aqueous solution by MOF/graphite oxide pellets: Preparation, characteristic, adsorption performance and mechanism”.*J.Eco.of .Ennv.safe.*164, pp. 289-296, 2018
- [102] Zhi Song, Yu-Long MA, Cong-Er Li.“The residual tetracycline in pharmaceutical wastewater was effectively removed by using MnO₂/graphene nanocomposite”. *J.Sci.Tot.Envio.* 651, pp. 580-590, 2019.
- [103] Yanhui Li a, Qiuju Dua, Tonghao Liua, Xianjia Pengb, Junjie Wanga, Jiankun Suna, Yonghao Wanga, Shaoling Wua, Zonghua Wanga, Yanzhi Xiaa, LinhuaXiaa. “Comparative study of methylene blue dye adsorption onto activated carbon, graphene oxide, and carbon nanotubes”. *J. Chem.Eng. Res, Des.* 91, pp. 361-368, 2013.

- [104] Qiliang Yanga, Pingxiao Wua,b,c,d,* , Juan Liua , Saeed Rehmana , Zubair Ahmeda , Bo Ruana , Nengwu Zhua. “Batch interaction of emerging tetracycline contaminant with novel phosphoric acid activated corn straw porous carbon: Adsorption rate and nature of mechanism”. *J.Envir.Res.*181, pp. 108-899, 2020.
- [105] Pyrzynska, ´ K., Bystrzejewski, M.,“Comparative study of heavy metal ions sorption onto activated carbon, carbon nanotubes, and carbon-encapsulated magnetic nanoparticles”. *Colloids Surf. A* 362, pp. 102–109, 2010.
- [106] Alessandro C. Martins , Osvaldo Pezoti , André L. Cazetta , Karen C. Bedin , Diego A.S. Yamazaki ,Gisele F.G. Bandoch , Tewodros Asefa, Jesuí V. Visentainer , Vitor C. Almeida.“Removal of tetracycline by NaOH-activated carbon produced from macadamia nut shells: Kinetic and equilibrium studies”. *J.Chemi.Eng.Jour.* 260, pp. 297-299,2015.
- [107] Guo, Y., Huang, W., Chen, B., Zhao, Y., Liu, D., Sun, Y., Gong, B. “Removal of tetracycline from aqueous solution by MCM-41-zeolite A loaded nano zero valent iron: synthesis, characteristic, adsorption performance and mechanism”. *J. Hazard. Mater.* 339, pp. 22,2017.

EQUILIBRIUM DATA FOR TETRACYCLINE :APPENDIX A

	303 K			313 K			323 K		
	Conc	Ce (mg/l)	qe (mg/g)	Conc	Ce (mg/l)	qe (mg/g)	Conc	Ce (mg/l)	qe (mg/g)
AC	10	0.29±0.01	48.52	10	0.29±0.01	48.550	10	0.23±0.01	48.852
	50	1.21±0.01	243.93	50	1.23±0.01	243.815	50	1.25±0.01	243.748
	100	4.48±0.01	477.56	100	2.95±0.01	485.218	100	2.82±0.01	485.856
	200	62.98±0.01	685.09	200	58.65±0.01	706.750	200	57.71±0.01	711.415
	400	264.43±0.01	677.85	400	252.98±0.01	735.071	400	244.50±0.06	777.500
	500	363.17±0.05	684.11	500	352.33±0.01	738.336	500	346.25±0.04	768.733
GO	10	3.332±0.01	33.34	10	1.395±0.01	43.026	10	0.639±0.01	46.804
	50	17.840±0.03	160.80	50	16.806±0.01	165.972	50	10.667±0.01	196.666
	100	56.624±0.03	216.88	100	54.676±0.02	226.619	100	45.528±0.03	272.358
	200	151.263±0.01	243.69	200	145.889±0.01	270.553	200	125.472±0.03	372.642
	400	333.797±0.05	331.02	400	327.564±0.05	362.181	400	317.247±0.01	413.763
	500	428.529±0.01	357.35	500	423.425±0.01	382.875	500	412.074±0.01	439.629
AC- GO	10	1.203±0.01	43.98	10	1.039±0.01	44.806	10	0.881±0.01	45.595
	50	7.574±0.03	212.13	50	7.070±0.03	214.649	50	6.163±0.03	219.183
	100	47.073±0.03	264.63	100	31.102±0.01	344.492	100	28.415±0.03	357.925
	200	131.113±0.01	344.43	200	122.973±0.01	385.135	200	121.227±0.03	393.866
	400	326.221±0.01	368.90	400	320.579±0.03	397.106	400	318.967±0.01	405.166
	500	422.820±0.03	385.90	500	417.112±0.03	414.442	500	414.761±0.03	426.196

EQUILIBRIUM DATA FOR DOXYCLINE :APPENDIX B

	303 K			313 K			323 K		
	Conc	Ce (mg/l)	qe (mg/g)	Conc	Ce (mg/l)	qe (mg/g)	Conc	Ce (mg/l)	qe (mg/g)
AC	10	0.271±0.03	48.65	10	0.106±0.03	49.47	10	0.073±0.03	49.64
	50	1.137±0.05	244.31	50	0.323±0.01	248.38	50	0.277±0.01	248.61
	100	7.003±0.05	464.98	100	5.164±0.01	474.18	100	5.244±0.01	473.78
	200	81.677±0.05	591.61	200	68.034±0.04	659.83	200	32.791±0.02	836.05
	400	254.713±0.03	726.43	400	222.331±0.05	888.35	400	199.499±0.02	1002.50
GO	10	3.550±0.04	32.25	10	3.227±0.03	33.87	10	2.047±0.02	39.77
	50	21.454±0.03	142.73	50	20.255±0.03	148.73	50	18.805±0.03	155.98
	100	51.556±0.03	242.22	100	50.620±0.03	246.90	100	50.357±0.02	248.22
	200	128.106±0.04	359.47	200	125.469±0.05	372.65	200	125.311±0.03	373.44
	400	315.741±0.04	421.29	400	312.050±0.03	439.75	400	303.667±0.04	481.67
AC- GO	10	1.417±0.01	42.91	10	1.352±0.03	43.24	10	1.286±0.03	43.57
	50	7.709±0.01	211.46	50	7.537±0.04	212.31	50	7.280±0.01	213.60
	100	48.999±0.04	255.00	100	35.540±0.04	322.30	100	35.422±0.02	322.89
	200	130.874±0.03	345.63	200	129.767±0.03	351.17	200	127.948±0.02	360.26
	400	311.312±0.03	443.44	400	309.098±0.03	454.51	400	308.623±0.03	456.88